MODELING AND OPTIMIZATION OF SLOPPING PREVENTION AND BATCH TIME REDUCTION IN BASIC OXYGEN STEELMAKING

The research described in this thesis is financially supported by
Danieli-Corus.

Modeling and optimization of slopping prevention and batch time reduction
in basic oxygen steelmaking,
C. Stroomer-Kattenbelt,
ISBN 978-90-9023126-6

Cover: detail shot of fire and smoke, C. Stroomer-Kattenbelt

Printed by Gildeprint Drukkerijen

MODELING AND OPTIMIZATION OF SLOPPING PREVENTION AND BATCH TIME REDUCTION IN BASIC OXYGEN STEELMAKING

PROEFSCHRIFT

ter verkrijging van
de graad van doctor aan de Universiteit Twente,
op gezag van de rector magnificus,
prof.dr. W.H.M. Zijm,
volgens besluit van het College voor Promoties
in het openbaar te verdedigen
op vrijdag 11 juli om 15.00 uur

door

Carolien Kattenbelt

geboren op 7 maart 1981

te Enschede

Dit proefschrift is goedgekeurd door de promotor
prof.dr.ir. B. Roffel

Summary

Because of increasingly stricter environmental regulations, steel plants are attempting to reduce the occurrence of (heavy) slopping, which can be accompanied by large ejections of dust. They are also aiming to increase their production capacity by e.g. investments in additional equipment and by improving logistics. Reduction of the batch time in basic oxygen steelmaking might contribute to the desired increase in production capacity if the converters are the bottleneck in production.

Currently the desired temperature and steel composition are met by application of a first principles static model, which determines the required raw material input. This model is sometimes perceived as complicated. The setpoints of the control variables such as the addition rates, the lance height and the oxygen blowing rate are based on standard operating procedures, which have been developed during many years of practical experience. Operators only deviate from these standard operating procedures when it is necessary, for instance, when slopping occurs. It may be expected, that both the batch time and the occurrence of slopping can significantly be reduced by optimizing operating settings.

The objective of this thesis is to develop a dynamic control strategy for basic oxygen steelmaking which both reduces the occurrence of slopping and increases the production capacity by reducing the batch time. The development of this strategy would greatly benefit from the continuous measurement of important process variables. However, due to the high temperatures and dusty environment involved, measuring of important process variables is difficult. It is therefore necessary to develop a dynamic process model that predicts important process variables. Dynamic modeling of the process enables dynamic

optimization. The feasibility of measurements, modeling of the process and dynamic optimization are studied subsequently in this thesis.

Chapters 1 and 2 contain an introduction and background information.

In chapter 3 the feasibility of the continuous measurement of the steel composition, the slag composition, the steel temperature and the foam height is investigated. The high temperature, dusty environment and the lack of reference measurements cause most measurements to be infeasible.
To validate dynamic models of system behavior, however, continuous measurements are needed. The decarburization rate and the accumulation rate of oxygen inside the converter can be used for validation of the steel and slag composition. The steel temperature can be approximated using the assumption that the steel temperature increases linearly with the amount of oxygen blown. For the validation of foam height no feasible continuous measurements was found and since the occurrence of slopping is neither detected nor recorded, a slop detection system is needed.

In chapter 4 a slop detection system is presented that can be used to detect the occurrence of slopping. The slop detection algorithm is designed based on the images taken by a camera viewing the converter mouth. With this algorithm 73% of the slopping batches were detected within 5 seconds and 94% of the non-slopping batches were correctly detected. The algorithm is relatively simple and can thus easily be used in on-line applications such as an alarm or a slop repression system.

In chapter 5 the first principles static model, which is sometimes perceived as complicated, is compared to a statistical static model, which requires less expert knowledge. Both static models are used to calculate the amount, composition and temperature of the raw material input (scrap, additions, hot metal, oxygen) with which the required steel temperature and steel carbon concentration can be reached.
Using Principal Component Analysis it is shown, that the inputs are highly correlated and that the data can be divided into two separate clusters. For each of the clusters a separate statistical model was developed using Partial Least Squares, since this technique can cope with highly correlated input data. The inputs have a similar influence on the steel carbon concentration and steel

temperature in the first principles model and in the PLS models. The PLS models are less accurate than the currently used first principles model and the PLS models are, therefore, not a good alternative.
The lower accuracy of the PLS models might be caused by the fact that important process variables, such as the heat loss, are estimated in the first principles model, but they are not used as inputs in the PLS models. The lower accuracy may also be caused by the fact that the assumption of linearity may not be valid.

In chapter 6 a dynamic process model for the main blow is developed, which describes the steel and slag composition. Since it is shown in chapter 3 that the steel and slag composition can be validated by the measured decarburization rate and the accumulation rate of oxygen, the step responses in these two signals are used to develop de main blow model. The measured step responses can be explained by a simple dynamic model consisting of a carbon and an iron oxide balance. The developed dynamic process model is only valid for the main blow and can thus not be used for the entire batch.

In chapter 7 the dynamic process model described in chapter 6 is extended in such a way that it calculates the temperature, steel composition and slag composition during the entire batch. In the dynamic process model the linear approximation described in chapter 3 is used to calculate the temperature. The steel and the slag composition are validated by the measured decarburization rate and accumulation rate of oxygen. The calculated decarburization rate and the measured decarburization rate correspond well during the entire batch. The variance accounted for in the decarburization rate and the accumulation rate of oxygen is 73% and 63% respectively.
The accuracy of prediction of the carbon concentration of the static model is higher than that of the dynamic model. This is due to the fact that the level of detail of the static model is higher than that of the dynamic model. The dynamic model does not make the static model redundant and the dynamic model should always be used in combination with the static model.

In chapter 8 the dynamic model described in chapter 7 is extended with a slop probability model. The majority of the slopping occurrences (61%) coincide with a maximum in the iron oxide concentration in the slag. This type of slopping is modeled using a statistical two layer hierarchical model. In the

first layer the slop sensitive period in the batch is identified using a boolean expression. In the second layer, the probability of slopping is calculated using a logistic model. The hierarchical model is simple, using only a small number of input variables. Nevertheless, it has an accuracy of prediction of 73% for slopping batches and 71% for non-slopping batches.

In chapter 9 the process is dynamically optimized with the goal to minimize the batch time while observing the slopping constraint. Using the dynamic model described in chapters 6 and 7 as the state equations and the slop probability model described in chapter 8 as a constraint, it is derived, that dynamic optimization results in a bang-bang control strategy in which the lance height and the oxygen blowing rate are either their minimum or their maximum value. Using the optimal strategy and a maximum oxygen blowing rate of $4.95.10^4$ $[\frac{nm^3}{h}]$ the batch time can be reduced with 4.6%. Using a maximum oxygen blowing rate of $5.5.10^4$ $[\frac{nm^3}{h}]$ the batch time can even be reduced with 12.4%. Due to modeling errors, this reduction in batch time may not be realizable when the calculated optimal strategy is applied in practice. The calculated optimal strategy, however, indicates the direction in which the currently used control strategy can be changed to reduce the batch time and to prevent slopping.

Samenvatting

Door steeds strenger wordende milieuwetgeving, proberen staalfabrieken (hevig) slobben, dat gepaard kan gaan met de uitstoot van stofdeeltjes, te voorkomen. Tegelijkertijd proberen ze hun productiecapaciteit te verhogen, bijvoorbeeld door investeringen in extra apparatuur en door verbetering van de logistiek. Een vermindering van de batchtijd in het oxystaalproces zou aan de gewenste toename in productiecapaciteit kunnen bijdragen als de converters de bottleneck in productie zijn.

Op dit moment wordt de gewenste staalsamenstelling en staaltemperatuur gehaald door toepassing van een fysisch statisch model, dat de benodigde hoeveelheid grondstoffen bepaalt. Dit model wordt soms ingewikkeld gevonden. De setpoints van stuurvariabelen zoals de toevoersnelheden, de lanshoogte en de zuurstofblaassnelheid zijn gebaseerd op standaard procedures, die ontwikkeld zijn op basis van vele jaren praktische ervaring. Operators wijken alleen van deze standaardprocedures af als dat nodig is, bijvoorbeeld als slobben optreedt. Het is te verwachten, dat zowel de batchtijd als het aantal keer dat slobben optreedt aanzienlijk kan worden verminderd door optimalisatie van de stuurvariabelen.

Het doel van dit proefschrift is het ontwikkelen van een dynamische stuurstrategie, die zowel het aantal keer dat slobben voorkomt als de batchtijd vermindert. Het ontwikkelen van deze strategie zou zeer geholpen zijn door de continue meting van belangrijke procesvariabelen. Door de hoge temperatuur en de stoffige omgeving is het echter moeilijk om belangrijke procesvariabelen te meten. Het is daarom noodzakelijk om een dynamisch procesmodel te ontwikkelen, dat de belangrijke procesvariabelen kan voorspellen. Door dynamische modellering van het proces is ook dynamische optimalisatie mogelijk. De haalbaarheid van

metingen, het modelleren van het proces en dynamische optimalisatie worden achtereenvolgens behandeld in dit proefschrift.

Hoofdstukken 1 en 2 bevatten een introductie en achtergrond informatie.

In hoofdstuk 3 wordt de haalbaarheid van de continue meting van de staalsamenstelling, de slaksamenstelling, de staaltemperatuur en de schuimhoogte onderzocht. De hoge temperatuur, de stoffige omgeving en het gebrek aan referentiemetingen zorgen ervoor dat de meeste continue metingen niet haalbaar zijn.
Om dynamische modellen van het proces te kunnen valideren zijn continue metingen echter wel noodzakelijk. De ontkolingssnelheid en accumulatiesnelheid van zuurstof in de converter kunnen voor validatie van de staal- en slaksamenstelling gebruikt worden. De staaltemperatuur kan worden benaderd door gebruik te maken van de aanname dat de staaltemperatuur lineair stijgt met de hoeveelheid geblazen zuurstof. Voor validatie van de schuimhoogte is geen haalbare continue meting gevonden en omdat slobben niet gedetecteerd of geregistreerd wordt is een slobdetectie systeem noodzakelijk.

In hoofdstuk 4 wordt een slobdetectie systeem gepresenteerd waarmee het plaatsvinden van slobben kan worden gedetecteerd. Het slobdetectiealgoritme is ontworpen gebaseerd op beelden die door een camera zijn opgenomen, die gericht staat op de bovenrand van de converter. Met dit algoritme is 73% van de slobbende ladingen binnen 5 seconden gedetecteerd en is 94% van de niet-slobbende ladingen correct herkend. Het algoritme is relatief eenvoudig en kan dus zonder problemen worden toegepast in on-line applicaties zoals een slobalarm of een slobrepressiesysteem.

In hoofdstuk 5 wordt het fysische statische model, dat soms ingewikkeld wordt gevonden, vergeleken met een statistisch statisch model, waarvoor minder specifieke model kennis noodzakelijk is. Beide statische modellen worden gebruikt om de hoeveelheid, de samenstelling en de temperatuur van de grondstoffen (addities, schrot, hot metal en zuurstof) te berekenen, bij welke de benodigde staaltemperatuur en koolstofconcentratie gehaald worden.
Door gebruik te maken van Principal Component Analysis is het aangetoond, dat de modelingangen sterk gecorreleerd zijn en dat de data in twee verschillende clusters opgedeeld kan worden. Voor elk van de clusters is een apart

statistisch model ontwikkeld met behulp van Partial Least Squares omdat deze techniek om kan gaan met gecorreleerde ingangsvariabelen. De ingangsvariabelen hebben in het fysische model en in de twee PLS modellen een soortgelijke invloed op de staaltemperatuur en koolstofconcentratie. De PLS modellen zijn minder nauwkeurig dan het op dit moment gebruikte fysische model en ze zijn dan ook geen goed alternatief.
De lage nauwkeurigheid van de PLS modellen zou veroorzaakt kunnen zijn doordat belangrijke procesvariabelen, zoals het warmteverlies, in het fysische model geschat worden, maar niet als inputs worden gebruikt in de PLS modellen. De lagere nauwkeurigheid zou ook veroorzaakt kunnen worden doordat de aanname van lineariteit mogelijk niet geldig is.

In hoofdstuk 6 is een dynamisch proces model voor de mainblow ontwikkeld, dat de staal- en slaksamenstelling beschrijft. In hoofdstuk 3 is aangetoond, dat de staal- en slaksamenstelling kunnen worden gevalideerd door de gemeten ontkolingssnelheid en accumulatiesnelheid van zuurstof in de converter. Daarom worden de stapresponsies in deze twee signalen gebruikt om het mainblow model te ontwikkelen. Het is aangetoond, dat de gemeten stapresponsies kunnen worden verklaard door een eenvoudig dynamisch model dat bestaat uit een koolstof- en een ijzeroxidebalans. Het ontwikkelde dynamische procesmodel is alleen geldig voor de mainblow en kan dus niet voor de gehele lading worden gebruikt.

In hoofdstuk 7 is het dynamische model, dat in hoofdstuk 6 is beschreven, op zo'n manier uitgebreid, dat de temperatuur, slaksamenstelling en staalsamenstelling gedurende de hele lading kunnen worden berekend. In het dynamische procesmodel wordt de lineaire benadering, die in hoofdstuk 3 is beschreven, gebruikt om de staaltemperatuur te berekenen. De gemeten en berekende ontkolingssnelheid komen nauw overeen gedurende de hele batch en de variance accounted for voor de ontkolingssnelheid en de accumulatiesnelheid van zuurstof in de converter is respectievelijk 73% en 63%.
De nauwkeurigheid van de voorspelling van de koolstofconcentratie van het staal is van het statische model groter dan die van het dynamische model. Dit komt doordat het detailniveau van het statische model groter is. Het dynamische model zal het statische model dan ook niet overbodig maken. Het dynamische model zal altijd in combinatie met het statische model gebruikt moeten worden.

In hoofdstuk 8 is het dynamisch model dat in hoofdstuk 7 is beschreven uitgebreid met een slobkans berekening. De meerderheid van de slobbers (61%) vinden tegelijkertijd met het maximum in het ijzeroxidegehalte in de slak plaats. Dit soort slobber is gemodelleerd met een statistisch tweelaags hierarchisch model. In de eerste laag wordt de slobgevoelige periode in de batch bepaald met behulp van een boolean vergelijking. In de tweede laag wordt de slobkans berekend met behulp van een logistic model. Het hierarchische model is eenvoudig en maakt gebruik van slechts een beperkt aantal input parameters. Desalniettemin heeft het een nauwkeurigheid van 73% voor slobbende ladingen en 71% voor niet slobbende ladingen.

In hoofdstuk 9 is het proces dynamisch geoptimaliseerd met het doel de batchtijd te minimaliseren terwijl tegelijkertijd slobben wordt voorkomen. Gebruikmakend van het dynamisch model beschreven in de hoofdstukken 6 en 7 als state equations en het slobkans model beschreven in hoofdstuk 8 als een constraint, is het af te leiden, dat dynamische optimalisatie resulteert in een bang-bang control strategie waarbij de lanshoogte en de zuurstofblaassnelheid ofwel hun minimum ofwel hun maximum waarde hebben.
De optimale strategie kan bij een maximum zuurstofblaassnelheid van $4.95.10^4$ $[\frac{nm^3}{h}]$ de batchtijd reduceren met 4.6%. Gebruikmakend van een maximum zuurstofblaassnelheid van $5.5.10^4$ $[\frac{nm^3}{h}]$ kan de batchtijd zelfs met 12.4% worden verkort. Deze vermindering van batchtijd zou, als de optimale strategie in praktijk wordt toegepast, mogelijk niet volledig gerealiseerd kunnen worden i.v.m. model mismatch. De berekende optimale strategie geeft echter een indicatie van de richting waarin de huidige stuurstrategie veranderd kan worden om de batchtijd te verminderen en slobben te voorkomen.

Contents

1

Introduction

In this introduction the current situation and recent developments in basic oxygen steelmaking are discussed. The ambition of steel plants to increase production capacity and the increasingly stricter environmental regulations call for a change in the control strategy of basic oxygen steelmaking. This thesis deals with the development of a dynamic control strategy for basic oxygen steelmaking. How the new control strategy can be accomplished is addressed in the thesis objective. The thesis structure will also be discussed.

1.1 Basic oxygen steelmaking

Basic oxygen steelmaking is a batch process in which steel is made from liquid iron [1; 2; 3]. The concentration of elements such as carbon, manganese and phosphorous have an impact on the steel quality (hardness, strength and toughness). For the steel to be cast, it needs to be at a predefined temperature. To achieve the predefined temperature and composition, oxygen is blown into a vessel that contains the liquid iron and that is lined with refractory bricks. The oxygen oxidizes the elements within the bath causing an increase in temperature and a reduction in concentration of undesirable elements. The formed liquid oxides float to the top of the bath forming a slag layer. The formed gaseous oxides such as carbon monoxide and carbon dioxide rise through this slag layer making it foamy. In certain cases the slag can foam to the extend, that part of it is thrown over the edge of the converter. This foam overflow is

called slopping.

1.2 Current situation

Static models are currently used to calculate the amount of raw materials needed in order to meet quality and temperature demands [4; 5; 6]. Furthermore, set points of control variables such as addition rates and oxygen blowing rates are currently based on standard operating procedures, which have been developed during many years of practical experience. The operator only deviates from these standard operating procedures when necessary. The most common reason for deviation from standard operating procedures is the occurrence of slopping.

1.3 Recent developments

During the 5th European Oxygen Steelmaking Conference in 2006, many steel plants have presented the changes they made in the operation of the process in order to increase their production capacity [7; 8; 9; 10; 11; 12; 13; 14; 15]. This has been achieved by investments in additional or better equipment, by improving logistics, by decreasing maintenance time, by decreasing refractory wear and by decreasing batch time by, for instance, increasing the oxygen blowing rate during the entire batch. They have also shown their ambition to continue to increase their annual steel production.
Another area that has attracted much attention lately is slopping. Heavy slopping can be accompanied by large ejections of dust. Due to increasingly stricter environmental regulations and increasing opposition from neighboring inhabitants [16; 17; 18; 19] many steel plants have attempted to reduce the occurrence of slopping.
The demand for an increase in production and a decrease in the occurrence of slopping seem to be conflicting. While an increase in production can be achieved by increasing the oxygen blowing rate, the same increase in oxygen blowing rate increases the gas generation rate inside the vessel. Research indicates, that under steady state conditions, an increase in gas generation rate increases the foam height and the chance of the occurrence of slopping [20; 21].

1.4 Thesis objective and scope

The aim of this thesis is to develop a dynamic control strategy for basic oxygen steelmaking with which the occurrence of slopping can be reduced and the annual production can be increased. The increase in production can be realized by decreasing the production time of a single batch.
Other strategies to increase production such as e.g. the purchase of additional equipment and improvement in logistics are beyond the scope of this thesis. Other possible additional effects that the change in control strategy may have, such as the effect on wear of the refractory bricks are also beyond the scope of this thesis.

1.5 Thesis structure

The development of a dynamic control strategy for basic oxygen steelmaking would be greatly aided by the continuous measurement of important process variables, by modeling of system behavior and by dynamic optimization studies. The feasibility of continuous measurements, the possibility of modeling the process and optimization of the process are investigated subsequently. This results in the following thesis structure:

Chapter 2 provides some additional background information regarding the process and generally used measuring equipment. The steel plant of which data is used in this thesis is discussed in more detail.

Chapter 3 deals with the feasibility of the continuous measurement of important process variables such as the composition of the steel, the composition of the slag, the steel temperature and the foam height. It is shown that due to the high temperatures and dusty environment involved and due to the lack of reference measurements most of the the suggested measurements are currently not feasible. Only the temperature can be estimated using a linear approximation based on the assumption of a self regulating temperature.
It is however recognized, that for the creation of a dynamic process model a continuous reference for the steel and slag composition would be helpful. The easily measurable decarburization rate and accumulation rate of oxygen could be used as such references.

Chapter 4 describes a slop detection system based on images recorded by a camera viewing the converter mouth. In chapter 3 it is concluded that the continuous measurement of the foam height is currently infeasible. In dynamic modeling and control of the process it would be helpful to have references of the foam height. However, in most steel plants slopping is neither detected nor recorded. Therefore, a slop detection algorithm is designed which is both accurate and sensitive and which can be applied in online applications.

Chapter 5 provides some additional background information on the static control models that are currently in use for the calculation of the necessary raw material input. The currently used first principle static model is sometimes perceived as complicated. Especially when it needs to be retuned because of changes in the process. This first principle model is therefore compared with a Partial Least Squares (PLS) statistical model which requires less expert knowledge. It is shown that the first principle model is more accurate than the PLS model. It is therefore concluded that, if enough expert knowledge is available, the first principle model is preferred.

Chapter 6 describes a dynamic process model for the main blow, that calculates the steel and slag composition. The model is developed based on the measured step responses in the decarburization rate and accumulation rate of oxygen to step changes in the oxygen blowing rate, the lance height and the addition rate of iron ore. It is shown, that the measured step responses can be described by a simple model consisting of a carbon and an iron oxide balance.

Chapter 7 describes how the dynamic process model developed in chapter 6 can be extended, so that it describes the steel and slag composition as well as the steel temperature during the entire batch. The dynamic model is validated by comparing it with the measured decarburization rate and accumulation rate of oxygen. It is shown, that the modeled and measured decarburization rate and accumulation rate of oxygen correspond well during the entire batch.

It is furthermore shown, that the accuracy of prediction of the carbon concentration at the end of the batch is lower than that of the first principles static model. It is therefore argued, that the dynamic model should always be used in combination with a static model.

Chapter 8 describes the extension of the dynamic model described in chapter 7 with a slop probability model. From observation it is shown that the majority of slopping batches start to slop when the iron oxide concentration in the slag is at its maximum level. It is shown, that these slopping batches can be modeled using a statistical two layer hierarchical model. The first layer of the model describes the slop sensitive period during the batch, while the second layer describes the slop probability of the batch. The resulting slop prediction model is simple using only a small number of input variables.

Chapter 9 describes dynamic optimization of basic oxygen steelmaking with the goal to minimize the batch time. In the optimization problem, the dynamic model described in chapters 6 and 7 is used as the state equations and the slop probability model described in chapter 8 is used as a constraint. It is shown, that dynamic optimization results in a bang-bang control strategy. The optimal control strategy both prevents the occurrence of slopping and reduces the batch time significantly.

Chapter 10 contains the most important conclusions.

Bibliography

[1] R. Boom, B. Deo, Fundamentals of steelmaking metallurgy, Prentice Hall International, Hemel Hempstead (1993)

[2] F. Oeters, Metallurgie der stahlherstellung, Springer-Verlag, Dusseldorf (1989)

[3] E.T. Turkdogan, Fundamentals of steelmaking, The institute of materials, London (1996)

[4] C.J. Kearton, Process model for oxygen converters, In: *70th steelmaking conference*, Scarborough (1968), 42-46

[5] D. DasGupta, J. Heidepriem, Verbesserung der temperaturtreffsicherheit eines statischen on-line-modells in einem LD-stahlwerk, *Stahl und eisen*, **102**(1982), 857-860

[6] C. Kubat, H. Taskin, R. Artir, A. Yilmaz, Bofy-fuzzy logic control for the basic oxygen furnace (BOF), *Robotics and autonomous systems*, **49**(2004), 193-205

[7] O. Bode, R. Bruckenhaus, Optimisation of steelplant logistics at Dillinger Hutte using simulation models, In: *5th European oxygen steelmaking conference*, Aachen (2006), 411-416

[8] J. Brockhoff, P. Broersen, M. Hartwig, H. Pronk, H. ter Voort, R. Mostert, A. Snoeijer, A. Overbosch, Towards 7 million tons of liquid steel per year at BOS2 Corus strip IJmuiden, In: *5th european oxygen steelmaking conference*, Aachen (2006), 417-424

[9] G. Simms, I. Blake, Port Talbot challenges, In: *5th european oxygen steelmaking conference*, Aachen (2006), 425-432

[10] A. Berghofer, R. Kromarek, Salzgitter Flachstahl GmbH increased the efficiency of its BOF shop, In: *5th european oxygen steelmaking conference*, Aachen (2006), 477-485

[11] J. Lilja, S. Ollila, H. Nevala, Decade of development in steelmaking at Ruukki production, In: *5th european oxygen steelmaking conference*, Aachen (2006), 494-500

[12] S. Takeuchi, K. Akahane, K. Sakai, Improvement of BOF productivity in no. 2 steelmaking plant at Kashima steel works, In: *5th european oxygen steelmaking conference*, Aachen (2006), 501-507

[13] S. Kim, D. Lee, High efficient converter operation scheme in Pohang No. 2 steelmaking plant, In: *5th european oxygen steelmaking conference*, Aachen (2006), 537-541

[14] Gol, L. Meier, K. Schneider, H. Schock, W. Laubach, Boosting production through optimal BOF modernization of ISDEMIR Iron and steelworks, In: *5th european oxygen steelmaking conference*, Aachen (2006), 542-549

[15] H. Moser, W. Hofer, K. Jandl, R. Apfolterer, H. Mizelli, Productivity increase and low hot metal LD-steelmaking at voest alpine Stahl GmbH, In: *5th european oxygen steelmaking conference*, Aachen (2006), 93-99

[16] Oppositie vergunning Corus blijft groeien, In: *Noordhollands dagblad*, 3 February 2006

[17] Dorpsraad kritiseert vergunning Corus, In: *Noordhollands Dagblad*, 9 October 2006

[18] Aanvraag revisievergunning Corus Staal, 14 October 2004 and additions of 29 April 2005

[19] Herziene ontwerpbeschikking wet milieubeheer, September 2006

[20] S. Jung, R.J. Fruehan, Foaming characteristics of BOF slags, In: *2000 ironmaking conference*, Pittsburgh (2000), 517-527

[21] K. Ito, R.J. Fruehan, Study on the foaming of CaO-SiO2-FeO slags: Part 1. Foaming parameters and experimental results, *Metallurgical transactions B*, **20B**(1989), 509-514

2

Background

Several process steps are required to make steel from the raw materials iron ore and cokes. Basic oxygen steelmaking (BOS), the subject of this thesis, is an important process step since it removes the majority of unwanted elements and increases the temperature of the molten steel. This chapter serves as background information for the remainder of the thesis. It contains a description of the steelmaking process, a detailed description of the basic oxygen steelmaking process and a detailed description of the steel plant of which data is used in this thesis.

2.1 Steelmaking process

Steel is produced from iron ore in several different process steps as is shown in figure 2.1.

2.1.1 Blast furnace

The first step is the continuous production of hot metal (HM) in the blast furnace by reducing iron ore with cokes and air. The hot metal is tapped from the blast furnace periodically. In figure 2.2 a schematic representation of a blast furnace is shown. When comparing typical compositions and temperatures of the hot metal and the liquid steel, which are shown in table 2.1, it can be seen that in additional process steps, the carbon, silicon, manganese, phosphorous

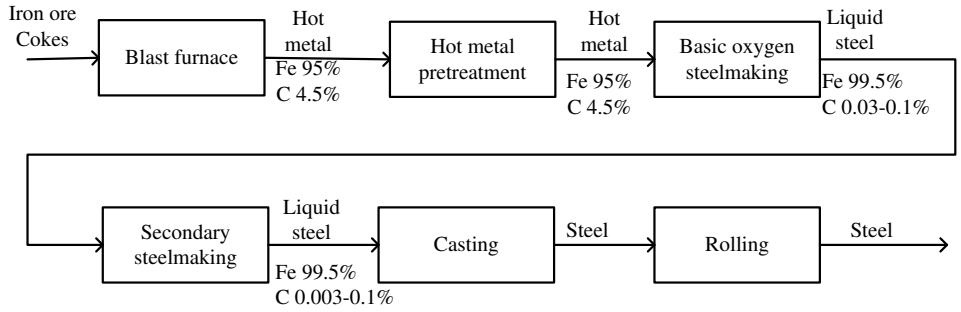

Figure 2.1: The process steps in which steel is produced.

and sulphur concentration have to be reduced and that the temperature has to be increased.
For a more detailed description of iron making the reader is referred to a book by Biswas [1].

Table 2.1: Typical composition of hot metal when tapped from the blast furnace and typical demanded steel qualities for basic oxygen steelmaking.

Component	Hot metal		Steel	
C	4.4-4.8	[w%]	0.035-0.1	[w%]
Si	0.4	[w%]	0	[w%]
Mn	0.4	[w%]	0.13	[w%]
P	0.06	[w%]	0.011-0.02	[w%]
S	0.02-0.04	[w%]	0.005	[w%]
Temperature	1300-1460	[C]	1555-1655	[C]

2.1.2 Hot metal pre-treatment

In most steel plants hot metal pre-treatment steps are used to reduce high concentrations of elements which are difficult to remove, or which can cause problems in subsequent process steps. The reduction of the high concentration is often conducted in separate processing units. Depending on plant strategy, the reduction of high concentrations can be performed in the blast furnace runner, in the torpedo's (transportation vessels for the hot metal), in a separate

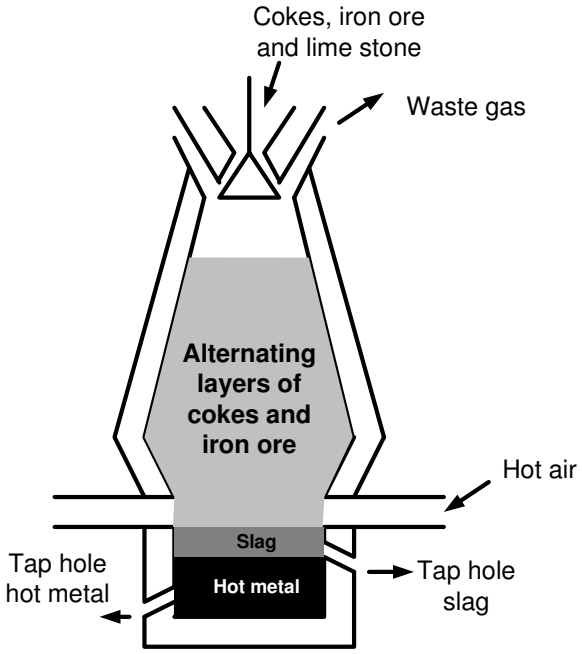

Figure 2.2: Schematic representation of a blast furnace.

converter (dephosphorisation converter) or in secondary steelmaking.
Hot metal pre-treatment can include desiliconisation, dephosphorisation and desulphurisation and is conducted by adding materials such as iron oxide, lime, fluorspar and calcium or magnesium based compounds. These materials can be introduced by either dumping them on the hot metal bath or introducing them with a carrier gas either through bottom tuyeres or through a lance.

2.1.3 Basic oxygen steelmaking

In basic oxygen steelmaking the majority of unwanted elements are removed and the temperature is increased. In basic oxygen steelmaking, the hot metal is tapped into a converter. In the converter oxygen is blown on top of the hot metal bath in order to oxidize elements in the hot metal, resulting in the

following reactions:

$$X + \frac{1}{2}nO_2 \rightarrow XO_n \tag{2.1}$$

Due to these exothermic oxidation reactions the carbon concentration (and other elemental concentrations) reduces and the temperature increases. After blowing for about 20 minutes (depending on the size and operation of the converter) the converter is tapped. During tapping, alloying materials can be added to increase the concentration of certain elements. Typical alloying materials are ferromanganese, siliconmanganese and ferrosilicon.
A more detailed description of basic oxygen steelmaking can be found in section 2.2 of this thesis and in books by Deo and Boom [2], Oeters [3] and Turkdogan [4].

2.1.4 Secondary steelmaking

In basic oxygen steelmaking the majority of unwanted elements are removed and the larger part of temperature increase is achieved. Processing units for secondary steelmaking can be used to make small adjustments in steel composition and temperature. The secondary steelmaking methods can be grouped into stirring processes, injection processes, vacuum processes and heating processes. A more extensive review of secondary steelmaking can be found in books by Boom and Deo [2] and by Stolte [5].

2.1.5 Casting

The liquid steel can be cast into blocks called ingots, alternatively, a more advanced casting technique, continuous casting, can be used. In figure 2.3 a schematic representation of a continuous caster is shown. In continuous casting liquid steel is continuously poured into a bottomless mould and at the same time a continuous steel casting is extracted. At the end of the continuous caster the cast steel is cut into pieces. Casting is more extensively described in books by Schwerdfeger [6] and by Irving [7].

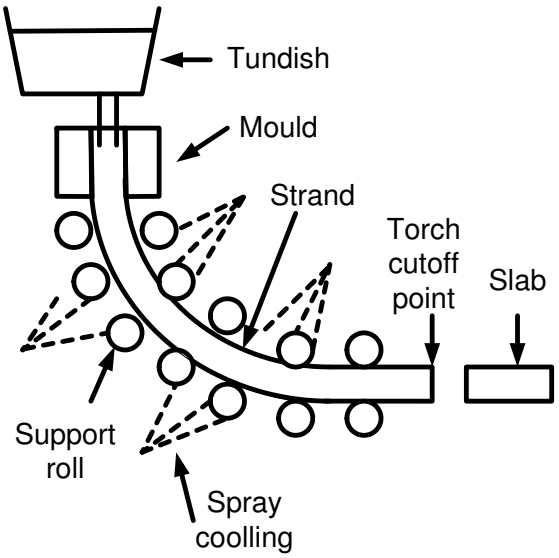

Figure 2.3: Schematic representation of a continuous caster.

2.1.6 Rolling

Rolling is needed to recrystallize the steel into a much finer grain structure giving the steel greater toughness and tensile strength. It also reduces the thickness of the steel plate.
In hot rolling, the steel is first preheated in a furnace in order to change the crystalline structure and to make it easier to roll. Then the steel is rolled by passing it between two rolls revolving at the same speed but in opposite directions.
Some types of steel are also cold rolled after hot rolling, mostly to make the steel thinner, to increase strength and to give the steel a bright and smooth surface. In cold rolling the steel is first cleaned with acid. It is then rolled at low temperatures using oils as a lubricant to reduce friction. After rolling, the steel can be coated with metals or paints in order to protect the steel surface or to give it special characteristics. Rolling is more extensively described in two books by Roberts [8; 9].

2.2 Detailed description of basic oxygen steelmaking

Basic oxygen steelmaking is an important process step in steelmaking, since it removes the majority of the unwanted elements and causes a large part of the necessary temperature increase. Both the process and the equipment used are described in more detail in this section.

2.2.1 Process description

The change in steel composition and steel temperature is achieved in a reactor called a converter shown in figure 2.4. The converter is operated in batch operation. During the batch, oxygen is blown onto the hot metal bath at supersonic speeds with an oxygen lance. Nitrogen and argon are blown through tuyeres in the bottom of the converter to improve converter mixing. The oxygen oxidizes elements within the bath. These oxidation reactions take place simultaneously or sequentially at a large number of sites including directly under the oxygen jet, at the interface between slag and bath and at the surface of iron droplets in the slag formed due to the force of the jet impact [2].
Two types of oxidation reactions can be distinguished. Direct oxidation occurs through the absorption of oxygen by the bath. This oxygen subsequently reacts with the other elements present.

$$\frac{1}{2}O_2 \rightarrow [O] \tag{2.2}$$

$$X + n[O] \rightarrow XO_n \tag{2.3}$$

In indirect oxidation, oxygen reacts with the iron in the bath and forms iron oxide. This iron oxide subsequently reacts with the elements within the bath.

$$Fe + \frac{1}{2}O_2 \rightarrow FeO \tag{2.4}$$

$$X + nFeO \rightarrow XO_n + nFe \tag{2.5}$$

The oxidation reactions are exothermic and increase the temperature of the metal bath. If nothing is done, the temperature of the metal bath would increase to more than the demanded temperature. Therefore at the start of the batch scrap is added to cool the metal bath.

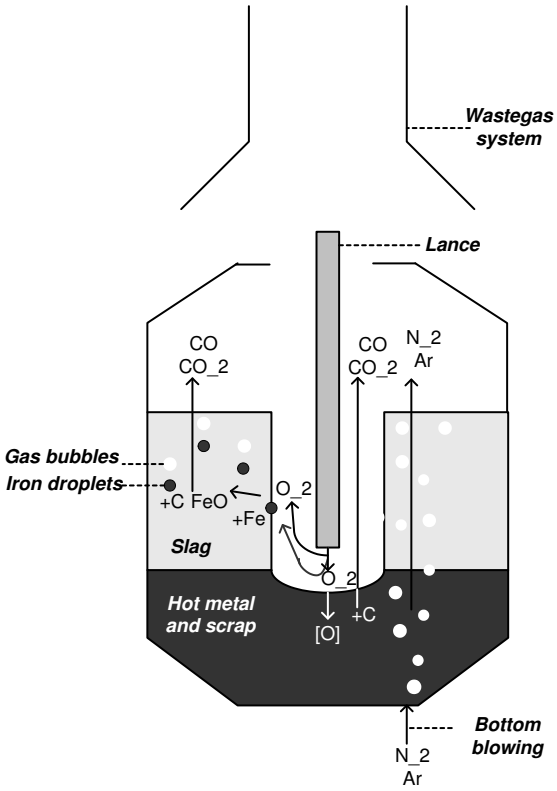

Figure 2.4: Schematic representation of converter.

The oxides formed through the oxidation reactions float to the top of the metal bath forming a slag layer. Additions are added at the beginning of the batch and during the batch in order to reduce wear of the refractory bricks lining the converter. An important property of the slag, that largely influences how much the slag erodes the converter lining, is the basicity (B).

$$B = \frac{W_{CaO}}{W_{SiO2}} \tag{2.6}$$

Where W_{CaO} and W_{SiO2} are the calcium oxide and silicium oxide content of the slag. The lower the basicity, the more the slag will erode the magnesium oxide bricks that line the converter. Furthermore, if not enough magnesium

oxide is present in the slag, magnesium oxide from the bricks will dissolve into the slag causing refractory wear.
The main additions used are dolomitic lime (consists of calcium oxide and magnesium oxide) and lime (consists of mainly calcium oxide). In some plants also slag (contains calcium oxide, magnesium oxide and silicium oxide) is used as an addition. Besides the reduction they cause in refractory wear, the additions also have a cooling effect. Sometimes also iron ore which introduces additional oxygen into the process is added during the batch as a cooling agent.
Carbon monoxide and carbon dioxide formed due to the oxidation of carbon leave the converter through the waste gas system. A part of the produced carbon monoxide and carbon dioxide flow directly adjacent to the oxygen lance, another part flows as bubbles through the slag. These bubbles in the slag cause the slag to foam. In some cases the volume of foam can become so large, that it is going over the edge of the converter. This undesirable effect is called slopping.

2.2.2 Measuring equipment

A few measuring devices are in general use in the more advanced steel plants. These measuring devices, shown in figure 2.5, include the sublance, the sonic meter or audiometer and equipment to measure waste gas flow, composition and temperature.

Sublance
The sublance is a long lance containing a cardboard probe which can take measurements at a desired point during the batch. The sublance probe is used to take a bath sample which is send to the laboratory for detailed analysis. The probe also contains a thermocouple with which the bath temperature can be measured. Often the probe also contains an indirect carbon concentration measurement.

Sonic meter
The sonic meter or audio meter is a microphone placed in the waste gas system which measures the sound coming from the converter. The sound spectrum is generally measured in a range between 5 and 1000 [Hz]. The sonic meter is generally used to gather information on the height of the foam layer [11; 12].

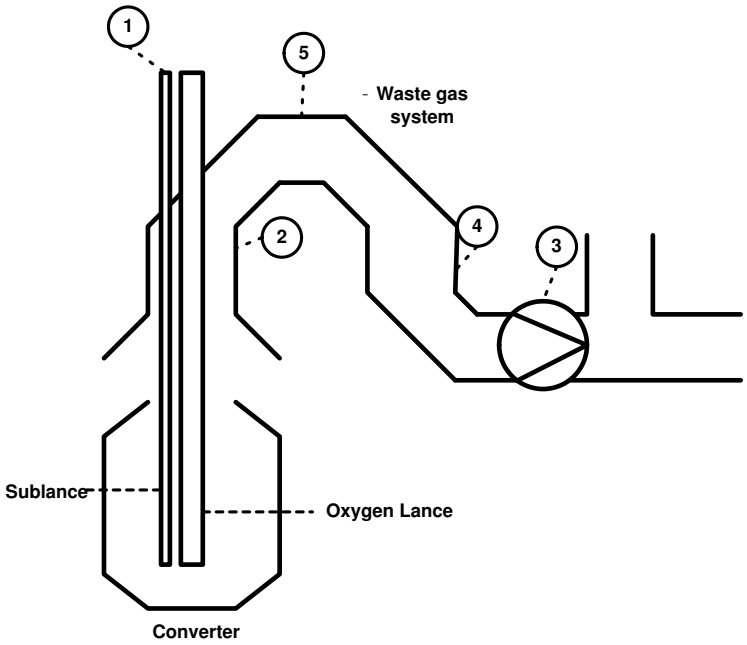

Figure 2.5: Measuring devices in primary steelmaking. 1. Sublance, 2. Sonic meter, 3. Waste gas flow, 4. Waste gas composition, 5. Waste gas temperature.

Waste gas flow, composition and temperature
In the waste gas system the waste gas flow, composition and temperature are usually measured. These measurements have been used to give information on the steel carbon concentration [13; 14], the accumulation of oxygen in the converter [11; 15] and the occurrence of slopping [13].

2.3 Steel plant of which data has been used

The data used in this thesis has been gathered at the OSF2 steel plant in IJmuiden, The Netherlands. In the OSF2 steel plant in IJmuiden, the annual production is nearly 7 million tons of liquid steel. Brockhoff et al. [16] give a short description of the equipment and the operating procedures of the OSF2. The hot metal coming from the blast furnace is treated in two desulpurisation

Table 2.2: Average batch in OSF2 IJmuiden, the Netherlands.

		OSF2
Hot metal	[tons]	275
Scrap	[tons]	71
Lime	[tons]	7.9
Dolomite	[tons]	4.4
Iron ore	[tons]	3.4
Slag	[tons]	3.7
Oxygen	$[nm^3]$	15300
Temperature HM	[C]	1395
C concentration HM	[w%]	4.4
Si concentration HM	[w%]	0.4
Mn concentration HM	[w%]	0.4
P concentration HM	[w%]	0.06
C concentration at end of batch	[w%]	0.05
Temperature at end of batch	[C]	1650

stations. The desulphurised hot metal is transported to three 325 ton converters. Normally all three converters are in operation (a three out of three practice). Only when one of the converters needs maintenance two out of three practice is used. The converter cycle time (time between the start of two subsequent batches) ranges from around 42 [min] in two out of three practice to 60 [min] in three out of three practice. The oxygen blowing rate in these converters is about 49500 $[\frac{nm3}{h}]$, causing typical batch times of around 20 minutes. In table 2.2 the raw material input data of an average batch is shown. The scrap used consists of a predefined mixture of several separate scrap types. The scrap types are defined based on the size and the composition of the scrap. Lime, dolomite, iron ore and slag are added at a certain addition rate following predefined addition schedules. Lance height, bottom blowing rate and oxygen blowing rate also follow predefined schedules and they are normally kept constant during the majority of the batch. Secondary steelmaking facilities consist of a ladle furnace, a vacuum degassing unit and two stirring stations.

Bibliography

[1] A.K. Biswas, Principles of blast furnace ironmaking, theory and practice, Cootha publishing house, Brisbane (1981)

[2] R. Boom, B. Deo, Fundamentals of steelmaking metallurgy, Prentice Hall International, Hemel Hempstead (1993)

[3] F. Oeters, Metallurgie der stahlherstellung, Springer-Verlag, Dusseldorf (1989)

[4] E.T. Turkdogan, Fundamentals of steelmaking, The institute of materials, London (1996)

[5] G. Stolte, Secondary metallurgy, Fundamentals processes applications, Verlag Stahleisen, Dusseldorf (2002)

[6] K. Schwerdtfeger, Metallurgie des stranggiessens, giessen und erstarren von stahl, Verlag Stahleisen, Dusseldorf (1992)

[7] W.R. Irving, Continuous casting of steel, The institute of materials, London (1993)

[8] W.L. Roberts, Cold rolling of steel, Manufacturing engineering and materials processing/2, Marcel Dekker Inc., New York (1978)

[9] W.L. Roberts, Hot rolling of steel, Manufacturing engineering and materials processing/10, Marcel Dekkers Inc., New York (1983)

[10] B. Snoeijer, P. Mink, A. Overbosch, M. Hartwig, H. ter Voort, J. P. Brockhoff, Improvement of converter processconsistency at BOS no. 2 Corus IJmuiden, In: *5th European oxygen steelmaking conference*, Aachen (2006), 186-193

[11] P. Nilles, R. Holper, Converter noise and off gas temperature measurements, tools for better BOF control, *C.R.M.*, **35**(1973), 23-32

[12] W. Birk, I. Arvanitidis, P. Jonsson, A. Medvedev, Physical modelling and control of dynamic foaming in LD-converter process, *IEEE transactions on industry applications*, **37**(2001), 1067-1073

[13] H. Zhi-gang, L. Liu, H. Ping, T. Mix-xiang, A dynamic off-gas model on a 150t BOF, *Steel times international*, April/May(2003), 11-16

[14] J.A. Glasgow, W.F. Porter, Development and operation of BOF dynamic control, *Journal of metals*, August(1967), 81-87

[15] W. Dorr, W. Lanzer, E. Weiler, H. Trenkler, Aussagefahigkeit der abgasmessung zur kenzeichnung des schlackenzustandes beim LD-verfahren, *Stahl und eisen*, **93**(1974), 876-884

[16] J. Brockhoff, P.G.J. Broersen, M. Hartwig, H.P. Pronk, H. ter Voort, R. Mostert, A.B. Snoeijer, A. Overbosch, Towards 7 million tons of liquid steel per year at BOS2 Strip IJmuiden, In: *5th European oxygen steelmaking conference*, Aachen (2006), 417-424

3

Feasibility of continuous measurements

It would be valuable if important process variables such as the steel composition, the slag composition, the steel temperature and the foam height could be measured continuously during the batch. This would greatly aid the creation and validation of dynamic process models and the development of a control strategy. However, the measurement of these variables is, in most cases, currently not feasible due to the high temperatures and the dusty environment involved and the lack of available reference measurements.
It is therefore suggested that dynamic process models can best be validated using the measured decarburization rate and accumulation rate of oxygen.

3.1 Introduction

In basic oxygen steelmaking static models ensure that demands for temperature and composition are met at the end of the batch [1]. However, variations in raw material quality and errors in raw material weighing limit the accuracy of these static models. If the steel and slag composition and the steel temperature could be measured continuously, deviations from target could be spotted at an early stage and could be corrected. Furthermore, static models do not predict and can thus not prevent slopping, which causes large problems in converter operation. It would therefore also be valuable if the foam height

could be measured continuously.
In this chapter the feasibility of the continuous measurement of the bath composition, slag composition, bath temperature and foam height is investigated.

3.2 Steel composition

Some research has been directed towards the direct continuous measurement of the steel composition [2; 3; 4]. Although these direct measurements seem very promising they have so far not successfully been applied in basic oxygen steelmaking or are only applicable during a limited part of the batch.
Other measurements of the steel composition are based on the decarburization rate. The decarburization rate $\frac{dC}{dt}$ can be calculated from the measured waste gas composition and flow.

$$\frac{dC}{dt} = \frac{\phi_{wg}(WG_{CO} + WG_{CO2})}{V_M} \tag{3.1}$$

In which V_M is the molar volume, ϕ_{wg} is the waste gas flow, WG_{CO} and WG_{CO2} are the volume fraction of carbon mono oxide and carbon dioxide in waste gas.
In figure 3.1 the measured decarburization rate of a typical batch is shown. There is a large delay between the moment when process conditions in the

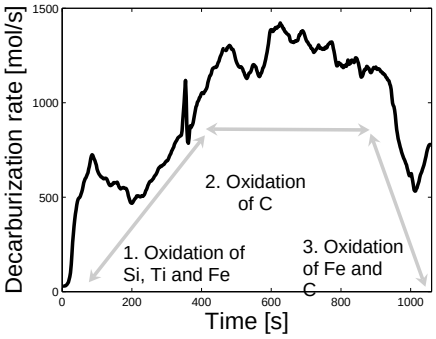

Figure 3.1: The decarburization rate of a typical batch.

converter change and the time the change is measured with waste gas equip-

ment. Therefore some researchers have focussed on reducing the delay time by finding a correlation between the decarburization rate and other measurements such as waste gas temperature and converter weight [5; 6; 7].

3.2.1 Carbon balance

An often reported inferential carbon concentration measurement uses a carbon balance in which the carbon leaving the bath is subtracted from the initial carbon concent [8; 9].

$$C(t) = C_0 - \int_0^t (\frac{dC}{dt} dt) \tag{3.2}$$

In which C_0 is the initial carbon content of bath and $C(t)$ is the carbon content in the bath. Unfortunately a large error in the calculated carbon concentration is introduced due to the inaccurate determination of the initial carbon concentration of the bath.

3.2.2 Carbon relationship

The second of the reported inferential carbon concentration measurements is based on a relationship between the final carbon concentration and the rate of carbon removal [8; 9; 10]. This method is only applicable at the end of the batch, where the low carbon concentration becomes a limiting factor for the decarburization rate. Disturbances introduced by, amongst others, the sublance measurement, converter additions and lance height and skirt movements influence the relationship between the carbon concentration and the decarburization rate [1]. Generally these disturbances do occur and therefore this carbon concentration measurement is not feasible.

3.3 Slag composition

The accumulation rate of oxygen inside the converter has been used as an indication of the slag composition [11]. The accumulation of oxygen $\frac{dO}{dt}$ can be described with an oxygen balance.

$$\frac{dO}{dt} = \frac{dO_{lance}}{dt} + \frac{dO_{additions}}{dt} - (\frac{dO_{wastegas}}{dt} - \frac{dO_{air}}{dt}) \tag{3.3}$$

Where $\frac{dO_{lance}}{dt}$ is the oxygen delivered through the lance, $\frac{dO_{additions}}{dt}$ is the oxygen delivered through additions, $\frac{dO_{wastegas}}{dt}$ is the oxygen leaving in waste gasses and $\frac{dO_{air}}{dt}$ is the oxygen entering the waste gas system through the inlet of air at the gap between the converter and the skirt.
In figure 3.2 the accumulation rate of oxygen of a typical batch is shown.

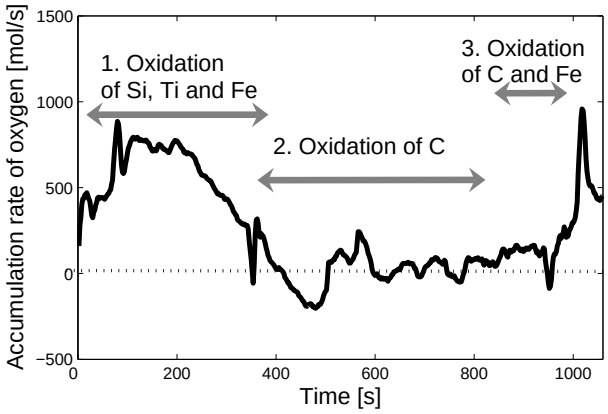

Figure 3.2: The accumulation of oxygen in the converter.

To calculate the composition of the slag from the total amount of accumulated oxygen in the converter Dorr et al. [11] made assumptions about the dissolution rate of additions. They also assumed an average pattern for the oxidation rate of silicon, manganese and phosphorous. Based on these assumption they calculated the oxygen that is used to form iron oxide O_{Fe}.

$$O_{Fe} = \int_0^t \frac{dO}{dt} dt - (O_{Si} + O_{Mn} + O_P) \tag{3.4}$$

Where O_{Si}, O_{Mn} and O_P is the amount of oxygen binding with silicium, manganese and phosphorous respectively. The authors concluded that the measuring errors in waste gas flow and waste gas composition in addition to the assumptions made, cause a large error in the calculated slag composition, which renders this slag composition measurement infeasible.

3.4 Steel temperature

Several direct temperature measurements have been presented in the literature [12; 13; 14; 15; 16; 17; 18]. Some were conducted through the oxygen lance [12; 13; 14] and only give a reliable temperature measurement after the batch has ended. Others were conducted through bottom tuyeres [15; 16; 17] or through the converter wall [18]. These have either (so far) not been applied to basic oxygen steelmaking, or they encountered operational problems, that still have to be solved, such as clogging of the tuyeres. The direct continuous measurement of temperature is therefore currently not feasible.
Some inferential temperature measurements have also been proposed [19; 20; 21] and will be discussed in this section. A special test was performed to provide references. In this test, for three batches, the temperature was measured multiple times during the batch using adapted drop-in sensors.

3.4.1 Energy balance of the converter

In the literature a dynamic energy balance of the converter is often used for calculation of the bath temperature during the batch [19; 20].

$$\frac{dQ_{steel}}{dt} = \frac{dQ_{reactionsconverter}}{dt} - \frac{dQ_{scrap}}{dt} - \frac{dQ_{additions}}{dt} - \frac{dQ_{slag}}{dt} - \frac{dQ_{heatloss}}{dt} \tag{3.5}$$

Where $\frac{dQ_{steel}}{dt}$ is the change in energy of the steel, $\frac{dQ_{scrap}}{dt}$ is the change in energy of the scrap, $\frac{dQ_{reactionsconverter}}{dt}$ is the change in energy due to reactions, $\frac{dQ_{additions}}{dt}$ is the change in energy due to additions, $\frac{dQ_{slag}}{dt}$ is the energy consumed by the slag and $\frac{dQ_{heatloss}}{dt}$ is the change in energy due to heatloss.
The main difficulty is that some processes, that highly influence the bath temperature, are complex. For instance, the melting of scrap depends on many factors, such as the size distribution and shape of the scrap, the bath temperature and the mixing of the bath [19; 22] and the dissolution of lime is influenced by the formation of a dicalcium silicate layer around the lime pellets [23; 24; 25]. With the small number of reference measurements available, these processes and their influence on the steel temperature can not be modeled accurately. Therefore, with the small number of reference measurements available, a temperature measurement based on an energy balance of the converter is not feasible.

3.4.2 Energy balance of the waste gas system

An alternative inferential temperature measurement is based on an energy balance of the waste gas system as is shown in figure 3.3 [21]. Steam from

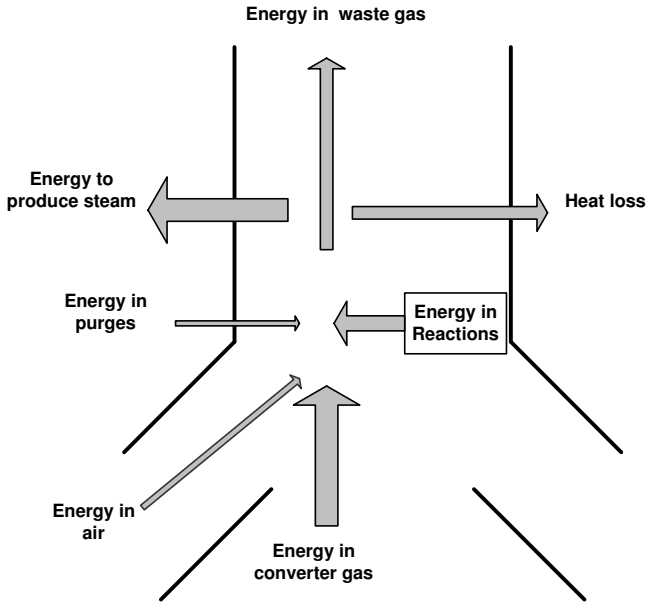

Figure 3.3: Energy balance of waste gas system.

purges and the oxygen from the air react with carbon monoxide from the converter gas generating heat. The waste gas cools down due to heat loss and due to the production of steam. Using room temperature as a reference and assuming that the energy contained in purges is negligible, the energy balance of the waste gas system can be described as:

$$\begin{aligned} \frac{dQ_{wastegassystem}}{dt} &= \frac{Q_{convertergas}}{dt} + \frac{dQ_{reactionswastegas}}{dt} \\ &\quad - \frac{dQ_{steam}}{dt} - \frac{Q_{heatloss}}{dt} - \frac{dQ_{wastegas}}{dt} \end{aligned} \tag{3.6}$$

Where $\frac{dQ_{wastegassystem}}{dt}$ is the energy which accumulates in the waste gas system, $\frac{dQ_{wastegas}}{dt}$ is the energy leaving waste gas system in the waste gasses,

$\frac{dQ_{convertergas}}{dt}$ is the energy entering the waste gas system from the converter gas, $\frac{dQ_{reactionswastegas}}{dt}$ is the energy released by reactions, $\frac{dQ_{steam}}{dt}$ is the energy used for steam production and $\frac{dQ_{heatloss}}{dt}$ is the energy lost to environment.
Since steam pressure, flow and temperature and waste gas composition, flow and temperature are measured, the energy contained in the steam and waste gas can easily be calculated. Using mass and component balances of the waste gas system, the amount of reaction that takes place and therefore the energy produced by reactions can also be calculated. To calculate the bath temperature, the accumulation of energy in the waste gas system, the difference between bath and converter gas temperature and the heat loss have to be modeled. With the small number of reference measurements available, this can not be done accurately and therefore a temperature measurement based on an energy balance of the waste gas system is not feasible.

3.4.3 Linear approximation

The last inferential temperature measurement that will be discussed is based on the assumption, that the temperature of the bath is (partly) self regulating as shown in figure 3.4. A higher temperature increases the dissolution rate of additions and the melting rate of scrap. The higher dissolution and melting rates will cool the bath and cause a smaller increase in temperature. Based on the approximation of a self regulating temperature, with a constant oxygen blowing rate a linear temperature profile can be assumed.

$$\frac{dT}{dt} = a_T VO2 \tag{3.7}$$

Where T is the steel temperature, a_T is the regression coefficient and $VO2$ is the oxygen blowing rate. Due to the charging of scrap the temperature drops significantly at the start of the batch. The initial condition for calculating the steel temperature during the batch is therefore:

$$T_0 = T_{hm} - \Delta T \tag{3.8}$$

Where T_0 is the initial steel temperature, T_{hm} is the measured hot metal temperature and ΔT is the bath temperature drop due to charging of scrap.
The coefficient a_T in equation 7.1 is chosen in such a way, that the modeled temperature at the end of the batch corresponds to the estimated temperature

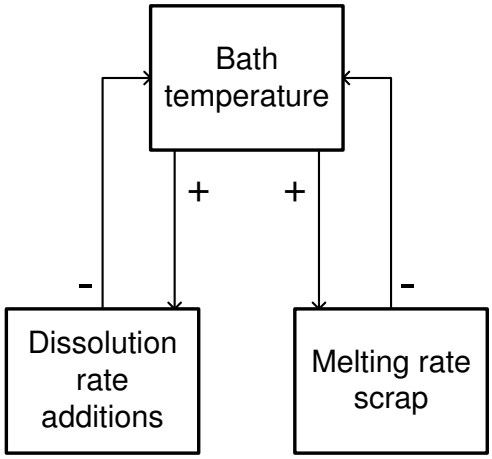

Figure 3.4: Self regulating mechanism of temperature.

at the end of the batch as calculated using a static process model [1]. The temperature drop can be estimated by minimizing the difference between the estimated and measured temperature of the reference batches. In figure 3.5 the estimated temperature of the three reference batches is shown.

3.5 Foam height

The direct foam height measurement reported in the literature is based on radio wave interferometry [26]. Its successful application is (so far) limited by operational problems such as skulling (adherence of molten steel to a cooled surface).
A number of inferential foam height measurements have been proposed [5; 21; 27; 28] and will be discussed in this section. The foam height is only known when slopping becomes visible at the converter mouth. Only the instances of slopping can be used as a reference.

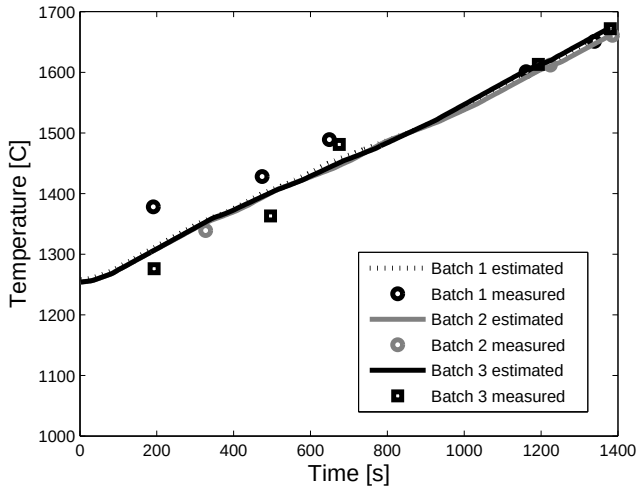

Figure 3.5: Estimated temperature during the batch for the three batches in which the temperature was measured multiple times.

3.5.1 Intensity of noise

Many researchers have used the relationship between the intensity of the noise measured by the sonic meter and the foam height to infer the foam height [5; 27; 28].

$$h = \frac{ln(\Phi_0) - ln(\Phi)}{\beta} \tag{3.9}$$

Where h is the foam height, Φ_0 is the magnitude of the sound spectrum of the noise produced in the converter, Φ is the magnitude of the sound spectrum measured by the sonic meter and β is the attenuation coefficient. The attenuation coefficient is frequency dependent.

There are, however, some factors that complicate the use of this measuring method. The source of the noise, for instance, is not known, but it is generally believed to be noise emitted by the oxygen jet itself, by the eddies generated at the impingement of the oxygen jet on the steel bath, by gas evolution and by CO combustion [5]. Different factors such as the oxygen blowing rate and the lance height affect these sources and thus the sound spectrum of the noise produced. Moreover, the degree of attenuation depends not only on the height of

the foam layer but also on the physical properties of the foam. Moxon et al.[29] report that for aqueous foams the attenuation of sound in a foam depends on the liquid content of the foam, the viscosity of the liquid, the bubble size and the foams particle loading, which all change during the batch. With the limited number of reference measurements, the effects of changes in the source of the noise and changes in the attenuation properties of the slag can not accurately be modeled. This foam height measurements is therefore infeasible.

3.5.2 Resonance in the noise

Nilles et al. mention that the noise originating from the converter is modified by the resonance properties of the empty parts of the vessel [5]. Since the modification depends on the size and shape of the empty parts of the vessel, the resonance frequencies can be used for the inferential measurement of the foam height. The converter is connected to the open air through a gap between the converter and the waste gas system. At a little distance from the sonic meter the waste gas system bends. A helpful analogy for the converter is a flute with one hole and a bend as is shown in figure 3.6. Benade [30] has shown, that -for flutes- some frequencies are reflected at open tone holes. Rostafinski [31] has shown, that curved ducts also reflect some frequencies. The resonance frequency depends on the length of the tube in which resonance can occur as well as the sound velocity.

$$f_{resonance} = \frac{nv}{4L} \tag{3.10}$$

Where n = 1, 2, 3 .. and in which $f_{resonance}$ is the resonance frequency, v is the sound velocity (typically 820 $[\frac{m}{s}]$ for CO gas of 1600 [K]) and L is the length of tube.
Just before slopping the height of the empty part of the converter suddenly changes and therefore at that moment a change in resonance frequency should also be observed. Since flutes and converters are no more than an useful analogy, it is not known which frequencies are reflected at the gap and at the bend. If however, most of the sound is reflected at the gap, the height of the empty part of the column is small and will suddenly approach zero and the resonance frequency will rapidly increase from >500 [Hz] until it suddenly disappears during slopping. On the other hand if the sound is not reflected at the gap, the height of the empty column is very large and the resonance frequency should be in the range of 20 [Hz] or even lower and it should increase

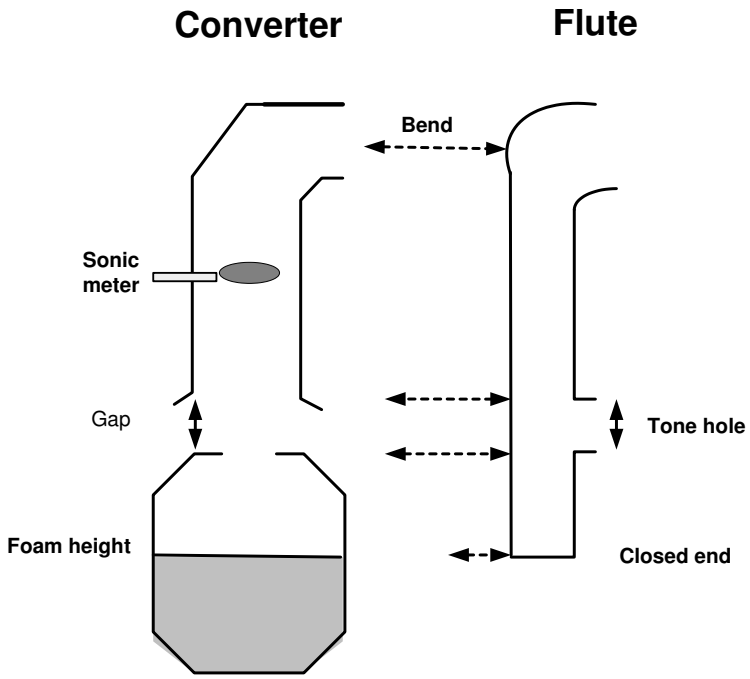

Figure 3.6: Analogy of a flute and a converter.

slightly due to slopping.
In the high frequency range (>500 [Hz]) only random noise is recorded and the microphone used cannot accurately record sound in the low frequency range (<20 [Hz]). Therefore, the inferential measurement of the foam height based on resonance frequencies is not feasible.

3.5.3 Heat absorption by the oxygen lance

It has been suggested, that the foam height can be inferred from the measured increase in temperature of the cooling water of the oxygen lance [21]. The heat flow to the oxygen lance depends, amongst others, on the foam height. Many

heat transfer processes, such as radiance from the steel bath, the slag and the converter wall, convection in the converter and convection in the waste gas system occur simultaneously. With the limited number of reference measurements these processes can not be modeled accurately. The increase in temperature of the cooling water of the oxygen lance can therefore not be used as an indirect measurement of the foam height.

3.6 Conclusions

The feasibility of the continuous measurement of process variables such as the steel composition, the slag composition, the steel temperature and the foam height is greatly hampered by the high temperatures and dusty environment involved on one hand and by the lack of reference measurements on the other. The high temperature and dusty environment have greatly complicated the application of direct measurements. The harsh conditions cause early breakdown of measuring equipment, making these measuring methods unusable for multiple batches. The lack of reference measurements limit the amount of relationships that can be modeled in indirect measurements. This causes most indirect measurements to be infeasible.
Many authors have attempted to develop dynamic process models [20; 32]. To verify these dynamic models some continuous reference measurements have to be available. The steel temperature can be approximated using the assumption that the steel temperature increases linearly with the amount of oxygen blown. The continuous measurement of the steel and slag composition is infeasible and can therefore not be used for validation of dynamic models. Although the decarburization rate and the accumulation rate of oxygen do not give information about the compositions themselves, they do contain information about the change in composition. The decarburization rate and the accumulation rate of oxygen inside the converter are therefore useful for validation of a dynamic process model.

Bibliography

[1] A.B. Snoeijer, A. Overbosch, M. Hartwig, H. ter Voort, J.P. Brockhoff, Improvement of converter process consistency at BOS no. 2, Corus IJmuiden, In: *5th european steelmaking conference*, Aachen (2006), 186-193

[2] N. Ramaseder, J. Gruber, J. Heitz, D. Baeuerle, W. Meyer, J. Hochoertler, VAI-CON Chem a new continuous chemical analysis system of liquid steel in metallurgical vessels, *Metallurgica Italiana*, **96**(2004), 60-63

[3] N. Ramaseder, J. Gruber, J. Heitz, D. Baueuerle, W. Meyer, J. Hochoertler, The continuous chemical analysis of liquid steel in metallurgical vessels with VAI-CON Chem system, *Revue de metallurgie-CIT*, **June**(2002), 509-516

[4] A. Sharan, Light sensors for BOF carbon control, In: *1998 steelmaking conference*, Toronto (1998), 337 - 345

[5] P. Nilles, R. Holper, Converter noise and off gas temperature measurements, tools for better BOF control, *C.R.M*, **35**(1973), 23-32

[6] H. Voll, D. Ramelot, Fast determination of decarburization rate by fumes temperature measurement, *C.R.M.*, **33**(1972), 11-19

[7] W. Grenfell, D.J. Bowen, BOF blow control by furnace weight, *Journal of metals*, **July**(1974), 17-24

[8] H. Zhi-gang, L. Liu, H. Ping, T. Mix-xiang, A dynamical off-gas model on a 150t BOF, *Steel times international*, **April/ May**(2003), 11-16

[9] J.A. Glasgow, W.F. Porter, Development and operation of BOF dynamic control, *Journal of metals*, **August**(1967), 81-87

[10] W. Dorr, W. Lanzer, E. Weiler, H. Trenkler, Aussagefahigkeit der abgasmessungen am LD-converter fur die processfuhrung, *Stahl und eisen*, **94**(1974), 381-386

[11] W. Dorr, W. Lanzer, Aussagefahigkeit der abgasmessung zur kenzeignung des schlackenzustandes beim LD-verfahren, *Stahl und eisen*, **93**(1973), 876-884

[12] S.T. Jensen, M.P. Bonin, W. Federoff, N. Rymarchyk, T. Smith, Lance-based sensing and vision systems, *Iron and steel technology*, **January**(2004), 69-73

[13] A. Fuchs, M.P. Bonin, S. Jensen, J. Sackos, D. Goldstein, N. Rymarchyk, D.R. Hardesty, New optical sensor for improved BOF control: lance based

temperature and laser distance measurement, *Iron and steel engineer*, **July**(1998), 25-31

[14] E. Fuchs, D. Hardesty, M. Bonin, J. Stackos, C. Smith, D. Goldstein, N. Rymarchyk, A new optical sensor for BOF lance-based temperature and range/contour measurement, In: *1998 steelmaking conference*, Toronto (1998), 359-367

[15] T. Lamp, H. Kochner, H. Lachmund, Y. Xie, D. Steyls, J. Borlee, L. Sancho, Innovative continuous online determination of steel melt temperature by direct optical measurement in the melt, In: *European commision technical steel research*, EUR 21428 EN 2005

[16] M. Pillwax, M. Hiebler, P. Juza, J. Steins, N. Ramaseder, VAI-ConCept a performance package for AOD converters, *AISE steel technology*, **September**(2003), 93-99

[17] M. Sugiura, R. Nakato, S. Nagata, E. Tsubota, T. Yamazaki, T. Tanaka, H. Kumazawa, W. Nagai, Development of new technique for continuous molten steel temperature measurement, *Nippon steel technical report*, **89**(2004), 23-27

[18] M. Burton, R.J.B. Turpin, The continuous metal temperature measurement of the LD/AC bath, In: *70th steelmaking conference*, Scarborough (1968), 70-76

[19] H.W. den Hartog, P.J. Kreijger, A.B. Snoeijer, Dynamic model of the dissolution of scrap in the BOF process, *C.R.M.*, **37**(1973), 13-22

[20] C. Chigwedu, J. Kempken, W. Pluschkell, A new approach for the dynamic process simulation of the BOF process, In: *5th European oxygen steelmaking conference*, Aachen (2006), 363-371

[21] A. Pons, Development of theoretical models for indirect measurements in basic oxygen steelmaking, master thesis University of Twente August 2006

[22] S. Asai, I. Muchi, Effect of scrap melting on the process variables in LD converter caused by the change of operating conditions, *Transactions ISIJ*, **11**(1971), 107-115

[23] B. Deo, P.K. Gupta, M. Malathi, P. Koopmans, A. Overbosch, R. Boom, Theoretical and practical aspects of dissolution of lime in laboratory experiments and in BOF, In: *5th European oxygen steelmaking conference*, Aachen (2006), 202-209

[24] F. Oeters, R. Scheel, Untersuchungen zur kalkauflosung in CaO-FeO-SiO2-schlacken, *Arch. eisenhuttenwes.*, **45**(1974), 575-580

[25] G. Konig, H. Rellenmeyer, K.H. Obst, Vorgange bei der auflosung von hart und weichbrandkalk in schlacken aus dem sauerstoffaufblas-konvertor, *Stahl und eisen*, **87**(1967), 1071-1077

[26] M.S. Millman, L. Baath, D. Malmberg, E. Price, Radiowave interferometry for BOS slag control, In: *Second international congress on the science and technology of steelmaking*, Swansea (2001), 309-320

[27] W. Birk, I. Arvanitidis, P. Jonsson, A. Medvedev, Physical modelling and control of dynamic foaming in LD-converter process, *IEEE transactions on industry applications*, **37**(2001), 1067-1073

[28] W. Birk, A. Medvedev, Foam level control in a water model of the LD converter process, *Control Engineering Practice*, **11**(2003), 49-56

[29] N.T. Moxon, A.C. Torrance, S.B. Richardson, The attenuation of acoustic signals by aqueous and particulate foams, *Applied acoustics*, **24**(1988), 193-209

[30] A.H. Benade, Fundamentals of musical accoustics, Oxford university press, New York, London (1976)

[31] W. Rostafinski, Transmission of wave energy in curved ducts, *Journal of the accoustic society of america*, **56**(1974), 1005-1007

[32] E. Graveland-Gisolf, P. Mink, A. Overbosch, R. Boom, G. de Gendt, B. Deo, Slag-droplet model: A dynamic tool to simulate and optimize the refining conditions in BOF, *Steel research international*, **74**(2003), 125-130

4

Slop detection using a camera

In basic oxygen steelmaking, foam overflow or slopping causes operational and environmental problems. It would be valuable to know when slopping occurs especially for modeling and control of the process. However, in the previous chapter it is shown, that the continuous measurement of the foam height is currently infeasible. Furthermore, in most steel plants slopping is neither detected nor recorded. In this chapter a slop detection algorithm is presented, which is based on images taken by a camera viewing the converter mouth. The proposed algorithm has a sensitivity and specificity of 0.74 and 0.94 respectively, is relatively simple and can easily be used in on-line applications. When using this algorithm, slopping is quickly detected and can be halted for the majority of slopping batches.

4.1 Introduction

Foam overflow, also called slopping, causes operational and environmental problems in basic oxygen steelmaking. Many different definitions of slopping exist. In this chapter slopping is defined as "the continuous overflow of material over the edge of the converter". The detection of the occurrence of slopping using a slop detection system is one of the ways by which slopping can be prevented. There are certain requirements a slop detection system should meet. A slop detection system should be accurate; it should predict slopping when it occurs and it should not be detected when nothing occurs. The slop detection

system should be able to work on-line if it is applied in a slop alarm or in an automatic slop repression system.
Slop detection is a type of binary classification [1]. In binary classification members of a set of objects are classified into two groups based on whether they have a certain property or not. This is often represented in a truth table as is shown in table 4.1. In the columns the classifying property is shown. In this

Table 4.1: Truth table

	True (slopping)	False (non-slopping)
Positive (detected)	True Positive (TP)	False Positive (FP)
Negative (not detected)	False Negative (FN)	True Negative (TN)

case the classifying property is slopping. The column marked True indicates the slopping batches and the column marked False indicates the non-slopping batches. In the rows the observation is shown. In this case the observation is the result of the slop detection system. Positive means, that slopping is detected, negative means, that slopping is not detected. In table 4.1 the upper left cell marked True Positive (TP) thus stands for the number of slopping batches that are correctly detected as slopping and the lower left cell marked False Negative (FN) stands for the number of slopping batches that are not detected. Together the True Positive cell and the False Negative cell contain all the slopping batches. The lower right cell marked True Negative (TN) is the number of non-slopping batches that are correctly detected and the upper right cell marked False Positive (FP) are the number of non-slopping batches that are detected as slopping. Together the True Negative cell and the False Positive cell contain all the batches that do not slop. To measure the performance of binary classification the concepts sensitivity and specificity are often used [1].

$$\text{Sensitivity} = \frac{\text{TP}}{\text{TP} + \text{FN}} \tag{4.1}$$

$$\text{Specificity} = \frac{\text{TN}}{\text{TN} + \text{FP}} \tag{4.2}$$

The sensitivity represents the proportion of slopping batches that is correctly recognized, while the specificity represents the proportion of non-slopping batches that is correctly recognized. Combined the sensitivity and the specificity are a

measure of the accuracy of the slop detection system. Other interesting properties that can also be calculated using the truth table are the proportion of slopping occurrences and the proportion of False Positives (false alarms).

$$\text{Proportion of slopping occurrences} = \frac{\text{TP} + \text{FN}}{\text{TP} + \text{FN} + \text{TN} + \text{FP}} \tag{4.3}$$

$$\text{Proportion of False Positives} = \frac{\text{FP}}{\text{TP} + \text{FP}} \tag{4.4}$$

Much research has focussed on the detection of slopping using measurements such as a sonic meter [2; 3; 4], vibrations of the oxygen lance or the converter [4; 5; 6; 7], waste gas measurements [8; 9; 10] and waste gas temperature [11; 12]. In these slop detection algorithms slopping is either detected when a certain boundary value is crossed or if the measured pattern deviates too much from the 'average' or 'expected' pattern. Unfortunately, the interdependency between these measurements and the foam height is influenced by changing and unmeasured variables such as the physical properties of the slag. Therefore, the accuracy of these algorithms is often limited.
Alternatively, slopping can also be detected using direct observations with, for instance, a camera. Some authors have developed a slop detection algorithm based on images from camera's viewing the tap-hole [13; 14; 15]. The position of these cameras may present some problems in maintenance. In this chapter a slop detection algorithm is presented, which is based on camera images taken with a camera viewing the converter mouth. The distance of the camera from the converter is more than ten meters. Due to the distance of the camera from the tap hole the required maintenance is minimal.
Gonzales and Woods [16] describe the different steps needed in digital image processing. First images have to be acquired. Then the prior knowledge gained by observing the acquired images has to be described in the knowledge base. Finally the detection algorithm can be constructed based on the knowledge base.
In the first two sections image acquisition and the knowledge base are discussed. In the third section a slop detection algorithm for separate images is developed. In the following section this algorithm is extended for movies. In the last two sections the results are discussed and compared to the literature and the conclusions are summarized.

4.2 Image acquisition

In figure 4.1 the experimental set-up is shown. A Basler A602 FC CMOS

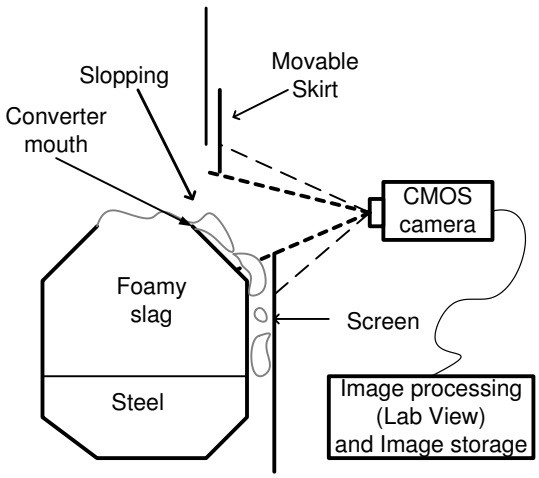

Figure 4.1: Experimental set-up.

camera is aimed at the gap between the lower part of the skirt and the upper part of a protective screen. From this position the camera has a clear view of the converter mouth. The position of the protective screen and the converter mouth are fixed, but the skirt height can vary. In the acquired image, shown in figure 4.2, part of the protective screen and part of the skirt are visible. The images are acquired and recorded at a rate of 2,5 frames per second with software designed in LabVIEW, using a shutterspeed of 5[ms] and a resolution of 480x640. During a plant trial the images of 230 batches were recorded.

4.3 Knowledge base

Images can consist of several different colored parts. In figure 4.2 for instance the majority of the colored part of the image can be seen under the line named "converter mouth". Unattached from this part also small red dots are present which are barely visible. These separate parts are called objects in this chapter. From observations it is known that images recorded by the camera can be

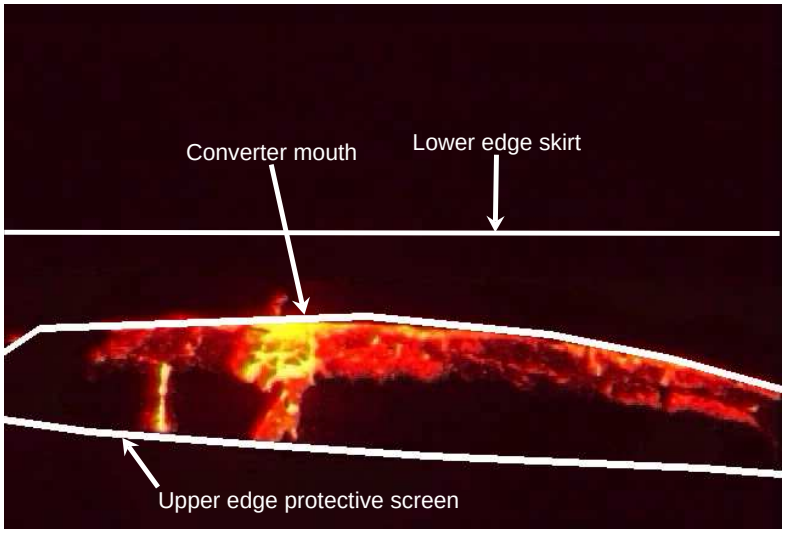

Figure 4.2: Example image (slopping).

subdivided in three distinct categories, namely inactive, fiery and slopping images. These images can be disturbed by phenomena such as over-exposure (large oval red objects, which are visible in several subsequent images in a movie) or sparks (small orange dots which are only visible during a limited time).
In inactive images hardly any converter activity can be seen. These images typically occur at the beginning and the end of the batch. Inactive images have thin horizontally positioned yellow and orange objects placed just above the converter mouth, which are visible in several subsequent images.
In fiery images quickly changing flame patterns can be seen. These images typically occur during the middle of the batch. Fiery images have yellow and orange objects which can take any shape and size, but which are usually large. These objects can be visible throughout the entire image, also in front of the protective screen and the skirt. Flames can appear suddenly and be visible in only a few subsequent images, or flames can be visible for a while in several

subsequent images in a movie.
In slopping images it can be seen, that part of the slag is dripping or pouring over the edge of the converter. These images can typically be seen during the middle of the batch (of which the majority occur around one third of the batch time). Slopping images have yellow and orange objects positioned vertically just above the protective screen. These objects are usually visible in several subsequent images in a movie.

4.4 Slop detection algorithm for separate images

In the knowledge base, described in the previous section, there are some differences in the description of the color, size and position of objects in an image. These differences can be used to attribute the images to the different categories and to remove disturbing phenomena from the image.
In the knowledge base most categories are described to have a yellow or orange color. Only over-exposures are described as red. Whether this color information can be used as a distinguishing property can be investigated by comparing the hue, saturation and intensity of samples of different images in the HSI (Hue Saturation Intensity) color space or by comparing red, green and blue values in the RGB (Red Green Blue) color space. Over-exposures have distinctly different blue color values. Typical histograms of the blue color plane of slopping images and overexposures are shown in figure 4.3.
In the knowledge base sparks are the only objects that are described as being small. Sparks can therefore clearly be distinguished from the other image objects by their size.
In the knowledge base it is described, that only slopping and fiery images can have objects with a position just above the upper edge of the protective screen. It is also described that while slopping images hardly ever have objects above the converter mouth, fiery images often have objects that can be visible in the entire image and thus also above the converter mouth. Therefore, if objects are visible just above the protective screen but not high above the converter mouth, the image is most likely a slopping image.
Properties such as the different blue color value for overexposed images, the different size of sparks and the different position of objects in slopping images, can be used to construct a slop detection algorithm, as shown in figure 4.4. If the image is thresholded in the blue image plane, a black and white image is

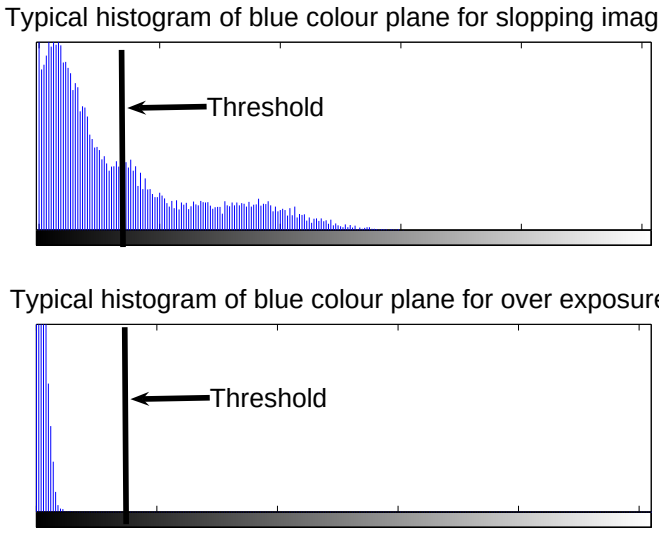

Figure 4.3: Typical histogram of blue image plane of a slopping image and an over-exposed image.

created from which over-exposures are removed. If then small objects are omitted, sparks are also removed from the black and white image. The position of the white objects can be used to detect the slopping images. In the proposed algorithm two parameters can be adjusted, namely the value of the threshold and the maximum size of the objects that are excluded. The calculation of sensitivity and specificity are based on a test set of 840 non-slopping and 1040 slopping images. In figure 4.5 the sensitivity and the specificity are shown for a range of thresholds and excluded sizes. The threshold and excluded sizes are represented by a relative value defined as the threshold divided by the finally selected threshold and the excluded size divided by the finally selected excluded size. The threshold and the excluded size were selected in such a way that that the algorithm has both a high sensitivity and a high specificity. At the finally selected threshold (represented by 1 in figure 4.5a) the sensitivity is 0.72. With a threshold twice as large (represented by 2 in figure 4.5a) the sensitivity is only 0.5. The value of the finally selected threshold and the finally selected excluded size was chosen in such a way that the specificity of the slop detection

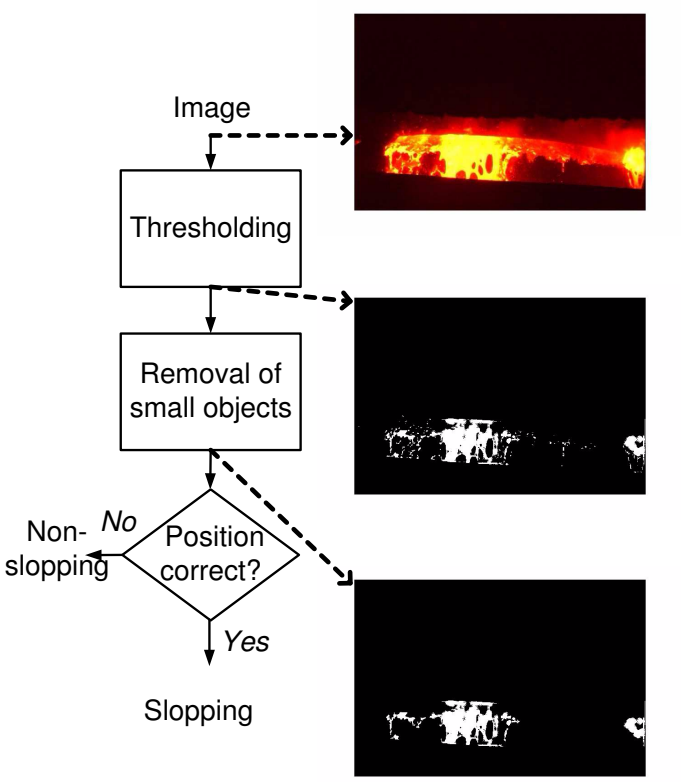

Figure 4.4: Slop detection algorithm.

system is high. The sensitivity and the specificity on separate images for the finally selected threshold and excluded size is 0.72 and 0.97 respectively. The result of application of the algorithm for separate images is shown in table 4.2. In this table the column marked True contains all the 1040 slopping images. Of the 1040 slopping images 749 were detected as slopping and and 291 were detected as non-slopping. The column marked False contains all the 840 non-slopping images. Of the 840 non-slopping images 25 were detected as slopping and 815 were detected as non-slopping.

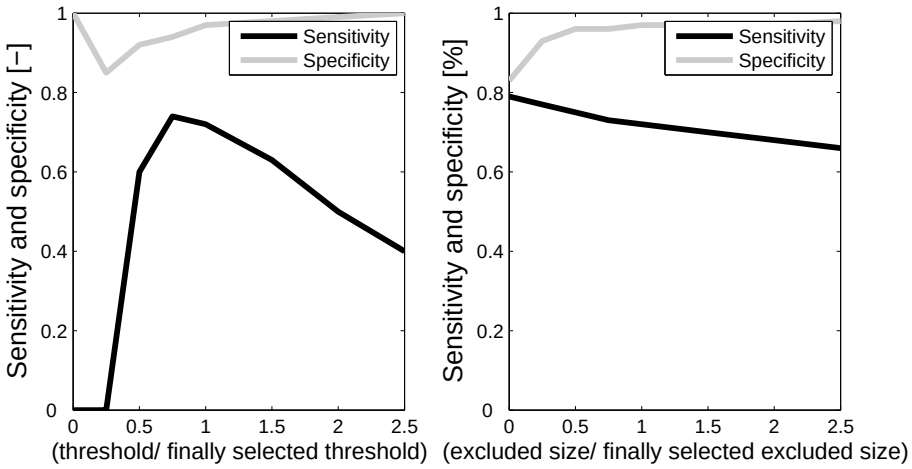

Figure 4.5: Sensitivity and specificity of the algorithm for different thresholds and excluded sizes.

Table 4.2: Results of slop detection algorithm for separate images.

	True (slopping)	False (non-slopping)
Positive (slopping detected)	749	25
Negative (slopping not detected)	291	815

4.5 Extension of algorithm for movies

In the knowledge base it is described, that when slopping occurs it lasts for a while and is thus visible in several subsequent images of a movie. This knowledge can be incorporated in the slop detection algorithm by using a "dynamic window" of several subsequent images. In this case a dynamic window of three seconds or 8 images was chosen. If inside this dynamic window half or more of the separate images is detected as slopping it is fairly certain that slopping is indeed occurring. Slopping can occur multiple times during a batch and is only correctly detected if it is detected within five seconds of the occurrence. Non-slopping is only correctly detected if the entire batch is detected as non-slopping. Calculation of sensitivity and specificity are based on 132

non-slopping batches and on 143 instances of slopping which occurred in 98 batches. The sensitivity and specificity of the algorithm is 0.73 and 0.94 respectively. The result of application of the slop detection algorithm for movies is shown in table 4.3.
In this table the column marked True contains all the 143 slopping instances. Of the 143 slopping instances 104 were detected as slopping and 39 were detected as non-slopping. The column marked False contains all the 132 non-slopping batches. Of the 132 non-slopping batches 8 were detected as slopping and 124 were detected as non-slopping. The proportion of slopping occurrences is 0.52 and the proportion of False Positives (or false alarms) is 0.07.

Table 4.3: Results of slop detection algorithm for movies

	True (slopping)	False (non-slopping)
Positive (slopping detected)	104	8
Negative (slopping not detected)	39	124

4.6 Discussion

In slop detection algorithms a trade-off has to be made between the sensitivity and the specificity of the system. A higher sensitivity can be achieved at the cost of a lower specificity and vice versa. In the described slop detection algorithm, based on the images taken by a camera viewing the converter mouth, the sensitivity and specificity are 0.73 and 0.94 respectively. The choice of a high specificity was intentional, because the specificity highly influences the confidence in and the usability of the algorithm. If the specificity of a slopping alarm is low, it would often go off when nothing is happening (false alarm or False Positive). Usually little attention will be paid to such an alarm. Counteractive measures could be taken automatically in a slop repression system based on the prediction of slopping by the slop detection algorithm. In that case a high specificity will ensure that these actions are not taken unnecessarily. This is important since counteractive measures can be costly, as is the case with anti-foaming agents. Counteractive measures may also increase production time, as is the case with a decrease in oxygen blowing rate.
Of the slop recognition algorithms described in the literature often important

indicators of the quality of the slop detection algorithm, such as its sensitivity and specificity, are not mentioned. To our knowledge the specificity of the slop detection algorithms described in the literature is never mentioned. In the literature the sensitivity of the algorithms is sometimes mentioned and it ranges between 0.67 and 0.92 [3; 4; 5; 9], or it is described by the reduction of the occurrence of slopping achieved when the algorithm is applied, which ranges from 50% to 95% [2; 6; 7; 13; 14; 15]. The sensitivity of our proposed slop detection algorithm is 0.73. Although the sensitivity of the proposed algorithm is within the range mentioned in the literature, it can strictly speaking not be compared to the sensitivity of these algorithms, because the specificity of the algorithms mentioned in the literature is not reported and an algorithm is always a compromise between sensitivity and specificity.

4.7 Conclusions

A slop detection algorithm was designed based on images taken by a camera viewing the converter mouth. The algorithm consists of thresholding the blue image plane, removing small objects and assessing the position of the remaining objects in the image. This algorithm is relatively simple and can thus easily be used in on-line applications.
In a large collective, of the 143 occurrences of slopping 73% were detected within 5 seconds of occurring and of the 132 non-slopping batches 94% were correctly detected as non-slopping.
If the slop detection algorithm was used in a slop repression system, it would quickly detect and stop slopping in the majority of the slopping batches. It would also ensure that slop repression measures are hardly ever taken unnecessarily and it thereby ensures, that no unnecessary costs are made or that production time is not unnecessarily increased.

Bibliography

[1] D.G. Altman, J.M. Bland, Diagnostic tests 1: sensitivity and specificity, *BMJ*, **308**(1994), 1552

[2] C. Bencini, A. Poli, Automation for refining and slag control in LD process

at AFP/ Piombino steel shop, In: *1993 steelmaking conference*, Dallas (1993), 193-198

[3] A.B. Snoeijer, A. Overbosch, M. Hartwig, H. ter Voort, J.P. Brockhoff, Improvement of converter process consistency at BOS no. 2, Corus IJmuiden, In: *5th european steelmaking conference*, Aachen (2006), 186-193

[4] T. Kanai, A. Sakai, J. Tani, S. Yoshida, N. Matsui, Development of a slopping prediction and control system in BOF operation, In: *2nd european oxygen steelmaking congress*, Taranto (1997), 267-275

[5] J.J. Pak, D.J. Min, B.D. You, Slag foaming and its suppression techniques in BOF steelmaking process, In: *1996 Steelmaking conference*, Pittsburgh (1996), 763-769

[6] H. Takezoe, T. Saito, K. Ebato, J. Katsuda, M. Azuma, S. Hato-Guchi, Some trials in the development of a slopping prediction technique in the BOF at Kakogawa works Kobe Steel Ltd., *ISIJ International*, **31**(1991), 1368-1370

[7] Y. Iida, K. Emoto, M. Ogawa, Y. Masuda, M. Onishi, H. Yamada, Fully automatic blowing technique for basic oxygen steelmaking furnace, *Transactions ISIJ*, **24**(1984), 540-546

[8] H. Zhi-Gang, L. Liu, H. Ping, T. Ming-Xiang, A dynamic off-gas model on a 150t BOF, *Steel times international*, **april/may**(2003), 11-16

[9] D. Merriman, Mass spectrometry for oxygen steelmaking control, *Steel Times*, **225**(1997), 439-443

[10] F. Meyer, N. Kaell, Slag control by means of complete gas analysis and converter sound measurement at the arbed LD-AC steelplant of Esch-Belval, In: *Mcmaster symposium on iron and steelmaking no 4.*, Ontario (1976), 5.1-5.23

[11] R.M. Mishizaki, L.E. Hambly, A.H. Lohbihler, Automatic slop control at Stelco's Hilton works, In: *67th steelmaking conference*, Chicago (1984), 163-169

[12] J.E. Lait, K.W. Heyer, G.K. Cuthill, BOF control using wastegas temperature, In: *Mcmaster symposium on iron and steelmaking no. 4*, Ontario (1976), 8.1-8.11

[13] H. Iso, K. Arima, M. Kanemoto, Y. Ueda, H. Yamane, Prediction and suppression of slopping in the converter, *Transactions ISIJ*, **28**(1988), 382-390

[14] H. Iso, H. Narita, M. Saito, N. Sakanashi, Y. Ueda, T. Yoshida, S. Ogata, T. Murata, Development of a closed OG system (ACOR), *Nippon steel technical report*, **31**(1986), 17-26

[15] M. Oda, M. Yoshino, Y. Muraki, T. Hasegawa, Development of the slopping predictive and suppressing system in LD converter, In: *6th international steel congress*, Nagoya (1990), 109-114

[16] R.C. Gonzales, R.E. Woods, Digital image processing, Prentice-Hall Inc, Upper saddle River, New Jersey (2002)

5

Static models for calculation of raw material input

In basic oxygen steelmaking static models are used to calculate the necessary raw material input. The first principles model that is currently used in the steel plant of which data is available is sometimes perceived as complicated, especially in cases where the model needs to be retuned. An example of when difficulties could arise is when the first principles model is installed in several different steel plants. For each different steel plant model parameters may need to be changed. Expert knowledge is required to identify which (combination of) model parameters need to be changed.
Retuning of statistical models requires less expert knowledge and a statistical model could, therefore, be a good alternative. Since the input data is highly correlated, the statistical model was constructed using Partial Least Squares. The standard deviation in the prediction of the carbon concentration and steel temperature is higher for the PLS model than for the first principles model. It was therefore concluded, that a PLS model is not a good alternative to replace the first principles model.

5.1 Introduction

The composition of liquid steel largely influences the strength, hardness and toughness of the finished product and for steel to be cast it needs to be at a predefined temperature. Therefore, most steel plants use static models to calculate the amount of raw material that needs to be charged in order to meet the composition and temperature requirements [1; 2; 3; 4; 5; 6; 7; 8; 9; 10].
The accuracy of prediction of these static models does not only depend on model accuracy but also on the accuracy of measurements of, amongst others, raw material input weight, temperature and composition [11]. The accuracy of prediction of the models presented in the literature can thus not be compared.
The first principles static model [12] that is currently used in the steelplant of which data is available, is sometimes perceived as complicated. Especially in cases where the model needs to be retuned because of changes in the process such as the use of a different lance height or addition pattern. Another example of retuning that may cause problems is when the first principles model is installed in several different steel plants. Retuning of statistical models requires less expert knowledge. In this chapter it is therefore investigated whether a statistical model is a good alternative if insufficient expert knowledge is present.
The raw material input data is highly correlated. Partial Least Squares (PLS) is a statistical technique that can cope with highly correlated input data. This technique will be used to construct the statistical model.
In the first section the theory on first principles static models is discussed. In the following section the theory on PLS models is discussed and a PLS model is constructed. In the last two sections the results are shown and the conclusions are drawn.

5.2 First principles model

The end of batch steel temperature and steel composition are often controlled with first principles static models, which calculate the required raw material input. In the literature these models are usually presented the other way around, thus with the raw material input data as input of the model and the steel composition and temperature as outputs of the model, as is shown in figure 5.1. Although many different variations of such first principles models exist, the general framework consists of an oxygen and an energy balance [1; 2; 3; 4; 5; 6].

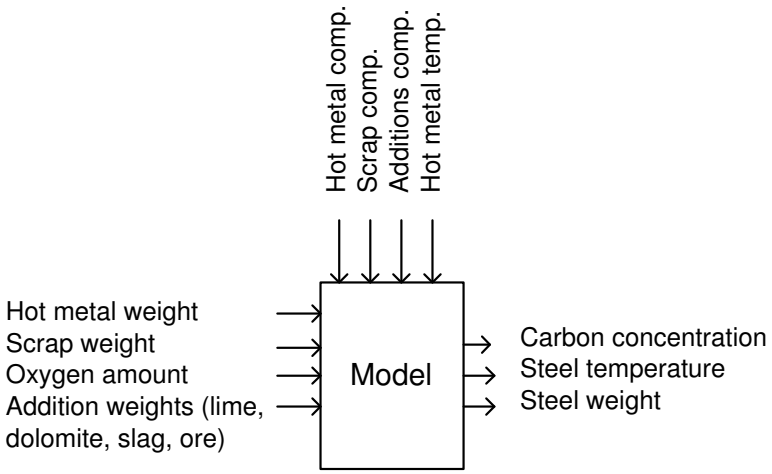

Figure 5.1: Input output diagram of static model for basic oxygen steelmaking.

In the oxygen balance the majority of the oxygen is supplied by the oxygen lance and the remainder of the oxygen is supplied by additions. The supplied oxygen is consumed by reactions, mainly by the oxidation of carbon and the oxidation of silicon.

$$O_{lance} + O_{additions} = O_{reactionsconverter} \tag{5.1}$$

In which O_{lance} is the oxygen supplied by the lance, $O_{additions}$ is the oxygen supplied by additions and $O_{reactionsconverter}$ is the oxygen consumed by the reactions occurring in the converter.
In the energy balance the energy supplied by reactions is used to increase the temperature of the steel and the slag and to dissolve the scrap and additions. Also a portion of the heat is lost to the environment.

$$Q_{reactionsconverter} = Q_{steel} + Q_{slag} + Q_{scrap} + Q_{additions} + Q_{heatloss} \tag{5.2}$$

In which $Q_{reactionsconverter}$ is the energy supplied by reactions in the converter, Q_{steel} is energy consumed by the steel, Q_{slag} is the energy consumed by the

slag, Q_{scrap} is the energy consumed by the scrap, $Q_{additions}$ is the energy consumed by the additions and $Q_{heatloss}$ is the energy lost to the environment.
Turkdogan [6] describes the energy balance for a specific batch in a 220 ton converter, as is shown in table 5.1. Although the amount and composition of each of the raw materials used varies from steel plant to steel plant and from batch to batch, the distribution of energy between the various terms in the energy balance can serve as an example.

Table 5.1: Energy balance of an example batch as given by Turkdogan. [6]

Heat generated by reactions	
C	58%
Si	25%
Fe	12%
Mn	3%
P	2%
Heat consumed	
Scrap	43%
Hot metal	27%
Heat loss	20%
Additions	10%

In the first principles models often also an iron balance and a slag balance are used to ensure that the required steel weight is met and the composition of the slag does not cause damage to the refractory bricks. Additionally a few assumptions are necessary to be able to calculate the oxygen and energy balance. Assumptions need to be made for the amount of heat loss, the amount of iron that reacts to iron oxide, the amount of carbon that reacts to carbon dioxide and the amount of manganese oxide and phosphorous oxide formed [1; 2; 3]. The model balances are usually supplemented with empirical relationships to account for these assumptions [4; 5].
In the first principles model, adaptation is used to cope with small drifts in time, such as a gradually changing lime composition [1; 3; 4]. In most cases an error term in the oxygen and heat balance is adapted. Other changes in the process, such as the use of a different lance height or addition pattern may require retuning of the model. In that case model parameters in the balances or in the empirical relations may need to be changed. Expert knowledge is required to identify which (combination of) model parameters need to be

changed.
Often the steel plant uses a sublance measurement to measure the steel temperature and carbon concentration at a certain point during the batch. In that case (an adapted version of) the static model is used to calculate the end of batch carbon concentration and steel temperature, using these measurements as additional inputs [7; 8; 9].

5.3 Partial Least Squares model

Partial Least Squares is a statistical technique that can cope with highly correlated data. The key behind this technique and other related techniques is the use of projection to examine and model high-dimensional data in a low dimensional "Latent Variable" (LV) subspace that describes most of the variability in the data. Roderigues et al. give a comprehensive explanation of these techniques [13]. Their overview will be closely followed in this chapter.
Principal Component Analysis (PCA) is a simplified form of PLS. It can be used to describe the variation amongst a block of variables such as, for instance, the input variables. In figure 5.2 several data points are plotted in a three dimensional space. Most of the variation lies along a line which is not necessarily parallel to any of the variable axes. This line, the first Principal Component (PC), passes through the average of the points and is chosen such that the projections of the points onto the line minimize their distances to the data in the least squares sense. The second Principal Component is the line that passes through the average and minimizes the projection distances in a direction that is orthogonal to the first Principal Component.
In matrix notation PCA is described as follows [14]:

$$X = TP^T + E \tag{5.3}$$

Where X is the data matrix, T is the scores matrix, P is the loadings matrix and E is the residual error.
A loading plot can be used to relate the Principal Components back to the original variables. Original variables are positively correlated if they are near each other in the loading plot and negatively correlated if they are in opposing quadrants of the loading plot. A scores plot can be used to show the relationship between samples.
A PCA model was constructed for a collective of 4085 batches containing the

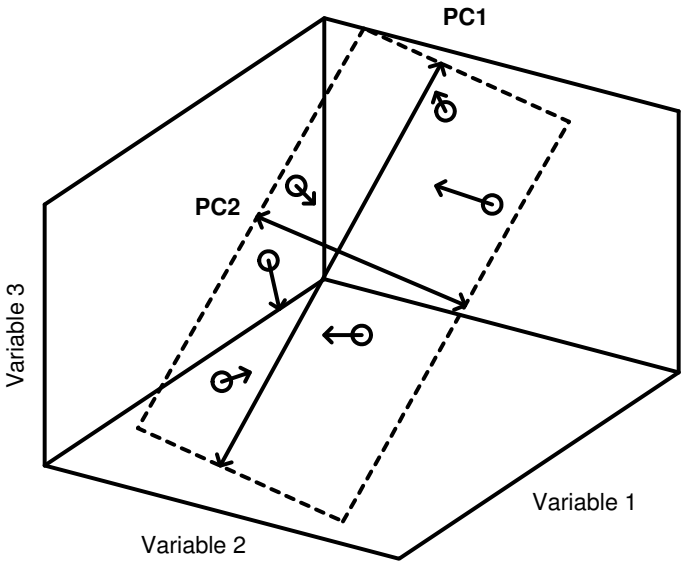

Figure 5.2: Concept of PCA analysis.

raw material input data and the measured steel carbon concentration and steel temperature. The data was autoscaled. In autoscaling, for each data point the mean is subtracted and the datapoint is divided by the standard deviation. Outliers were removed. The 21 input variables were reduced to only 3 Principal Components. The number of Principal Components was selected based both on the ratio of successive eigenvalues as well as the minimum in the root-mean-square error of the cross-validation [15]. The variance explained by these three Principal components is approximately 47%.
In figure 5.3 the loading plots of the three Principal Components of the PCA model and the scores plot for the first and second Principal Component are shown. In this figure W_{scrapt} is the total amount of scrap charged, $W_{scrap1}, ...,$ W_{scrap8} are the amount of the specific scrap types charged, W_{hm} is the amount of hot metal charged, W_{ore} is the amount of iron ore charged, W_{lime} is the amount of lime charged, W_{slag} is the amount of slag charged, $W_{dolomite}$ is the amount of dolomite charged, T_{hm} is the hot metal temperature, C_{hm}, Si_{hm}, Ti_{hm}, Mn_{hm} and P_{hm} are the hot metal carbon, silicon, titanium, manganese and phosphorous concentrations, C_{st} is the steel carbon concentration and T_{st}

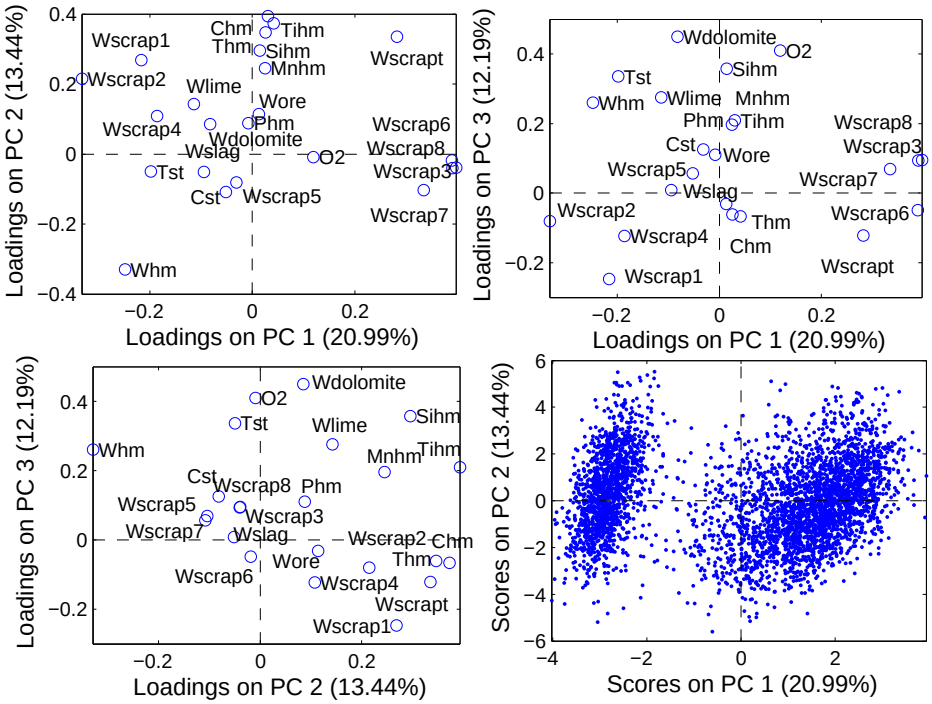

Figure 5.3: Loading plot and scores plot.

is the steel temperature.

In the three loading plots in figure 5.3 it can be seen, that the hot metal temperature (T_{hm}) and the hot metal carbon concentration (C_{hm}) are situated near each other and that they are therefore positively correlated. This correlation can be explained physically since the hot metal is saturated with carbon and the saturation carbon concentration depends on the hot metal temperature. However, correlations found need not have an underlying physical cause.

In figure 5.3 the amount of hot metal charged (W_{hm}) and the amount of scrap charged (W_{scrapt}), for instance, are at opposite quadrants in the loading plots. This implies that these variables are negatively correlated. The negative correlation between the amount of hot metal charged and the amount of scrap charged can be explained by the fact that the steel plant produces roughly the same amount of steel for each batch. Thus, if a smaller amount of hot metal

is used, the reduced iron input needs to be compensated by an increase in the amount of scrap charged.
It can also be seen in figure 5.3, that the hot metal silicon content (Si_{hm}) and the amount lime and dolomite charged (W_{lime}, $W_{dolomite}$) are positioned near each other. This implies that these variables are positively correlated. This positive correlation can be explained by the aim to have a certain slag basicity to prevent erosion of the converter lining. If the hot metal silicium content is higher, more lime and/or dolomite need to be charged to reach the same basicity.
In figure 5.3, the model outputs, the steel carbon concentration (C_{st}) and the steel temperature (T_{st}) are also shown. The steel carbon concentration is located near the origin in the three loading plots. The steel temperature is also located near the origin in the loading plot for the first and the second Principal Component. This may indicate, that there is little correlation between the steel carbon concentration and the input variables and between the steel temperature and the input variables. This may cause some problems when predicting the steel carbon concentration and steel temperature from the input variables using a statistical model. It may be, that important process variables that influence the steel temperature and carbon concentration are not measured.
In the scores plot in figure 5.3 two different clusters of samples can be seen. The two clusters are formed due to a difference in the demanded steel temperature. The partition in clusters suggests, that two separate statistical models are necessary to predict the steel carbon concentration and steel temperature.

Partial Least Squares (PLS) is a method for predicting Y variables from X variables when variables are correlated [13]. Like PCA, PLS extracts latent factors that are functions of all the variables, but PLS extends PCA by extracting factors from both X and Y. The latent X factors are selected with the goal of explaining both X and Y variables. Both X and Y are modeled with so-called outer relationships:

$$X = TP^T + E \tag{5.4}$$

$$Y = UQ^T + F \tag{5.5}$$

An the relationship between X and Y is modeled through the so-called inner relationship:

$$U = BT \tag{5.6}$$

Where X is the data matrix of the input variables, Y is the data matrix of the output variables, T and U are the scores matrices, P and Q are the loadings matrices, E and F are the residual error and B is the regression matrix.
A collective of 4085 batches was divided into two separate data sets based on the clusters in the PCA model. For both data sets a PLS model was constructed that uses the charged amount of hot metal, scrap, iron ore, slag, lime and dolomite, the hot metal temperature and the hot metal carbon, silicon, titanium, manganese and phosphorous concentration as inputs and the temperature and carbon concentration measured by the sublance as outputs. The data was auto scaled, outliers were removed. The number of Latent Variables was selected based on the root-mean-square error of the cross-validation [15]. For both models the 21 input variables were reduced to 7 Latent Variables.
The regression coefficients of the PLS models are shown in table 5.2.

Table 5.2: Values of the regression coefficients of the PLS models. If value is between -0.2 and 0.2 it is omitted.

Variable	T model 1	T model 2	C model 1	C model 2
W_{scrapt}	-0.30	-0.44		
W_{scrap4}			0.26	
W_{hm}			0.24	0.32
T_{hm}	0.20	0.24		
C_{hm}		0.20		
Si_{hm}	0.32	0.24		
W_{lime}	-0.22			
W_{ore}	-0.23	-0.35		-0.26
W_{slag}	-0.22	-0.24		
$W_{dolomite}$				0.24
$Oxygen$	0.32	0.34	-0.56	-0.42

Only those regression coefficients are shown for which the value is higher than 0.2 or lower than -0.2.
Although, the relationships between the inputs and the outputs of the PLS models need not be causal, it would be of interest to see whether these relationships can be explained physically and whether they are similar to the relationships in first principles static models.
The steel temperature depends on the energy balance described in equation 5.2. In table 5.1 it can be seen, that the majority of the energy is generated

by the oxidation of carbon and silicon. This explains the positive influence of the hot metal carbon and silicon concentration and the amount of oxygen on the steel temperature in the PLS models. In table 5.1 it can be seen, that the energy is consumed by the scrap, the hot metal and additions. This explains the negative influence of the amount of scrap, iron ore, lime and slag on the steel temperature in the PLS models. The heat inside the converter at the start of the batch depends on the amount of hot metal charged and the hot metal temperature. The higher the initial heat, the higher the steel temperature. This explains the positive influence of the hot metal temperature on the steel temperature in the PLS models.
The steel carbon concentration depends on the oxygen balance described in equation 5.1. Part of the oxygen is consumed by the oxidation of carbon. If more oxygen is supplied then more carbon can oxidize and the steel carbon concentration will be lower. This explains the negative influence of oxygen and the oxygen supplying iron ore on the carbon concentration in the PLS models. If more hot metal is added, the carbon content of the converter at the start of the batch is higher. This explains the positive influence of the hot metal weight on the steel carbon concentration in the PLS models. The other relationships with the steel carbon concentration in the PLS model are more difficult to explain.

5.4 Results

The measured and predicted carbon concentration and steel temperature at the sublance measurement for both PLS models are shown in figure 5.4. The standard deviation of the first principles model was reported by Snoeijer et al. [12]. The standard deviation of the PLS models was calculated for the validation sets of both PLS models combined. The standard deviation of the first principles model and the PLS models are shown in table 5.3. The first

Table 5.3: Standard deviation of prediction of temperature and carbon concentration of first principles and PLS static models.

	First principle model	PLS models
Temperature [K]	11.6-11.7	13.4
Carbon concentration [$.10^{-3}w\%$]	52-62	88.0

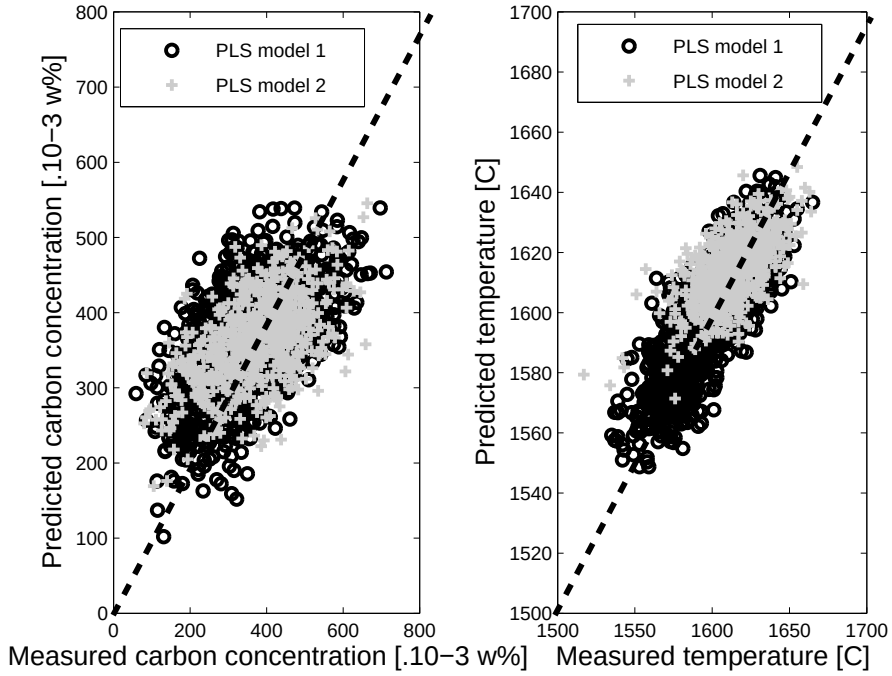

Figure 5.4: Accuracy of prediction.

principles and the PLS models were constructed based on data from the same steel plant. However, a different dataset was used to construct the models. This may have a slight influence on the calculated standard deviation.

5.5 Discussion

The difference in the standard deviation of prediction of the carbon concentration and the steel temperature between the first principles model and the PLS models is quite remarkable. It would be interesting to investigate why the PLS models may have a high standard deviation.
The PLS models are linear models. It may be the case that the assumption that the outputs can be predicted using a linear model is not valid. To in-

vestigate this, T and U in equation 5.6 can be plotted. If the data points in such a plot can be described using a linear equation, linearity may be assumed. Linearity is investigated in figure 5.5 for t_1 and u_1 for both PLS models. It

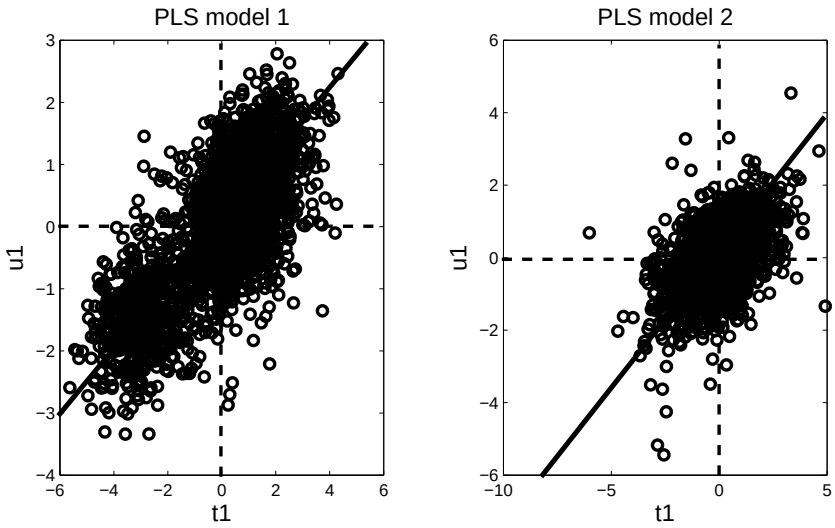

Figure 5.5: Correctness of assumption of linearity.

can be seen, that although the data points in both plots could be described using a linear equation, the data points form clouds and they could also be described using equations that are not linear. The assumption, that the outputs can be described using a linear model may therefore not be valid, but it is not immediately clear whether a non-linear fit would improve the model.
In the PCA model it was shown that the steel carbon concentration and the steel temperature are located near the origin in the loading plots. This may indicate, that there is little correlation between the steel carbon concentration and the input variables and between the steel temperature and the input variables. It may be that important process variables that influence the steel temperature and carbon concentration are not measured and that they are, therefore, not used as inputs in the PLS models. In the first principle model empirical relationships are used to estimate, for instance, the amount of heat loss, the amount of iron that reacts to iron oxide, the amount of carbon that reacts to carbon dioxide and the amount of manganese oxide and phosphorous

oxide formed. These estimated process variables are not measured and are therefore not used in the PLS models.

5.6 Conclusions

In this chapter it was investigated whether a statistical model would be a good alternative for the currently used first principles model. The first principles model is sometimes perceived as complicated, especially in cases when the model needs to be retuned. Retuning of a statistical model requires less expert knowledge.
Using Principal Component Analysis it was shown, that the input data is highly correlated. In the scores plot of the PCA model it could be seen, that the data can be separated in two different clusters. The two clusters are formed due to a difference in further treatment. The partition in clusters suggests, that two separate statistical models are necessary to predict steel carbon concentration and steel temperature.
Because the input data is highly correlated Partial Least Squares was selected to calculate the two statistical models. It was shown, that the input variables have a similar influence on the steel carbon concentration and steel temperature in the first principles model and in the PLS models. It was also shown, that the standard deviation in the prediction of the carbon concentration and steel temperature is higher for the PLS models, than for the first principles model. This may be due to the fact that PLS models assume that the outputs can be described using linear equations. It was shown, that the assumption of linearity may not be valid. Another cause for the higher standard deviation of the PLS models may be that important process variables, such as for instance the amount of heatloss, that are estimated in the first principles model are not used as inputs in the PLS models since they are not measured.
Because of the higher standard deviation, the PLS models are not a good alternative for the first principles model.

Bibliography

[1] C.J. Kearton, Process model for oxygen converter, In: *70th steelmaking conference*, Scarborough (1968), 42-46

[2] S. Kimura, M. Kimura, K. Semura, R. Misumi, S. Nishina, T. Ohmori, Improvement of calculation models for BOF, In: *1998 steelmaking conference*, Toronto (1998), 401-402

[3] U. Grethe, J. Kempken, R. Schramm, R. Klingenberg, Blocon modularized and adaptable BOF process model of high performance, In: *1996 steelmaking conference*, Pittsburgh (1996), 133-146

[4] D.J. Buchanan, J. Fear, R.A. Gordon, Computer control of the DOFASCO No. 2 BOF meltshop, In: *64th steelmaking conference*, Warrendale (1981), 203-213

[5] H. Mizelli, H. Moser, R. Tober, Restructuring of converter level 2 automation system, In: *5th european oxygen steelmaking conference*, Aachen (2006), 287-292

[6] E.T. Turkdogan, Fundamentals of steelmaking, The insitute of materials, London (1996)

[7] J. Flavio Viana, L.F. Andrade de Castro, Converter oxygen blowing model based on neural networks, In: *ScanmetII - 2nd international Conference on process development in iron and steelmaking*, Lulea (2004), 199-206

[8] A. Frattini Fileti, T. Pacianotto, A. Pitasse Cunha, Neural modeling helps the BOS process to achieve aimed end-point conditions in liquid steel, *Engineering applications of artificial intelligence*, **19**(2006), 9-17

[9] I. Cox, R. Lewis, R. Ransing, H. Lasczewski, G. Berni, Application of neural computing in basic oxygen steelmaking, *Journal of Material processing*, **120**(2002), 310-315

[10] C. Kubat, H. Taskin, R. Artir, A. Yilmaz, Bofy-fuzy logic control for the basic oxygen furnace, *Robotics and autonomous systems*, **49**(2004), 193-205

[11] D. DasGupta, J. Heidepriem, Verbesserung der temperaturtreffsicherheit eines statischen on-line-modells in einem LD-stahlwerk, *Stahl und eisen*, **102**(1982), 857-860

[12] A.B. Snoeijer, P. Mink, A. Overbosch, M. Hartwig, H. ter Voort, J.P. Brockhoff, Improvement of converter process consistency at BOS no. 2

Corus IJmuiden, In: *5th european oxygen steelmaking conference*, Aachen (2006), 186-193

[13] R.N. Roderigues, R.D. Tobias, Multivariate methods for process knowledge discovery: the power to know yor process, *Statistics, data analysis and data mining*, paper 252-26

[14] B. Roffel, B. Betlem, Process dynamics and control, modeling for control and prediction, John Wiley and sons Ltd, Chichester (2006)

[15] PLS toolbox 3.5 manual. Eigenvector (2004)

6

Dynamic model for the main blow

In the control and optimization of basic oxygen steelmaking it is important to have an understanding of the influence of control variables on the process. However, important process variables such as the composition of the steel and slag can not be measured continuously. The decarburization rate and the accumulation rate of oxygen, which can be derived from the generally measured waste gas flow and composition, are an indication of changes in steel and slag composition. The influence of the control variables on the decarburization rate and the accumulation rate of oxygen can best be determined in the main blow period.
In this chapter the measured step responses of the decarburization rate and the accumulation rate of oxygen to step changes in oxygen blowing rate, lance height and the addition rate of iron ore during the main blow are presented. These measured step responses are subsequently used to develop a dynamic model for the main blow. The model consists of an iron oxide and a carbon balance and an additional equation describing the influence of the lance height and the oxygen blowing rate on the amount of iron droplet formed due to the impact of the oxygen jet. With this simple dynamic model the measured step responses can be explained satisfactorily.

6.1 Introduction

To improve control of basic oxygen steelmaking and to enable dynamic optimization, the process should be modeled dynamically. To develop a dynamic model, the influence of changes in control variables, such as the lance height, the oxygen blowing rate and the addition rates on the process should be known. How the behavior of the process changes with time under the influence of changes in control variables can be investigated using an experimental approach [1; 2]. In this approach the value of control variables is deliberately changed. One possibility is to change the control variables by making a step change and monitor the process variable response.
In the literature little information is published on step responses in basic oxygen steelmaking [3; 4; 5; 6]. It is however known, that an increase in oxygen input, either due to an increase in oxygen blowing rate [3; 4; 5] or due to the addition of ore [5], increases the decarburization rate. Furthermore, Anderson et al. [6] published the delay between the occurrence of a change in a control variable such as the iron ore addition rate and a change in decarburization rate.
In this chapter the step response to changes in control variables is determined experimentally in the first section. Using the measured step responses a simplified process model is developed in the following section. In the next section the measured and simulated step responses are compared. Finally the conclusions are summarized.

6.2 Experimental

Due to the high temperatures and dusty environment involved in basic oxygen steelmaking, important process variables such as the steel composition and steel temperature can not be measured continuously. Therefore in most steelplants indirect measurements, such as waste gas flow, temperature and composition, are used to monitor the process. The decarburization rate and the accumulation rate of oxygen inside the converter, which are commonly derived from the waste gas measurements, can be used as an indication of the change in composition of the steel and the slag respectively [7; 8]. The decarburization

rate $\frac{dC}{dt}$ can be given by:

$$\frac{dC}{dt} = \frac{\phi_{wg}(WG_{CO} + WG_{CO2})}{V_M} \tag{6.1}$$

Where ϕ_{wg} is the measured waste gas flow, WG_{CO} and WG_{CO2} are the measured percentage of carbon monoxide and carbon dioxide in the waste gasses and V_M is the molar volume. The measured accumulation rate of oxygen inside the converter $\frac{dO}{dt}$ can be given by:

$$\frac{dO}{dt} = \frac{dO_{lance}}{dt} + \frac{dO_{additions}}{dt} - (\frac{dO_{wastegas}}{dt} - \frac{dO_{air}}{dt}) \tag{6.2}$$

Where $\frac{dO_{lance}}{dt}$ is the measured rate at which oxygen is blown into the converter, $\frac{dO_{additions}}{dt}$ is the measured rate in which oxygen in additions enters the converter, $\frac{dO_{wastegas}}{dt}$ is the measured rate at which oxygen leaves the converter through the waste gasses and $\frac{dO_{air}}{dt}$ is the measured rate at which air enters the waste gas system through the gap between the converter and the skirt.
It is important that a measured step response accurately describes the influence of the change in a control variable. This is easiest during a period in the batch in which the decarburization rate and accumulation rate of oxygen remain constant, when no changes in control variables occur. Boom and Deo [3] describe this period as the main blow period.
The step changes occurring during normal operation in a data set of 1006 batches were studied. The step changes in oxygen blowing rate, lance height and the addition rate of iron ore during main blow were determined. The number of observations found of a particular step change depends on the time for which that step change is well defined. For example, if this time is 50 [s], then the number of observed step changes in the oxygen blowing rate is 11. If the time is increased to 60 [s] then the number of observations reduces to only 5. For each type of step change the time for which this step change is well defined is selected in such a way, that the number of observations exceeds ten. Details of the step changes, such as the selected time, the number of observations and the average step size are shown in table 6.1.
To minimize the influence of disturbances on the step response, the step response of several different observations of a step change were averaged. Normalization of the step response to zero starting conditions will make this possible. It is assumed that for the result to be meaningful at least ten observations of a particular step change should be averaged. The average normalized step

Table 6.1: Steps found in data set

Independent step	Duration step	Observations	Average size of step
O2 rate increase	50 [s]	11	2500 [nm3/h]
Lance up	90 [s]	43	7 [cm]
Lance down	60 [s]	14	7 [cm]
Ore start	120 [s]	247	8 [kg/s]
Ore stop	90 [s]	48	8 [kg/s]

responses of the step change in oxygen blowing rate, lance height and the addition rate of iron ore on the decarburization rate and accumulation rate of oxygen are shown in figure 6.1. A decrease in oxygen blowing rate is not shown in this figure, since not enough well defined steps of this type were present in the available data set.

6.3 Process model

The measured step responses can be simulated using a process model. In basic oxygen steelmaking, reactions can take place at a number of sites including the slag foam where reactions take place between the iron droplets and the oxidizing slag and the hot spot directly under the oxygen jet [3].
Meyer et al. [9] have analyzed ejections of slag and metal emulsions from the tap hole. They have shown that a substantial portion of the liquid metal is emulsified into the slag during the batch. The authors concluded, that at the height of refining most decarburization occurs within the slag-metal emulsion. It is therefore assumed that the majority of reaction takes place at the interface between the iron droplets and the slag. Decarburization at the iron droplets in the slag occurs through a reaction with iron oxide.

$$Fe + \frac{1}{2}O2 \rightarrow FeO \tag{6.3}$$

$$C + FeO \rightarrow CO + Fe \tag{6.4}$$

In the main blow period mainly carbon and iron are oxidized. Silicium and titanium have already been oxidized before this period. If it is assumed that the oxidation of manganese, phosphorous and sulphur is negligible during the

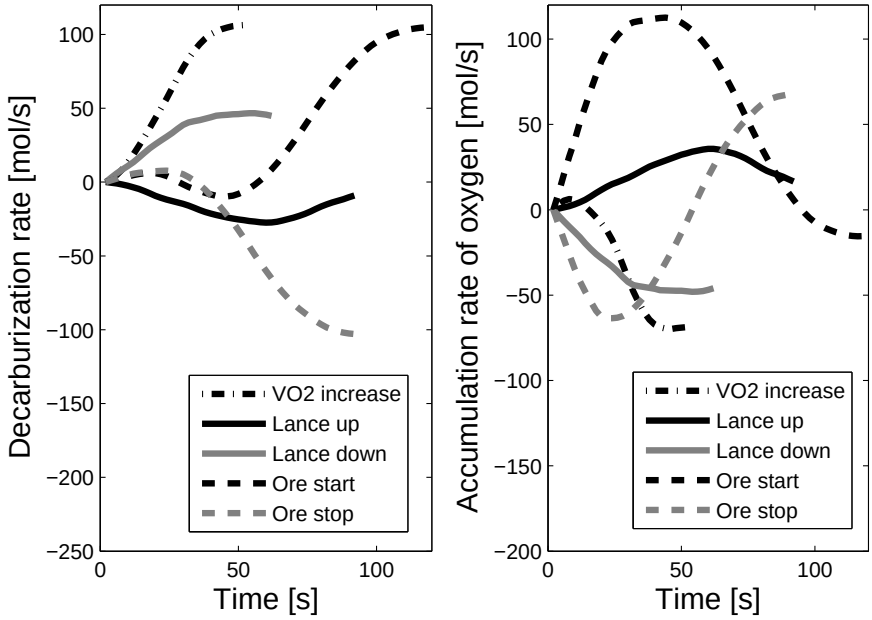

Figure 6.1: Influence of step changes on decarburization rate and accumulation rate of oxygen (experimental).

main blow, the accumulation rate of oxygen in the converter can be calculated using an iron oxide balance.

$$\frac{dO}{dt} = \frac{dFeO}{dt} = \frac{dFeO_{lance}}{dt} + \frac{dFeO_{addition}}{dt} - (1 + pCO2)\frac{dC_{reaction}}{dt} \qquad (6.5)$$

Where $\frac{dFeO}{dt}$ is the change of iron oxide content in the slag, $\frac{dFeO_{lance}}{dt}$ is the change in iron oxide due to the oxygen blown by the lance, $\frac{dFeO_{addition}}{dt}$ is the change in iron oxide due to the additions, $pCO2$ is the percentage of carbon dioxide formed and $\frac{dC_{reaction}}{dt}$ is the rate of decarburization.
Ghosh [10] has performed experiments in which oxygen was blown into a small induction furnace filled with carbon containing iron. He observed a complete consumption of the supplied oxygen and a continuous breaking and reforming of the oxide film. Since no oxygen was detected in the waste gas, it is assumed that all oxygen supplied by the lance is instantly converted to iron oxide.

$$\frac{dFeO_{lance}}{dt} = 2VO_2 \tag{6.6}$$

Where VO_2 is the measured amount of oxygen blown through the lance. The amount of carbon in the steel bath changes due to decarburization and due to the dissolving of scrap. The model will be used to simulate the measured step responses, which last at most 120 seconds. It is assumed that the influence of the dissolving of scrap on the change in carbon content in the steel can be neglected for such a short period. It is also assumed that the change in steel volume is negligible.

$$\frac{dC}{dt} = -\frac{dC_{reaction}}{dt} = -V_{steel}\frac{d[C]}{dt} \tag{6.7}$$

Where V_{steel} is the volume of steel in the converter and $[C]$ is the carbon concentration in the bath.
Several researchers performed experiments in which a small carbon containing iron droplet was dropped into a slag [11; 12; 13]. They observed that the decarburization rate increased with increasing temperature, carbon concentration and iron oxide concentration. It is therefore assumed, that the decarburization reaction is rate limited and first order in carbon and iron oxide.

$$\frac{dC_{reaction}}{dt} = V_{steel}Ae^{\frac{-Ea}{RT}}[C][FeO] \tag{6.8}$$

Where A is the frequency factor, Ea is the activation energy, R is the gas constant, T is the bath temperature, $[FeO]$ is the iron oxide concentration in the slag and $[C]$ is the carbon concentration in the steel.
Since the density of the steel and the slag is difficult to determine the reaction rate is calculated using the molar carbon and iron oxide concentration. Since it is assumed, that the steel volume is constant it is incorporated in the constant k_0.

$$\frac{dC_{reaction}}{dt} = k_0e^{\frac{-Ea}{RT}}[C^*][FeO^*] \tag{6.9}$$

Where k_0 is a reaction rate constant, $[FeO^*]$ is the molar iron oxide concentration in the slag and $[C^*]$ is the molar carbon concentration in the steel.
It has been shown, that the lance height and the oxygen blowing rate affect the amount of iron droplets that are formed due to jet impact [14; 15; 16]. An increase in oxygen blowing rate increases the mass of iron droplets formed [14],

while, above a certain lance height, an increase in lance height decreases the mass of iron droplets formed [14; 15]. The mass of iron droplets in the slag affects the reaction surface between the iron droplets and the slag at which part of the decarburization reaction takes place. This effect is modeled by assuming that the reaction rate constant changes if the lance height and oxygen blowing rate change.

$$k_0 = a + bVO_2 - cH_{lance} \tag{6.10}$$

Where a, b and c are model constants, VO_2 is the oxygen blowing rate and H_{lance} is the lance height. Equation 6.10 is only valid for a limited range of lance heights and oxygen blowing rates, which are typical during main blow.
In contrast to what the calculation of the accumulation rate of oxygen in equation 6.2 suggests, the added iron ore cannot react immediately. Instead, the temperature of the iron ore needs to increase before it can dissolve. This heat up period is modeled as a time lag. Since this time lag is not incorporated in the calculation of the measured accumulation rate of oxygen (equation 6.2), it is also not shown in the measured step response of the accumulation rate of oxygen to a step change in the iron ore addition rate in figure 6.1. This explains why the measured step response in the decarburization rate hardly changes in the first 60 seconds, while the measured step response in the accumulation rate of oxygen in the converter changes significantly during this period.
Since the iron ore is added as lumps, the dissolution rate of iron ore is not uniform. The blown oxygen first has to react to iron oxide before it can react with carbon. When the oxygen blowing rate changes, it will take some time before the iron oxide content of the bath changes accordingly. Similarly, when lance height and oxygen blowing rate are changed it will take some time before the mass of droplets in the slag is changed accordingly. Therefore, an averaged iron ore addition rate, oxygen blowing rate and lance height are used as inputs to equations 6.5 and 6.10. Averaging is a way to model a dynamic effect.

6.4 Comparison measurements and model

The measured step responses can be simulated using the model presented in the previous section. The initial values of variables in the model and the size of steps are similar to those typical during the main blow. The activation energy and initial iron oxide concentration were selected in such a way, that at stationary input conditions the decarburization rate and accumulation rate

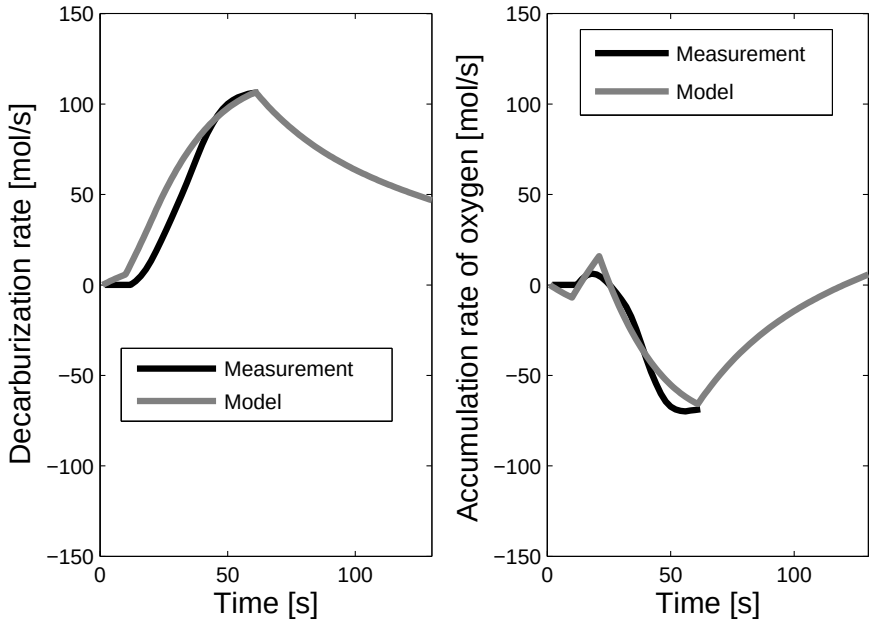

Figure 6.2: Modeled and measured influence of an increase in the oxygen blowing rate on decarburization rate and accumulation rate of oxygen.

of oxygen remain more or less constant. The constants a, b and c and the delay and the size of averaging windows were adjusted to fit the model to measurement results.

The measured and modeled step response to an increase in oxygen blowing rate, an increase and a decrease in lance height and the start and stop of an ore addition are shown in figures 6.2, 6.3 and 6.4. In these figures, the step changes occurred at $t = 10[s]$. In figure 6.2 it can be seen that the modeled and measured step response to an increase in oxygen blowing rate correspond well. At 10 seconds the oxygen blowing rate is increased. At this moment the increased oxygen input causes an increase of the iron oxide content in the slag (equation 6.5). This can be seen as the initial small and brief increase in the accumulation rate of oxygen. The increase in oxygen blowing rate also increases the amount of iron droplets formed (equation 6.10), thereby increasing the decarburization rate (equation 6.9). The increase in

decarburization rate decreases the iron oxide content in the slag (equation 6.5). The increase in decarburization rate and the decrease in iron oxide content can both be seen in figure 6.2 between 10 and 70 seconds. At around 70 seconds the mass of iron droplets in the slag no longer increases and has reached a stable level. At this point, the decreased iron oxide concentration in the slag reduces the decarburization rate (equation 6.9) until a decarburization rate is reached (at around 130 seconds) at which oxygen consumption again matches the oxygen supply.
In figure 6.3 it can be seen that the modeled and measured step response to an increase and a decrease in lance height correspond well. At 10 seconds

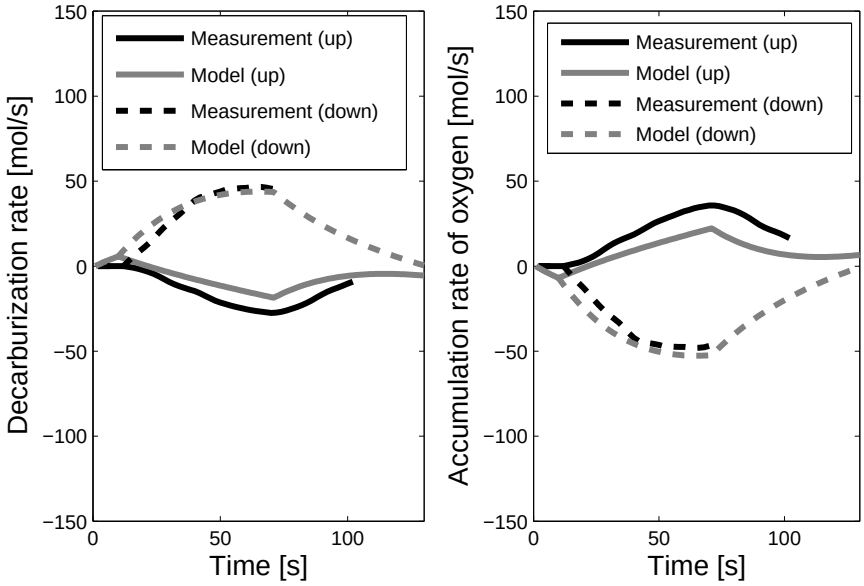

Figure 6.3: Modeled and measured influence of an increase and a decrease in the lance height on the decarburization rate and accumulation rate of oxygen.

the lance height is increased. The increase in lance height causes a decrease in the mass of iron droplets formed (equation 6.10), which in turn decreases the decarburization rate (equation 6.9) and consequently increases the iron oxide content of the bath (equation 6.5). The decrease in the decarburization rate and the increase in the accumulation rate of oxygen can both be seen in

figure 6.3 between 10 and 70 seconds. At around 70 seconds the mass of iron droplets in the slag no longer diminishes. At this point, the increased iron oxide concentration in the slag increases the decarburization rate (equation 6.9) until oxygen consumption matches oxygen supply. The step response to a decrease in lance height can be explained in a similar manner.
In figure 6.4 it can be seen that the modeled and measured step response to the start or stop of an iron ore addition correspond reasonably well. At

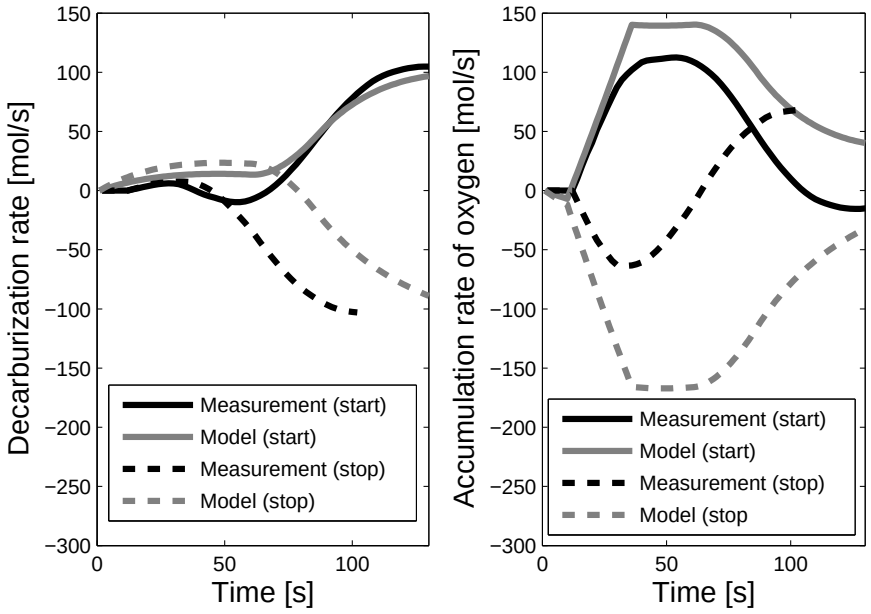

Figure 6.4: Modeled and measured influence of an increase and a decrease in iron ore addition rate on the decarburization rate and accumulation rate of oxygen.

10 seconds an ore addition is started. Initially the temperature of the iron ore increases and there is no effect of the ore addition on the decarburization rate, as can been seen in figure 6.4. (There is an effect on the accumulation rate of oxygen during this period. This is because the delay caused by the heating up period is not considered in calculating the measured accumulation rate of oxygen in equation 6.2). Then at around 60 seconds the ore starts

to dissolve and it increases the iron oxide content in the slag (equation 6.5). The increased iron oxide content causes an increase in the decarburization rate (equation 6.9) which can be seen in figure 6.4. The step response to the stop of ore addition can be explained in a similar manner. The difference between model and experiment for the stop of an iron ore addition is larger. Other dynamic effects may play a role and could explain part of this difference.

6.5 Conclusions

The average normalized step response to step changes in lance height, oxygen blowing rate and addition rate of iron ore during the main blow were determined in a data set containing 1006 batches. These step responses were satisfactorily simulated using a process model consisting of an iron oxide and a carbon balance and an additional equation describing the influence of the lance height and oxygen blowing rate on the amount of iron droplets in the slag and thereby on the decarburization rate.
It was found, that an increase in the oxygen blowing rate and the iron ore addition rate both cause an increase in the decarburization rate. Both step changes increase the oxygen supply to the converter. This increased oxygen supply is eventually matched by an equal increase in oxygen consumption and thus in an increase in the decarburization rate.
In addition it was found, that a decrease in lance height and an increase in oxygen blowing rate both cause a temporary (additional) increase in the decarburization rate. It is known that both lance height and oxygen blowing rate influence the amount of iron droplet formed due to jet impact. A decrease in lance height and an increase in oxygen blowing rate both increase the amount of iron droplets in the slag. Since part of the decarburization reaction takes place between these iron droplets and the slag, the increase in reaction surface between the iron droplets and the slag causes an increase in decarburization rate. The increased decarburization rate diminishes the iron oxide concentration in the slag, which in turn again decreases the decarburization rate.
It was also found, that a step change in the iron ore addition rate does not have an immediate effect on the decarburization rate. The delay is most likely caused by the time needed to increase the temperature of the iron ore.

Bibliography

[1] G. Stephanopoulos, Chemical process control: an introduction to theory and practice, Prentice Hall, New Jersey (1984)

[2] B. Roffel, B. Betlem, Process dynamics and control: Modeling for control and prediction, John Wiley and sons Ltd, Chichester (2007)

[3] B. Deo, R. Boom, Fundamentals of steelmaking metallurgy, Prentice hall international, Hemel Hempstead (1993)

[4] F. Oeters, Metallugie der stahlherstellung, Springer-Verlag, Berlin (1989)

[5] P.J. Kreijger, Zusammenhang zwischen konvertervolumen und sauerstoffaufblasgeschwindigkeit, *Stahl und eisen*, **96**(1976), 957-960

[6] D. Anderson, W.J. Henderson, advanced online blowing control of the BOS process, In: *International oxygen steelmaking congress*, Linz (1987), 595-607

[7] H. Zhi-Gang, L. Liu, H. Ping, T. Ming-Xiang, A dynamical off-gas model on a 150t BOF, *Steel times international*, **April/May**(2003), 11-16

[8] W. Dorr, W. Lanzer, Aussagefahigkeit der abgasmessung zur kennzeigung des schlackenzustandes, *Stahl und eisen*, **93**(1973), 187-884

[9] H.W. Meyer, W.F. Porter, G.C. Smith, J. Szekely, Slag-metal emulsions and their importance in BOF steelmaking, *Journal of metals*, **July**(1968), 35-42

[10] D.N. Ghosh, Kinetics of decarburization of Fe-C melts, part 1 high carbon levels, *Ironmaking and steelmaking*, (1975) no. 1, 36-44

[11] T. Gare, G.S.F. Hazeldean, Basic oxygen steelmaking decarburization of binary Fe-C droplets and ternary Fe-C-X droplets in ferruginous slags, *Ironmaking and steelmaking*, (1981) no. 4, 169-181

[12] E.W. Mulholland, G.S.F. Hazeldean, M.W. Davies, Visualisation of slag metal reactions by X-ray fluorscopy: decarburization in basic oxygen steelmaking, *Journal of the iron and steel institute*, **September**(1973), 632-638

[13] D.J. Min, R.J. Fruehan, Rate of reduction of FeO in slag by Fe-C drops, *Metallurgical transactions B*, **23B**(1992), 29-37

[14] Q.L. He, N. Standish, A model study of droplet generation in BOF steelmaking, *ISIJ International*, **30**(1990), 305-309

[15] W. van der Knoop, B. Deo, A.B. Snoeijer, G. van Unen, R. Boom, A dynamic slag-droplet model for the steelmaking process, In: *4th international conference on molten slags and fluxes*, Sendai (1992), 302

[16] A. Patuzzi, H. Alerl, Stochastisches verfahren zur schlackenreglung, *Stahl un eisen*, **110**(1990), 81-84

7

Dynamic modeling of the entire batch

In basic oxygen steelmaking static models are widely used to predict carbon concentration and temperature at the end of the batch. To improve control of the process it would be required to know the carbon concentration and temperature during the batch. In the previous chapter a dynamic model for the main blow, a period in the batch during which the decarburization rate is more or less constant, was presented. In this chapter, this main blow model is extended such that it estimates the bath temperature and composition of both bath and slag during the entire batch.

The model was validated using the measured decarburization rate and accumulation rate of oxygen. The measured and the estimated decarburization rate and accumulation rate of oxygen correspond well over the entire batch. Also the calculated steel and slag compositions during the batch are similar to those published in the literature. It can therefore be said that the important dynamic phenomena that influence the decarburization rate and the accumulation rate of oxygen have been modeled successfully.

The accuracy of the prediction of carbon concentration and temperature at the sublance measurement of the static model is higher than that of the dynamic model. The dynamic model should therefore be used in combination with a static model.

7.1 Introduction

In basic oxygen steelmaking, static models are used to control the end of batch carbon concentration and temperature [1]. Important process variables such as temperature and carbon concentration cannot be measured continuously due to high temperatures and the dusty environment and are therefore not known during the batch. A dynamic model which predicts the carbon concentration and temperature during the batch would improve control of the process. Many authors have published dynamic models in which the carbon concentration and temperature are predicted [2; 3; 4]. Their models usually consist of a very detailed physical description of the phenomena involved. These models are subsequently used for off-line studies in order to anticipate new situations such as the introduction of a new practice.
In the previous chapter a dynamic model for the main blow has been presented. The main blow is a period during the middle of the batch in which mainly carbon is oxidized and where the decarburization rate is more or less constant. The presented main blow model consists of an iron oxide balance, a carbon balance and some additional equations describing the decarburization rate. In this chapter the dynamic model for the main blow will be extended such that it can estimate the bath temperature and the composition of both bath and slag during the entire batch. Van Lith [5] describes a modeling approach, which will be followed in this chapter. A separate section is dedicated to each of the steps described in the modeling approach. The author states, that the first step in modeling is the formulation of model objectives and model requirements and the selection of key variables. The second step involves the basic modeling of the process, which consists of the formulation of the process hypothesis, the process structure and the model framework. Subsequently the unknown process parameters are estimated and identified. Finally the model performance is evaluated. In the last sections some results are shown and the conclusions are summarized.

7.2 Model objectives and model requirements

The dynamic model should be verifiable with continuous measurements and should at least describe the carbon concentration and the temperature during the batch. The available measurements, that indirectly give information about

the carbon concentration of the bath and the composition of the slag are the decarburization rate and accumulation rate of oxygen, which can be calculated from waste gas composition and waste gas flow. In figure 7.1 the decarburization rate and accumulation rate of oxygen for a typical batch are shown. The

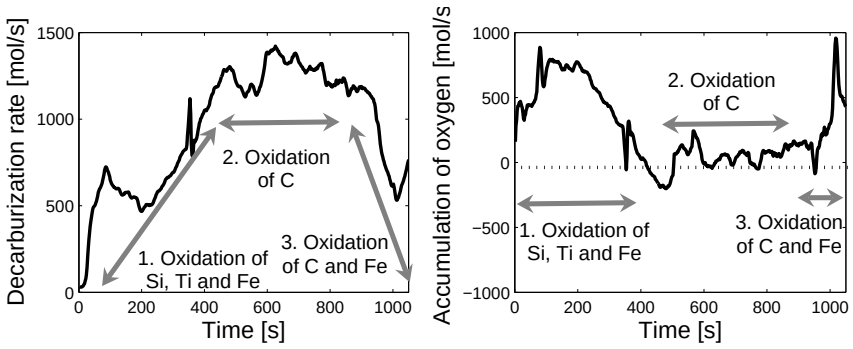

Figure 7.1: Decarburization rate and accumulation rate of oxygen of a typical batch.

shape of the trajectory of the decarburization rate and the accumulation rate of oxygen are each mainly determined by the oxidation of silicon, titanium and iron at the beginning of the batch, by oxidation of carbon during the middle of the batch (main blow period), and by the oxidation of iron at the end of the batch. Therefore, at least these four bath components need to be modeled. In the slag, the corresponding oxides, and magnesium oxide and calcium oxide -which are added to reduce refractory wear- need to be modeled.
The temperature is normally not measured during the batch. However, in order to be able to verify a modeled temperature trajectory a special test was performed in which the temperature was measured multiple times during the batch, for three batches. This was done using adapted Quick-tap drop-in sensors. The selected key variables are Fe, C, Si and Ti for the bath composition, FeO, SiO_2, TiO_2, CaO and MgO for the slag composition and T for the bath temperature.

7.3 Basic modeling

7.3.1 Process hypothesis and process structure

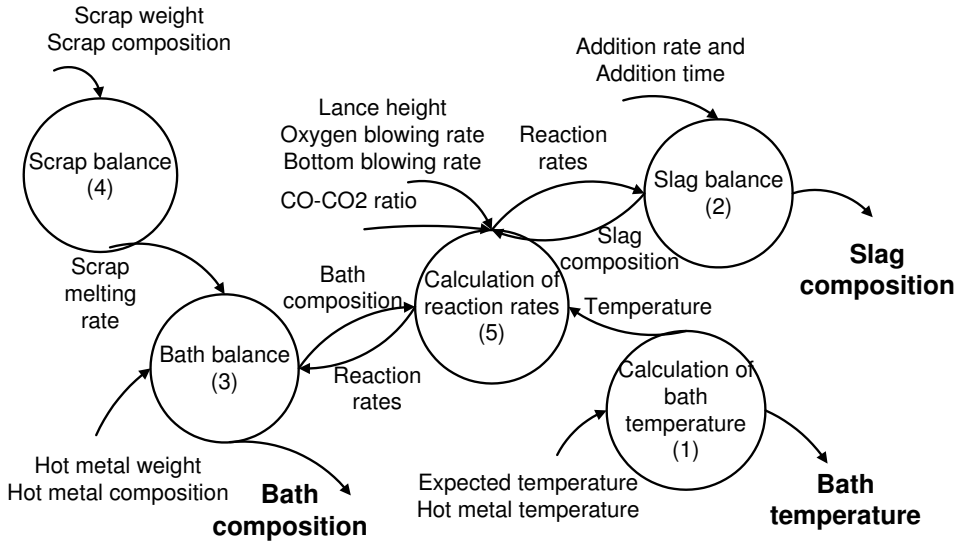

Figure 7.2: Data flow diagram of hybrid dynamic model which predicts carbon concentration and temperature in a LD-converter.

The key variables can be described directly using state equations. The numbers listed in this text refer to the numbers shown in the dataflow diagram in figure 7.2.
The bath temperature (1) can be approximated using the measured hot metal temperature and the expected bath temperature at the end of the batch. The change in slag composition (2) depends on the accumulation of oxides from additions and oxides formed by reactions. The bath composition (3) changes as a result of reactions and the melting of scrap (4). The reaction rate (5) may depend on the concentration of the elements in the bath, the concentration of oxides in the slag, the bath temperature, the carbon monoxide to carbon dioxide ratio in the waste gas, the lance height and the oxygen blowing rate.
The iron oxide balance and carbon balance in the main blow model, described in chapter 6, describe the change in slag composition and the change in bath

composition during the main blow and they will both be extended such that they can be used for the entire batch. The equations for the rate of the decarburization reaction in the main blow model, can be used as a starting point for the calculation of the reaction rate for the entire batch.

7.3.2 Model framework

Due to the small number of temperature reference measurements only a simplified temperature model can be developed. In chapter 3 it was shown, that the steel temperature can be approximated using the assumption that the steel temperature increases linearly with the amount of oxygen blown. This approximation is based on the assumption that the temperature is (partly) self-regulating as shown in figure 7.3. A higher temperature increases the dis-

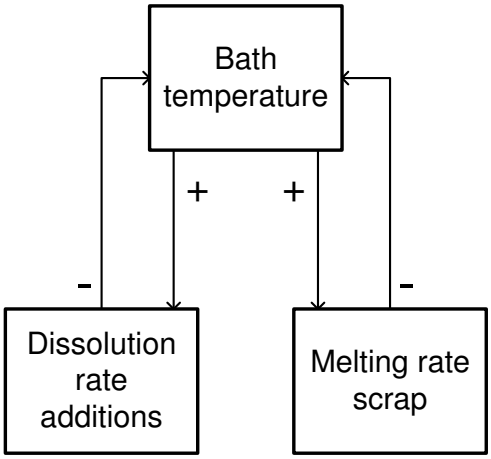

Figure 7.3: Self regulating principle of the bath temperature in basic oxygen steelmaking.

solution rates of additions and the melting rate of scrap. The higher dissolution and melting rates in turn cool the bath and cause a smaller increase in bath temperature. Based on the approximation of a self-regulating temperature a linear temperature profile is assumed.

$$\frac{dT}{dt} = a_T VO2 \tag{7.1}$$

With T is the steel temperature, a_T is the regression coefficient and $VO2$ is the oxygen blowing rate. Due to the charging of scrap the temperature drops significantly at the start of the batch. The initial condition when calculating the steel temperature during the batch is therefore:

$$T_0 = T_{hm} - \Delta T \tag{7.2}$$

Where T_0 is the initial steel temperature, T_{hm} is the measured hot metal temperature and ΔT is the bath temperature drop due to charging of scrap.
The coefficient a_T in equation 7.1 is chosen in such a way that the modeled temperature at the end of the batch corresponds with the estimated temperature at the end of the batch as calculated by the static model [1].
The change in iron oxide composition of the slag can be described by extending the iron oxide balance of the main blow model described in chapter 6. To describe the change in iron oxide during the entire batch the oxidation of silicon and titanium also need to be considered:

$$\begin{aligned}\frac{dFeO}{dt} = \; & \frac{dFeO_{lance}}{dt} + \frac{dFeO_{addition}}{dt} - (1 + pCO_2)\frac{dC_{reaction}}{dt} \\ & - \sum_{Si,Ti} n \frac{dX_{reaction}}{dt}\end{aligned} \tag{7.3}$$

Where $\frac{dFeO}{dt}$ is the change of iron oxide content in the slag, $\frac{dFeO_{lance}}{dt}$ is the change in iron oxide due to the oxygen blown by the lance, $\frac{dFeO_{addition}}{dt}$ is the change in iron oxide due to the additions, $pCO2$ is the percentage of carbon dioxide formed, $\frac{dC_{reaction}}{dt}$ is the decarburization rate, $\frac{dX_{reaction}}{dt}$ is the change in bath content due to oxidation of element X, in this case silicon and titanium and n is a stoichiometric coefficient.
Ghosh [6] has performed experiments in which oxygen was blown into a small induction furnace filled with carbon containing iron. He observed a complete consumption of the supplied oxygen and a continuous breaking and reforming of oxide film. Since no oxygen was detected in the waste gas, it is assumed that all oxygen is converted to iron oxide.

$$\frac{dFeO_{lance}}{dt} = 2VO_2 \tag{7.4}$$

Where VO_2 is the measured amount of oxygen blown with the lance.
The change in slag composition needs to be described not only for iron oxide, but also for silicium oxide, titanium oxide, calcium oxide and magnesium oxide. This change is caused by additions and in some cases also by reactions:

$$\frac{dXO_n}{dt} = \frac{dX_{reaction}}{dt} + \frac{dXO_{n,addition}}{dt} \tag{7.5}$$

Where $\frac{dXO_n}{dt}$ is the change in content of oxide XO_n in slag and $\frac{dXO_n,addition}{dt}$ is the measured amount of component XO_n added.
The change in bath composition for carbon, silicium, titanium and iron can be described by the generalization of the carbon balance of the main blow model described in chapter 6. The change in bath composition during the entire batch is not only caused by reactions but also by the melting of scrap:

$$\frac{dX}{dt} = -\frac{dX_{reaction}}{dt} + \frac{dX_{scrap}}{dt} \tag{7.6}$$

Where $\frac{dX}{dt}$ is the change in bath content of element X and $\frac{dX_{scrap}}{dt}$ is the change in bath content of element X due to scrap dissolution. It is assumed that the scrap dissolution rate is constant:

$$\frac{dX_{scrap}}{dt} = n_x a_{scrap} \tag{7.7}$$

Where a_{scrap} is the scrap dissolution rate which is thus independent of temperature, scrap type and scrap size and n_x is the fraction of element X in the scrap.
The reaction rate for the decarburization reaction can be described similar as in the main blow model.

$$\frac{dC_{reaction}}{dt} = k_0 e^{\frac{-Ea}{RT}} [C^*][FeO^*] \tag{7.8}$$

$$k_0 = a + bVO_2 - cH_{lance} \tag{7.9}$$

Where k_0 is a reaction rate constant, Ea is the activation energy, R is the gas constant, T is the bath temperature, $[FeO^*]$ is the molar iron oxide concentration in the slag, $[C^*]$ is the molar carbon concentration in the steel, a, b and c are model constants, VO_2 is the oxygen blowing rate and H_{lance} is the lance height.

The last of these two equations is however only valid for lance heights and oxygen blowing rates that are typical during the main blow. When lance height and oxygen blowing rate are outside this range, usually during the first part of the batch, a constant k_0 can be used instead.

$$k_0 = k_{0eq} \tag{7.10}$$

Where k_{0eq} is a constant value for k_0 at the start of the batch.
The oxidation of silicon and titanium only occur in the first few minutes of the batch, where the temperature change is relatively small. It is therefore assumed that their reaction rates can be calculated with a simplified version of the equation for the rate of decarburization in the main blow model. Because of the difference in stoichiometric coefficient a different reaction order in iron oxide is chosen.

$$\frac{dSi_{reaction}}{dt} = k_{Si}[Si^*][FeO^*]^2 \tag{7.11}$$

$$\frac{dTi_{reaction}}{dt} = k_{Ti}[Ti^*][FeO^*]^2 \tag{7.12}$$

7.4 Estimation of unknown parameters

The model described in section 7.3 contains a number of unknown parameters. The scrap melting rate (a_{scrap}) was chosen in such a way, that all scrap has become liquid at 70-80 % of the total batch time. The temperature drop due to the addition of scrap at the start of the batch (ΔT) was estimated using three batches in which the temperature was measured multiple times during the batch. The modeled and measured temperatures for these batches are shown in figure 7.4. The carbon monoxide to carbon dioxide ratio (p_{CO2}) was chosen as the average measured ratio during the batch, measured with waste gas analysis. The reaction rate constant of the oxidation of silicon and titanium ($k_{Si,Ti}$) was chosen in such a way, that the modeled and measured accumulation rate of oxygen correspond at the beginning of the batch.
The reaction rate constant (k_0) of the decarburization reaction can be estimated with a proportional-estimator.

$$(k_0)_i = (k_0)_{i-1} + g(\frac{dC}{dt}_{measured} - \frac{dC}{dt}_{calculated})_{i-1} \tag{7.13}$$

Where g is the gain and i is a discrete time instant. The values for a, b, c and E_a are the same as in the previous chapter. The activation energy of

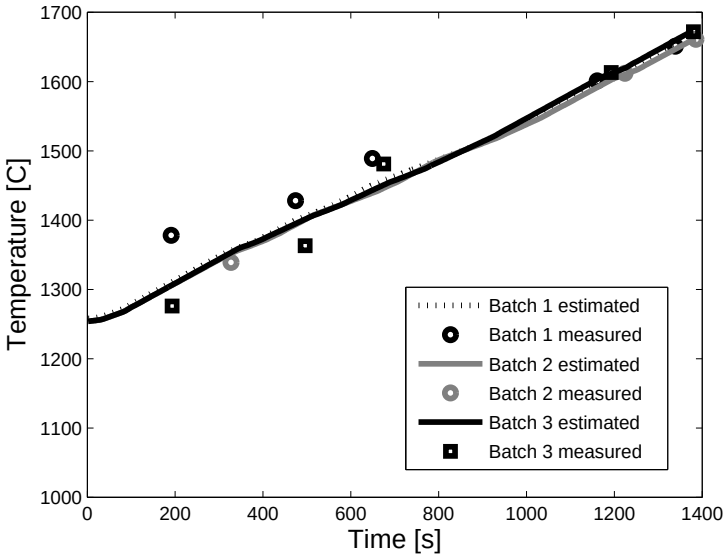

Figure 7.4: Fit of the modeled temperature (equation 7.1) for three batches in which the temperature was measured multiple times during the batch.

the decarburization reaction (E_a) has a value for which the estimated reaction rate constant of the decarburization reaction (k_0) remains constant during the batch if there is no change in input variables such as the lance height and oxygen blowing rate. The parameters a, b, c and k_{0eq} have a value for which the difference between the estimated reaction rate constant (equation 7.13) and the modeled reaction rate constant (equation 7.9) is minimized.

7.5 Model Evaluation

The stated model objective and model requirements are that the dynamic model should at least describe the carbon concentration and the temperature during the batch and that the dynamic model should be verifiable with continuous measurements. The fit of a modeled dynamic signal can be represented

by the variance accounted for (VAF):

$$VAF = 100(1 - \frac{var(\hat{y} - y)}{vary}) \tag{7.14}$$

Where var is the variance, $\hat{y}$ is the model value and y is the measured value. The modeled temperatures can only be verified for the three batches in which the temperature was measured intermittently. The variance accounted for in the temperature for these three batches is 96 %. In figure 7.4 it is shown that measured and modeled bath temperatures correspond well during the entire batch. The average variance accounted for for the decarburization rate and the accumulation rate of oxygen for a collective of over 700 batches is 74% and 63% respectively. The measured and the modeled decarburization rate are shown in figure 7.5. The modeled decarburization rate and accumulation

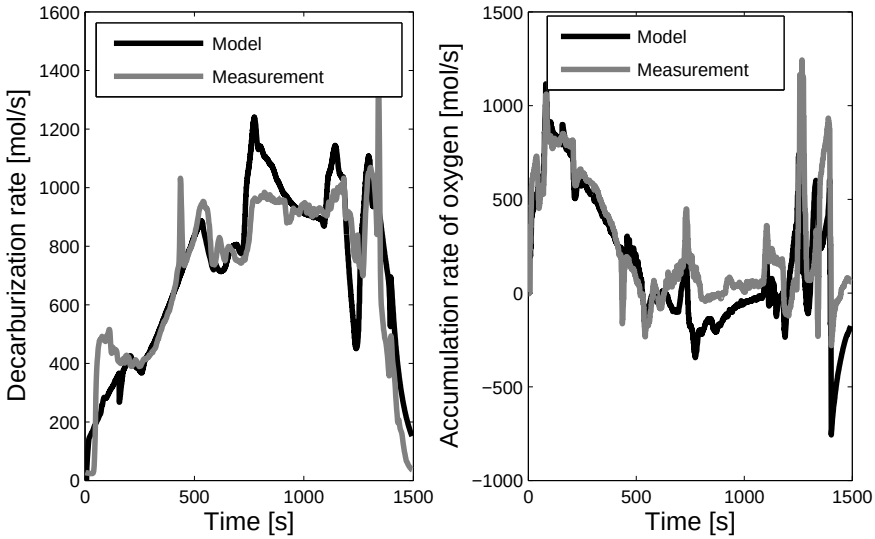

Figure 7.5: Measured and predicted decarburization rate and accumulation rate of oxygen of a typical batch.

rate of oxygen follow the trends in the measured signals well. The described dynamic model predicts the carbon concentration and bath temperature. The dynamic model is verified with continuous measurements. The dynamic model therefore meets the model objectives and requirements.

7.6 Results

Not only the general trend in the decarburization rate and accumulation rate of oxygen as described in section 2 is followed. Also the changes in the decarburization rate and accumulation rate of oxygen caused by changes in control variables are followed well. The lance height, oxygen blowing rate and the addition rate of iron ore corresponding to the batch shown in figure 7.5 are shown in figure 7.6. In the batch shown in figure 7.5 the lance height and oxy-

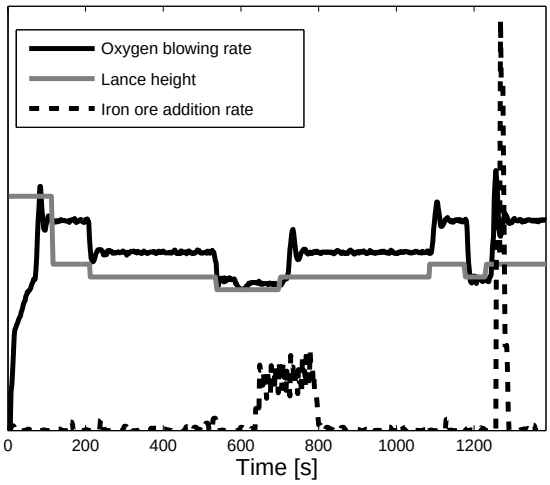

Figure 7.6: Lance height, oxygen blowing rate and iron ore addition rate corresponding to decarburization rate and accumulation rate shown in figure 7.5.

gen blowing rate have been changed simultaneously. When the lance height was increased, the oxygen blowing rate was increased as well and when the lance height was decreased the oxygen blowing rate was decreased as well. In equation 7.9 it is shown that both changes have an opposite effect on the decarburization rate. In this case the effect of the oxygen blowing rate is the largest. The effects can be seen in both measurement and model. At around 250 [s] the oxygen blowing rate was decreased, this caused a decrease in decarburization rate. Between 550 and 700 [s] and again between 1200 and 1300 [s] the oxygen blowing rate was decreased causing a decrease in decarburization

rate. At around 1100 [s] the oxygen blowing rate was increased. This caused an increase in the decarburization rate. Between 600 and 800 [s] iron ore is added. This causes an increase in the decarburization rate which can be observed for both the measurement and the model.
With the dynamic model the change in steel and slag composition during the batch can be calculated. A typical trajectory of the steel and slag composition is shown in figure 7.7. The calculated steel and slag composition are similar

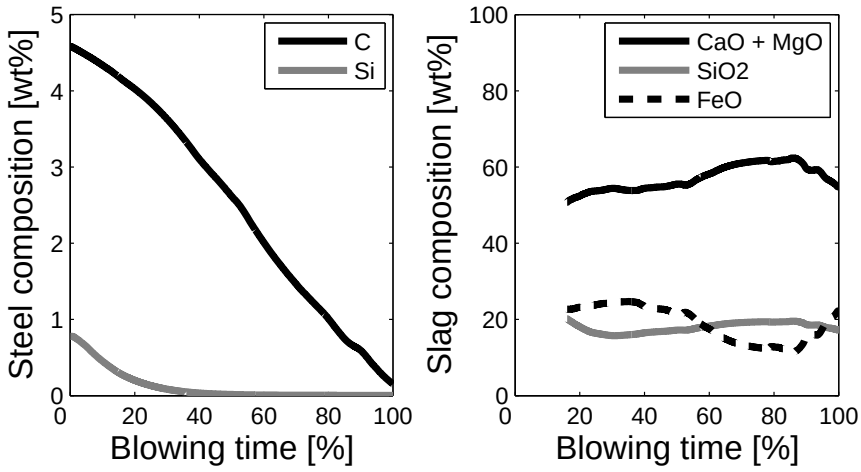

Figure 7.7: Predicted steel and slag composition for a typical batch.

to those found in the literature [7]. The silicon is almost completely oxidized in the first few minutes of the batch and during the entire batch a constant decrease in carbon concentration can be observed. Also similar is the typical change in iron oxide concentration, which is high in the first part of the batch, then reduces and increases again in the last part of the batch.
It would be of interest to compare the accuracy of prediction of the carbon concentration and the bath temperature of the dynamic model with the static models used to calculate necessary raw material input described in the literature [1]. The accuracy of prediction of both models at the intermediate sublance measurement is compared in table 7.1. The standard deviation of the static model is lower than that of the dynamic model. This is according to expectation since the level of detail of the static model is much higher than

Table 7.1: Accuracy of prediction of carbon composition and temperature at sublance measurement of the static and the dynamic model.

	static model	dynamic model
std carbon [.10^{-3}w%]	52-62	95
std temperature [K]	11.6-11.7	11.6-11.7

that of the dynamic model. The dynamic model should therefore be used in combination with the static model.

7.7 Conclusions

The calculated and measured decarburization rate and accumulation rate of oxygen correspond well during the entire batch, as can be seen in figure 7.5. The variance accounted for in the decarburization rate and the accumulation rate of oxygen is 74% and 63% respectively. Also the calculated steel and slag compositions during the batch are similar to those measured in earlier publications. It can therefore be said that the important dynamic phenomena that influence the carbon concentration of the bath have successfully been modeled. The accuracy of prediction of the static model is higher than that of the dynamic model. The dynamic model should therefore be used in combination with the static model, in which the static model is used to calculate the necessary raw material input and the dynamic model is used to describe the temperature and the steel and slag composition during the batch.

Bibliography

[1] A.B. Snoeijer, P. Mink, A. Overbosch, M. Hartwig, H. ter Voort, J.P. Brockhoff, Improvement of converter process Consistency at BOS no. 2, Corus IJmuiden, In: *5th European Oxygen Steelmaking Conference*, Aachen (2006), 186-193

[2] E. Graveland-Gisolf, P. Mink, A. Overbosch, R. Boom, G. de Gendt, B. Deo, Slag droplet model a dynamic tool to simulate and optimize conditions in BOF, *Steel research int.*, **74**(2003), 125-130

[3] C. Blanco, E. Garcia, M. Rendueles, L.F. Sancho, M. Diaz, Analysis of kinetic data in industrial steel converter for the operation control, In: *5th European oxygen steelmaking conference*, Aachen (2006), 115-122

[4] C. Chigwedu, J. Kempken. W. Pluschkell, A new approach for the dynamic process simulation of the BOF-process, *5th European Oxygen steelmaking conference*, Aachen (2006), 363-371

[5] P. van Lith, Hybrid Fuzzy-First principles modelling, PhD thesis University of Twente (2002)

[6] D.N. Ghosh, Kinetics of decarburization of Fe-C melts, part 1 high carbon levels, *Ironmaking and steelmaking*, (1975) no. 1, 36-44

[7] R. Boom, B. Deo, Fundamentals of steelmaking metallurgy, Prentice Hall International, Hemel Hempstead (1993)

8

Statistical slop prediction model

Slopping or foam overflow is a problem in basic oxygen steelmaking. Slopping can be prevented if it can be predicted by a model. In the literature research has been published when slopping occurs during a batch and which factors affect the foam height in steady state experiments. In this chapter both types of information are combined in a statistical two layer hierarchical slop prediction model.
The inputs of the presented model are the raw material input data and the physical properties of the slag, which were estimated with a dynamic model, which has been described in chapters 6 and 7. The first hierarchical layer predicts when slopping occurs during a batch based on boolean expressions. The second hierarchical layer predicts the probability of slopping based on a logistic model. The resulting slop prediction model is relatively simple, using only a small number of input variables. Nevertheless it predicts 73% of the slopping batches and 71% of the batches that do not slop correctly.

8.1 Introduction

In basic oxygen steelmaking small gas bubbles are created due to the oxidation of large amounts of carbon. These gas bubbles rise through a slag phase thus creating a foam. Slopping or foam overflow can be a major problem in

converter operation.
In a foam the gas bubbles are separated by thin films also called Plateau borders [1; 2]. Gravity causes the liquid to drain out of the Plateau borders, reducing the thickness of the liquid film at the top of the foam thereby eventually causing the foam bubbles to collapse. The rate of foam collapse depends on the thickness of the Plateau borders at the top of the foam and thus on the physical properties of the slag. The rate of foam formation depends on the rate of gas formation.
Some research has been conducted on when slopping occurs during a batch [3]. Furthermore, many steady state experimental studies have been performed to investigate the factors that influence the foam height [4; 5; 6; 7; 8]. One of the ways to prevent slopping is by predicting it based on a model that combines the knowledge of foaming described in the literature. The information available on slopping is twofold. On the one hand information is available on when slopping occurs and on the other hand it is known which factors influence the foam height. These two types of information can best be combined in a two layer hierarchical model.
A problem in modeling of slopping is that neither the foam height itself, nor the physical properties that influence the foam height can be measured continuously and they are therefore not exactly known during the batch. Although the physical properties that influence the foam height have been identified with steady state experiments, it is not exactly known how all these factors combined influence the foam height [4], nor can the steady state experiments directly be used to develop a model [9]. Since the available physical knowledge is not precise, the two layers of the hierarchical slop prediction model can best be described using statistical methods.
How slopping can be predicted using the available physical knowledge is described in this chapter. First the theory on slopping is described. Subsequently the knowledge when slopping occurs and which factors affect it is used to construct a slop prediction model. In the following sections the results are discussed and the conclusions are summarized.

8.2 Theory

Some research has been done when slopping occurs during a batch [3]. Chernyatevich et al. [3] have found that, with a constant oxygen supply rate and lance

height above the bath, the maximum level of the foam is usually attained on the termination of the vigorous oxidation of silicon when the carbon elimination reaction is still not intensively developed and the slag has a high iron oxide content and is fluid. Furthermore they found, that a change in the level of the lance, a change in the oxygen blowing rate and the addition of oxidants, such as iron ore, can cause the onset of slopping.
Much research has been done to identify why some batches slop and others do not. Most researchers conducted steady state experiments in which foam is generated by bubbling a gas through a nozzle. They changed variables such as slag composition, slag temperature and bubble rate and studied the influence on the steady state foam height. In these experiments it was found that an increase in slag temperature decreased the foam height [4; 6; 7; 8]. It was also found that the slag composition has a significant influence on the foam height. An increase in iron oxide concentration, for instance, was found to decrease the foam height [4; 7]. Another important factor influencing the foam height is the size and amount of particles present. Large particle of e.g. cokes and coal ($> 1mm$) were found to decrease the foam height [5; 8], while small particles were found to increase the foam height [6; 8].
Since it is difficult to measure the physical properties of the slag continuously in basic oxygen steelmaking, some researchers have focussed on predicting the slop sensitivity of an entire batch based on raw material input data instead [10].

8.3 Modeling

Information on when a batch slops on the one hand and information on which factors influence the probability of slopping on the other hand can best be combined in a two layer hierarchical model as is shown in figure 8.1. In a campaign of 1006 batches the instances of slopping were identified using camera observation as described in chapter 4. Of the 1006 batches 42% slopped and some of the slopping batches slopped multiple times during the batch. In figure 8.2 the times at which the batches start to slop are shown. Most of the slopping occurrences (61%) start around 300 to a little before 500 [s] after the start of the batch. These slopping occurrences coincide with the termination of silicon oxidation and the start of carbon oxidation. The remainder of slopping occurrences (39%) start after this period when oxidation of carbon is in full

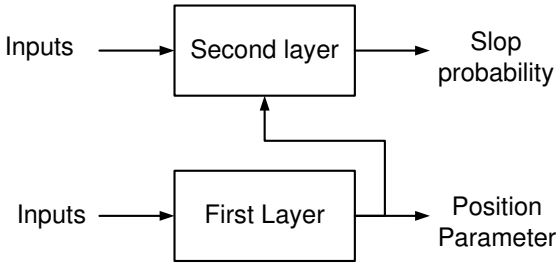

Figure 8.1: Two layer hierarchical slop prediction model.

progress. About half of the slopping batches that occur when oxidation of carbon is full progress are directly preceded by a change in lance height, a change in oxygen blowing rate or by the addition of iron ore. The observation, that most slopping occurrences start at the termination of silicon oxidation and that of the remaining slopping occurrences many are preceded by changes in lance height, oxygen blowing rate or the addition of iron ore is in accordance with the findings of Chernyatevitch [3].
Since the majority of slopping batches start to slop at the termination of the oxidation of silicon, this type of slopping batch will be modeled. The time at which slopping occurs is well defined and can best be modeled by a boolean expression.

$$\text{if } D < E \text{ Position} = 1 \tag{8.1}$$

$$\text{if } D \geq E \text{ Position} = 0 \tag{8.2}$$

In which Position is a parameter which is either 0 or 1 and which describes whether slopping can occur at a given time. The first layer of the model thus states whether slopping could occur at a certain time during the batch.
The raw material input data as well as the physical properties of the slag, such as its composition and temperature, have been shown to influence the foam height. Both the physical properties of the slag at the onset of slopping and the raw material input of the batch can thus be used as inputs for the second layer of the hierarchical model. Since the probability of slopping should in reality always remain between 0 and 1, the probability of slopping can best be modeled using a logistic model [11].

$$\eta = b_1 + b_2\text{Position} + b_3x_1 + ... + b_{n+2}x_n \tag{8.3}$$

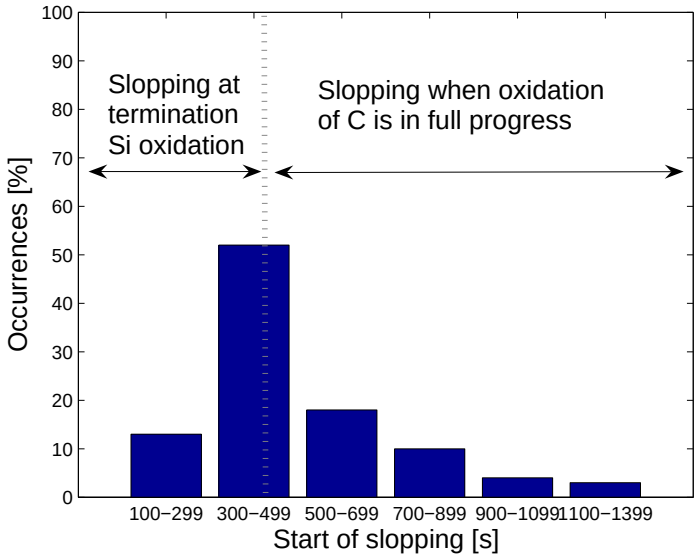

Figure 8.2: Observed start of slopping.

$$P = \frac{e^{\eta}}{1 + e^{\eta}} \tag{8.4}$$

In which P is the probability of slopping, η is a regression parameter for slopping, x_1 till x_n are the input variables and b_1 to b_{n+2} are regression coefficients.

8.4 Results

Unfortunately the physical properties of the slag can not be measured continuously. The physical properties can however be estimated using the dynamic process model described in chapters 6 and 7. To reduce the model error the measured decarburization rate was used to estimate the reaction rate constant of the decarburization reaction in this model. The estimated slag composition and temperature of a typical batch and the time at which this batch slops are shown in figure 8.3. The batch starts to slop just after the oxidation of silicon. In figure 8.3 it can be seen that this period coincides with a maximum in iron oxide content. The boolean expression in the first layer of the model therefore

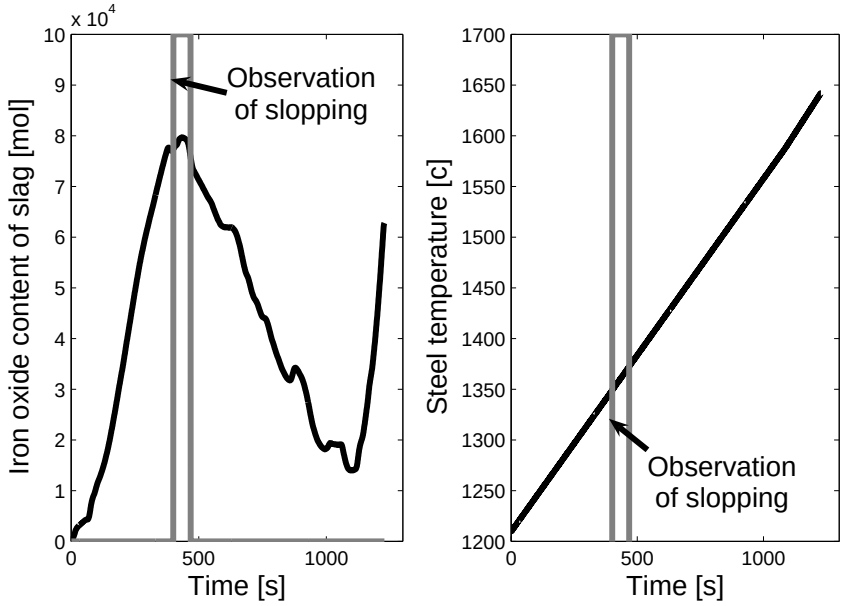

Figure 8.3: Iron oxide content and temperature during the batch as well as when slopping occurs.

evaluates whether the iron oxide content is near a local maximum.

$$\text{if } (FeO_{localmax} - FeO) < \epsilon \text{ Position} = 1 \tag{8.5}$$

$$\text{if } (FeO_{localmax} - FeO) \geq \epsilon \text{ Position} = 0 \tag{8.6}$$

Where $FeO_{localmax}$ is the iron oxide content in the local maximum and ϵ is a predefined error margin. Using this expression 76% of the calculated slop positions overlap with the observed slop positions. In the other batches slopping occurs near the calculated slop position.
The second layer of the hierarchical model has been constructed using a bottom up approach. Only those physical properties and raw material input data that improve the accuracy of the model significantly have been added. The second layer of the model is defined as:

$$\eta = b_1 + b_2\text{Position} - b_3[FeO^*] - b_4\text{Heavyscrap} - b_5[C^*] \tag{8.7}$$

$$P = \frac{e^{\eta}}{1 + e^{\eta}} \tag{8.8}$$

In which $[FeO^*]$ is the molar iron oxide concentration, Heavyscrap is the weight of one of the scrap types, $[C^*]$ is the carbon concentration in the steel, η is a regression parameter for slopping and P is the probability of slopping.
Since the slop prediction model is a statistical model, the relationship between the inputs and the slop probability need not be causal. However, it would be interesting to see if the influence of the inputs on the slop probability in the model can be explained physically.
It can be seen, that in the model, the iron oxide concentration has a negative influence on the slop probability. This is consistent with findings in steady state experiments, in which it was found that an increase in iron oxide concentration decreases the foam height [4; 7].
The model also states a negative influence of the charged amount of heavy scrap on the slop probability. The dynamic model used, bases its estimation of the temperature on a linear approximation as can be seen in figure 8.3. This is a simplification and in reality the amount and types of scrap used influence the temperature. Simulation studies by Graveland et al. [12] have shown, that the use of a higher percentage of heavy scrap causes a higher temperature in the first part of the batch. The negative influence of the heavy scrap weight on the slop probability is therefore consistent with the findings in steady state experiments, in which it was found that an increase in temperature decreases the slop probability [4; 6; 7; 8].
The model furthermore states a negative influence of the carbon concentration in the steel on the slop probability. The cause for this relationship is not completely clear, but since the carbon concentration and the process time are correlated, it may point towards an influence of the process time instead.
For some batches in the collective the dynamic model could not be used because necessary input data was not available. Of the collective of 1006 batches the slop probability could be calculated for 460 non-slopping batches and for 172 batches that only slopped at the termination of the oxidation of silicon. In figure 8.4 the calculated slop probability of a typical batch is shown. In this figure, it can be seen that the slop probability is highest when slopping is observed. If it is assumed, that slopping only occurs when the probability of slopping is above 0.60, then 73% of the slopping batches and 71% of the non-slopping batches are correctly detected. Slop detection is a type of binary classification and can be presented in a truth table [13] as is shown in table

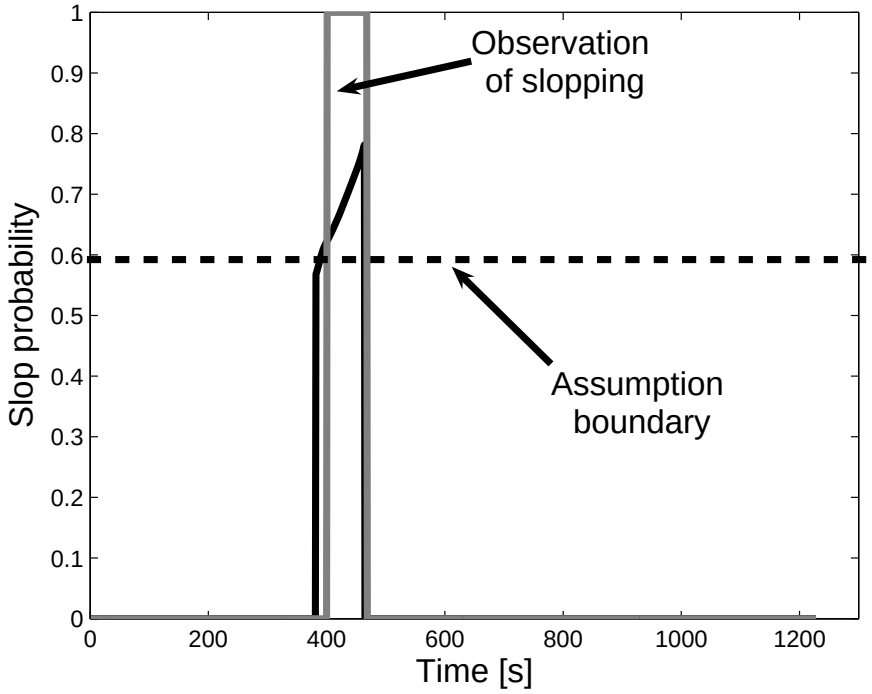

Figure 8.4: Calculated slop probability of a typical batch.

8.1. The truth table and its properties are more extensively covered in chapter 4. In the columns the classifying property is shown. The column marked True represent the batches that slop at the termination of silicon oxidation and the column marked False represents the non-slopping batches. In the rows the prediction of the slop probability model is shown. The row marked Positive indicates that slopping is predicted and the row marked Negative indicates that slopping is not predicted. Of the 172 slopping batches 126 were predicted to be slopping and 46 were predicted to be non-slopping. Of the 460 non-slopping batches 133 were predicted to be slopping and 327 were predicted to be non-slopping.

Table 8.1: Truth table for slop prediction model.

	True (slopping)	False (non-slopping)
Positive (slopping predicted)	126	133
Negative (slopping not predicted)	46	327

8.5 Conclusions

The majority of the slopping occurrences (61%) coincide with the termination of silicon oxidation. This type of slopping batch has been modeled using a statistical two layer hierarchical model. As input variables the raw material input data as well as the physical properties of the slag, as estimated by a dynamic model, were used. The slop probability model is simple, using only a small number of input variables. Nevertheless, it predicts 73% of the slopping batches and 71% of the batches that do not slop correctly.

Bibliography

[1] P. Kozakevitch, Foams and emulsions in steelmaking, *Journal of metals*, **July**(1969), 57-65

[2] D.L. Weaire, S. Hutzler, The physics of foams, Clarendon Press, Oxford (1999)

[3] A.G. Chernyatevich, E.Y. Zarvin, N. Borisov, I. Volovich, Mechanisms of the formation of ejections and spatter from basic oxygen furnaces, *Steel in the USSR*, **10**(1976), 54-59

[4] M. Zamalloa, T. Utigard, Slag foaming in FeO-CaO-SiO2 slags, In: *1992 steelmaking conference proceedings*, Toronto (1992), 581-590

[5] Y. Zhang, R.J. Fruehan, Effect of carbonaceous particles on slag formation, *Metallurgical and materials transactions B*, **26B**(1995), 813-819

[6] K. Ito, R.J. Fruehan, Study on the foaming of CaO-SiO2-FeO slags Part 1 Foaming parameters and experimental results, *Metallurgical transaction B*, **20B**(1990), 509-514

[7] S. Jung, R.J. Fruehan, Foaming characteristics of BOF slags, In: *2000 ironmaking conference*, Pittsburgh (2000), 517-527

[8] K. Wu, W. Qian, S. Chu, Q. Niu, H. Luo, Behavior of slag foaming caused by blowing gas in molten slags, *ISIJ international*, **40**(2000), 954-957

[9] A. Kapilashrami, M. Gornerup, A.K. Lahiri, S. Seetharaman, Foaming of slags under dynamic conditions, *Metallurgical and materials transactions B*, **37B**(2006), 109-117

[10] A.B. Snoeijer, P. Mink, A. Overbosch, M. Hartwig, H. ter Voort, J.P. Brockhoff, Improvement of converter consistency at BOS no. 2 Corus IJmuiden, In: *5th European oxygen steelmaking conference*, Aachen (2006), 186-193

[11] P. McCullagh, J.A. Nelder, Generalized linear models 2nd. ed., Chapman and Hall, London (1989)

[12] E. Graveland-Gisolf, P. Mink, A.B. Snoeijer, E. Barker, R. Boom, D. Dixit, B. Deo, The new generation slag droplet model, In: *SCANMET II, 2nd international conference on process development in Iron and Steelmaking*, Lulea, (2004),

[13] D.G. Altman, J.M. Bland, Diagnostic tests 1: sensitivity and specificity, *BMJ*, **308**(1994), 1552

9

Theoretical dynamic optimization

In recent years there is a trend to increase the production capacity in steelmaking. This has mostly been achieved by the purchase of new equipment, improvement of logistics and improvement of maintenance. Alternatively, the production capacity can be increased by minimization of the batch time in basic oxygen steelmaking, if this process step is the bottleneck. In this chapter minimization of the batch time by application of dynamic optimization is discussed. Using the dynamic model described in chapters 6 and 7 and a constraint to prevent slopping described in chapter 8, it is derived, that dynamic optimization results in a bang-bang control strategy in which the lance height and the oxygen blowing rate are either at their minimum or their maximum value.
Currently, the set point of control variables are based on standard operating procedures and were developed during many years of practical experience. In these standard operating procedures a certain maximum oxygen blowing rate is used. The oxygen lance is, however, able to supply oxygen at a higher rate. The optimal strategy reduces the batch time with 61 [s] or 4.6% on average. When the higher maximum oxygen blowing rate is used, the batch time is reduced with 165 [s] or 12.4% on average. Due to modeling errors, the reduction in batch time may be different when the calculated control strategy is applied in practice. The calculated optimal strategy, does, however, indicate the direction in which the currently used control strategy can be changed to reduce the batch time.

9.1 Introduction

In industry, processes can be optimized to achieve certain goals, such as the minimization of energy consumption, the minimization of costs or the minimization of production time. Optimization problems can be divided into static optimization problems and dynamic optimization problems. Static optimization problems consist of determining the optimal value of a parameter or variable, while dynamic optimization problems consist of determining the optimal trajectory of a parameter or variable and thus the optimal value of that parameter or variable in time [1; 2; 3].
Both static and dynamic optimization of steelmaking processes is covered in the literature [4; 5; 6; 7; 8]. Static optimization is used to either minimize production costs by optimizing material input data [4], or to minimize the emission of CO_2 by optimizing scrap input [5]. Dynamic optimization is mainly applied to the operation of the Electric Arc Furnace (EAF) [6; 7; 8]. Dynamic optimization of EAF operation has been used to optimize the nett-benefit of post combustion, to minimize the air-in leakage and to minimize production costs. Although Cordova et al. [7] mention their intention to dynamically optimize the use of post-combustion oxygen in basic oxygen steelmaking, to our knowledge dynamic optimization has, until now, not been applied to basic oxygen steelmaking.
In recent years there has been a trend to increase the production capacity in steelmaking. This has mostly been achieved by investments in additional equipment, improvement of logistics and by decreasing maintenance time [9; 10; 11; 12]. Minimization of the batch time in the basic oxygen steelmaking converter might contribute to the desired increase in production capacity, if the converter is the bottleneck in production.
In this chapter dynamic optimization of basic oxygen steelmaking with the goal to minimize batch time will be discussed. In the first section the problem formulation is given. In second section the optimal control trajectories for the oxygen blowing rate and the lance height are discussed. Subsequently the results of application of these optimal control trajectories are shown. The following sections contain a discussion and the conclusions.

9.2 Problem formulation

Optimization problems consist of an objective function, a set of state equations constituting the process model and conditions which, for instance, define the initial value of variables in the model. Some optimization problems also contain constraints [1; 2; 3]. The objective function, the state equations, the conditions and constraints are discussed in subsequent subsections.

9.2.1 Objective function

The objective is to minimize the production time of a particular batch. This can be described by the minimum time problem:

$$J = \int_{t0}^{tf} dt = t_f - t_0 \tag{9.1}$$

In which J is the objective function, t_0 is the time at the start of the batch and t_f is the time at the end of the batch.

9.2.2 State equations

In chapters 6 and 7 a dynamic model of the basic oxygen steelmaking process is described, that can be used for dynamic optimization. This dynamic model is based on a given data set and is generally only valid for a range of control variables that occur within this data set. The addition patterns and bottom blowing patterns have been developed using many years of practical experience to ensure that additions dissolve and that converter mixing is adequate. The influence of converter mixing on the process and the influence of process variables on the dissolving rate of additions is not taken into account in the mentioned dynamic process model. In order to assure that the additions dissolve and that mixing is correct, bottom blowing and addition patterns should not be changed when optimizing. The control variables are therefore the oxygen blowing rate (VO_2) and the lance height (H_{lance}).

The state equations describing the model are:

$$
\begin{aligned}
f1 = \quad \dot{T} \quad &= a_T(t) VO_2 && (9.2)\\
f2 = \quad \dot{FeO} \quad &= 2VO_2 + A_{FeO} \\
&\quad -(1 + pCO_2)(a + bVO_2 - cH_{lance}) e^{\frac{-Ea}{RT}} [C^*][FeO^*] && (9.3)\\
&\quad -2k_{Si}[Si^*][FeO^*]^2 - 2k_{Ti}[Ti^*][FeO^*]^2 \\
f3 = \quad \dot{CaO} \quad &= A_{CaO}(t) && (9.4)\\
f4 = \quad \dot{MgO} \quad &= A_{MgO}(t) && (9.5)\\
f5 = \quad \dot{SiO2} \quad &= A_{SiO2}(t) + k_{Si}[Si^*][FeO^*]^2 && (9.6)\\
f6 = \quad \dot{TiO2} \quad &= A_{TiO2}(t) + k_{Ti}[Ti^*][FeO^*]^2 && (9.7)\\
f7 = \quad \dot{C} \quad &= S_C(t) - (a + bVO_2 - cH_{lance}) e^{\frac{-Ea}{RT}} [C^*][FeO^*] && (9.8)\\
f8 = \quad \dot{Si} \quad &= S_{Si}(t) - k_{Si}[Si^*][FeO^*]^2 && (9.9)\\
f9 = \quad \dot{Ti} \quad &= S_{Ti}(t) - k_{Ti}[Ti^*][FeO^*]^2 && (9.10)\\
f10 = \quad \dot{Fe} \quad &= S_{Fe}(t) - 2VO_2 \\
&\quad +(1 + pCO_2)(a + bVO_2 - cH_{lance}) e^{\frac{-Ea}{RT}} [C^*][FeO^*] && (9.11)\\
&\quad +2k_{Si}[Si][FeO]^2 + 2k_{Ti}[Ti^*][FeO^*]^2
\end{aligned}
$$

Where fn are the state equations, $A_x(t)$ are the addition rates for the oxides, $S_x(t)$ the scrap dissolving rates for the specific element, T is the steel temperature, CaO, MgO, SiO_2, TiO_2, FeO are the calcium oxide, magnesium oxide, silicium oxide, titanium oxide and iron oxide content in the slag, C, Si, Ti, Fe are the steel carbon, silicium, titanium and iron content, a, b and c are constants, Ea is the activation energy, R is the gas constant, $[C^*]$, $[Si^*]$, $[Ti^*]$ are the carbon, silicon and titanium molar concentration in the steel, $[FeO^*]$ is the molar iron oxide concentration in the slag, k_{Si} and k_{Ti} are the reaction rate constants for silicium and titanium and pCO_2 is the carbon mono oxide carbon dioxide ratio in the waste gasses.

9.2.3 Conditions

The initial conditions of all the states are known and can be calculated based on batch raw material data.

$$x_i(t_0) = x_{i0} \qquad (9.12)$$

At the end of the batch the demanded carbon concentration should be reached.

$$X_C(t_f) = X_{C,demanded} \tag{9.13}$$

Where $X_{C,demanded}$ is the demanded carbon concentration.

9.2.4 Constraints

There are a number of constraints necessary. The model is only valid in a certain range. Therefore, the control variables need to be between predefined values.

$$a_1 < VO_2 < a_2 \tag{9.14}$$

$$a_3 < H_{lance} < a_4 \tag{9.15}$$

Where a_1, a_2, a_3, a_4 are the bounds in the control variables. In addition, slopping must be prevented. A slop prediction model was described in chapter 8.

$$\eta = b_1 + b_2 Position - b_3[FeO^*] - b_4 \text{Heavyscrap} - b_5[C^*] \tag{9.16}$$

Where b_1, b_2, b_3, b_4, b_5 are constants, Position is a variable which depends on the value of FeO, Heavyscrap is the weight of the heavy scrap charged and η is a regression parameter for slopping. The slop probability (P) can be expressed as:

$$P = \frac{e^\eta}{1 + e^\eta} \tag{9.17}$$

If the slop probability exceeds 0.60 it is probable that slopping occurs. An inequality constraint to prevent slopping can therefore be described as:

$$P \leq 0.6 \rightarrow g(x) = 0.6 - P \geq 0 \tag{9.18}$$

Where $g(x)$ is the inequality constraint, which depends on the states. There are several ways to incorporate inequality constraints in the optimization problem. One approach is to define a new state variable [1].

$$f11 = g(x)^2 k \tag{9.19}$$

Where k is a step function defined by:

$$k = K \text{ if } g(x) \geq 0 \tag{9.20}$$

$$k = 0 \text{ if } g(x) < 0 \tag{9.21}$$

Where K is a constant.

9.3 Optimal control strategy

In optimization problems Pontryagins minimum principle can be used to find the optimal control trajectory. The minimum principle states that a necessary condition for solving a dynamic optimization problem is that the controls should be chosen such as to minimize the Hamiltonian. An introduction to this principle can be found in books by Ramirez, Kamien and Schwartz and Agrawal and Fabien [1; 2; 3].
The Hamiltonian is defined as [1]:

$$H = F(x, u, t) + \Sigma_{i=1}^{i=N} \lambda_i f_i \tag{9.22}$$

Where H is the Hamiltonian, f_i are the state equations and λ_i are the costates. The controls appear linear and bounded in the Hamiltonian, implying that the optimal value for the controls are either at their minimum or their maximum value [1]. During the batch, these control variables may switch from their minimum value to their maximum value and vice versa. This type of control strategy is commonly referred to as bang-bang control.
The goal is to reach the demanded carbon concentration as quickly as possible, in such a manner that slopping does not occur. The batch time is at its minimum when the oxygen blowing rate is at it's maximum value and the lance height is at its minimum value. The lance height only has a small effect on the batch time.
Slopping occurs during the slop sensitive period, when the iron oxide content in the slag has just reached a maximum. The slop probability depends on the amount of heavy scrap charged, the iron oxide concentration in the slag and the carbon concentration in the steel during this slop sensitive period. By changing the control variables the iron oxide concentration and the carbon concentration can be influenced. However, the influence of the controls on the iron oxide concentration is largest. Slopping is less likely to occur when the iron oxide concentration in the slag is high during the slop sensitive period.
In figure 9.1 the iron oxide concentration for three different control trajectories for a typical batch is shown. The black line shows the calculated iron oxide concentration in the slag, when the oxygen blowing rate is $4.2.10^4$ $[nm^3/h]$ and the lance height is 160 [cm]. In the first period of the batch the blown oxygen oxidizes part of the iron and the iron oxide concentration increases until it reaches a maximum in the slop sensitive period. Then part of the iron oxide is used to oxidize carbon and the iron oxide concentration decreases. At

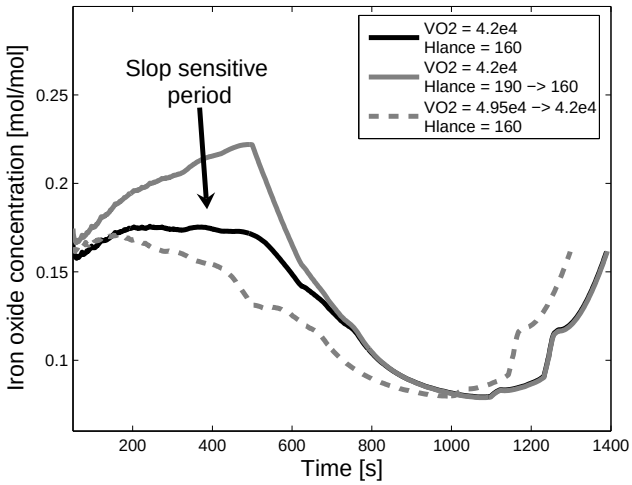

Figure 9.1: Influence of steps in lance height and oxygen blowing rate on iron oxide concentration in the slag.

the end of the batch part of the blown oxygen is used to oxidize iron, due to the diminished carbon concentration, and the iron oxide concentration again increases.

The gray line shows the calculated iron oxide concentration in the slag, when the oxygen blowing rate is $4.2.10^4$ $[nm^3/h]$ and the lance height is 190 [cm] and is reduced to 160 [cm] at t=500 [s]. It can be seen, that the higher lance height during the first part of the batch causes an increased iron oxide concentration in the first part of the batch. It can also be seen, that the batch history with respect to lance height changes does not seem to affect the final batch time.

The dotted gray line shows the calculated iron oxide concentration in the slag, when the oxygen blowing rate is $4.95.10^4$ $[nm^3/h]$ and is reduced to $4.2.10^4$ $[nm^3/h]$ at t=500 [s] while the lance height is 160 [cm]. It can be seen, that the higher oxygen blowing rate during the first part of the batch causes a lower iron oxide concentration in the first part of the batch. It can also be seen that the final batch time is affected by the batch history with respect to changes in oxygen blowing rate.

Since slopping is less likely to occur when the iron oxide concentration in the slag is high, slopping can be prevented by using a high lance height and a low

oxygen blowing rate during the slop sensitive period. To prevent slopping and to minimize the batch time, the lance height should be at its maximum value at the start of the batch and be reduced to its minimum value after the slop sensitive period has elapsed. The oxygen blowing rate must be at its minimum value during the slop sensitive period. However, the duration of the oxygen blowing rate at its minimum value should be kept as short as possible.

9.4 Results

When minimizing the batch time, the oxygen blowing rate and the lance height need to be between predefined boundaries. During normal operation (the standard batch), the oxygen blowing rate is slowly increased at the start of the batch and the lance height is high, due to safety reasons. In the last part of the batch the steel temperature and carbon concentration are measured. To enable this measurement the oxygen blowing rate is lowered. At the start of the batch, the optimized batch should have a similar oxygen blowing rate as the standard batch, for safety reasons. The optimized batch should also have a similar temporary reduction in oxygen blowing rate at the end of the batch as the standard batch to enable the measurement of the steel temperature and carbon concentration.
The models on which the optimization is based are valid in a certain range (oxygen blowing rate between $3.5.10^4$ and $4.95.10^4$ $[nm^3/h]$ and lance height between 150 and 220 [cm]). In the optimal batch, the lance height and oxygen blowing rate should remain between these boundaries. The oxygen lance can, however, supply oxygen up to rates of $5.5.10^4$ $[nm^3/h]$. Since the oxygen blowing rate highly influences the batch time, it would be interesting to explore the influence of using this higher oxygen blowing rate.
In figure 9.2 the standard and the optimal oxygen blowing rate and lance height and the resulting iron oxide concentration and slop probability of a typical batch are shown. All batches look fairly similar to this one. In the standard batch the slop probability exceeds 0.6 at around 440 [s] and slopping occurs. In the optimal batch the maximum lance height is used and additionally the oxygen blowing rate is reduced to its minimum value for a short time to prevent slopping. Both measures cause a higher iron oxide concentration during the slop sensitive period and thereby decrease the slop probability to below 0.6.

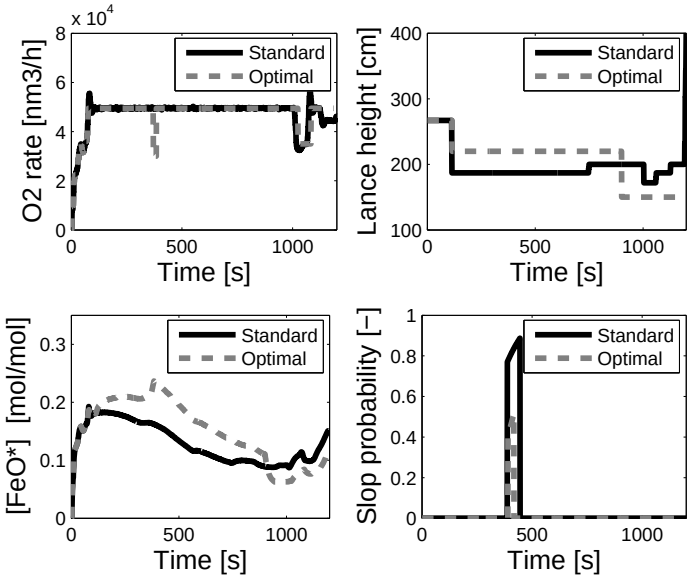

Figure 9.2: Standard and optimal trajectory of a batch where the oxygen blowing rate has to be reduced during the slop sensitive period.

It is interesting to investigate whether the batch time is sensitive to the time at which the oxygen blowing rate is decreased. In figure 9.3 the time at which the oxygen blowing rate is decreased and the corresponding duration of the decrease in oxygen blowing rate for which slopping is prevented are shown. If the oxygen blowing rate is not reduced during the batch, slopping is predicted at 440 [s]. It is not possible to prevent slopping by decreasing the oxygen blowing rate after this time, thus the region after 440 [s] is infeasible. In the region from 140 [s] before the slop sensitive period up to just before the slop sensitive period itself the required duration of the oxygen blowing rate decrease is between 15 and 25 [s]. The batch time will be only slightly different for this region and the batch time is therefore only moderately sensitive to the time at which the oxygen blowing rate is reduced.
It seems counterintuitive that a short decrease in oxygen blowing rate a long time before the slop sensitive period would prevent slopping. Because, when the oxygen blowing rate is increased again the slop sensitive period has not been passed. Figure 9.3, for instance, suggests, that slopping can be prevented

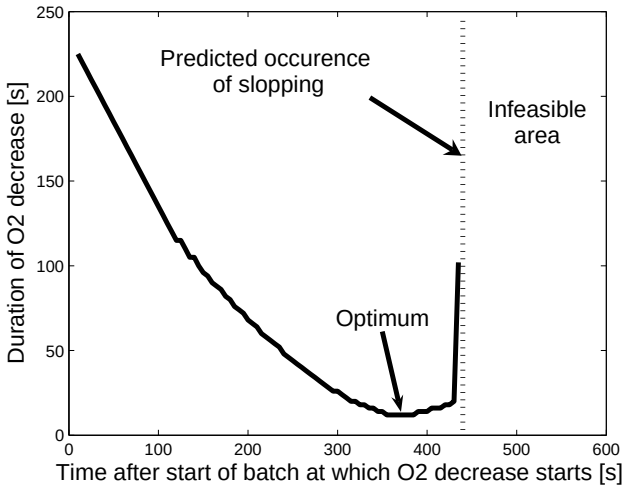

Figure 9.3: Start and duration of oxygen blowing rate at the minimum value.

if the oxygen blowing rate is decreased for 25 [s] at t = 310 [s]. This means, that if the suggested preventative measure is taken, the oxygen blowing rate is again at its maximum long before the slop sensitive period at 440 [s]. In figure 9.4 the calculated iron oxide concentration is shown for the situation where the oxygen blowing rate is at its maximum during the entire batch and for the situation where the oxygen blowing rate is decreased for 25 [s] at t=310 [s]. It can be seen, that the calculated iron oxide concentration is higher at $t = 440$ [s] for the situation where the oxygen blowing rate has briefly been decreased. The higher iron oxide concentration in the slag causes the difference in the calculated slop probability.

The reduction in batch time that can be achieved by using the optimal trajectory is on average 61 [s] or 4.6% for a maximum oxygen supply rate of $4.95.10^4$ $[nm^3/h]$ and 165 [s] or 12.4% for a maximum oxygen supply rate of $5.5.10^4$ $[nm^3/h]$.

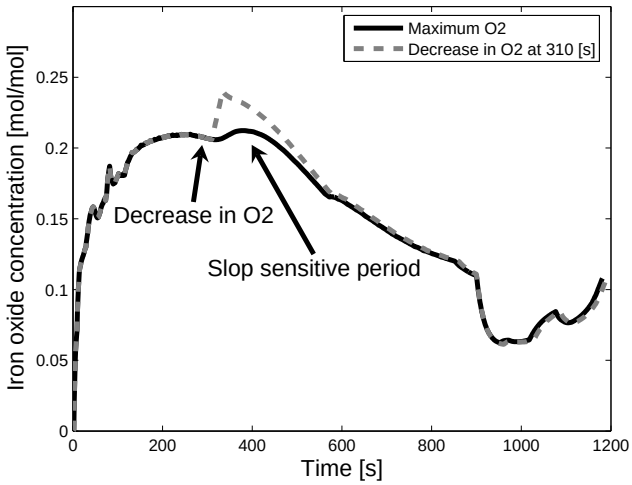

Figure 9.4: Calculated iron oxide concentration in slag for a batch with a maximum oxygen blowing rate and for a batch with a decrease in oxygen blowing rate at $t = 310$ [s] for 25 [s].

9.5 Discussion

The models used for optimization may contain a modeling error. The reduction in batch time, that is stated in this chapter, might therefore deviate from the calculated reduction when implementing the calculated optimal strategy. Furthermore, the used models were estimated based on a data set that only contains standard batches. Optimization changes the control strategy considerably and application of the optimal strategy might cause other unforseen effects. For example, the lime dissolution rate is known to depend on the iron oxide concentration in the slag [14; 15]. The changes in the control strategy have an effect on the iron oxide concentration in the slag (as is shown in figure 9.2). These changes might thus also influence the dissolution rate of lime. Additionally, the difference in control trajectory may cause differences in, for instance, heat losses. These secondary effects have not been taken into account in the model.

9.6 Conclusions

Dynamic optimization of basic oxygen steelmaking results in a control strategy in which controls are either at their minimum or their maximum values. During the batch, these control variables may switch from their minimum value to their maximum value and vise versa.
A high lance height reduces the slop probability, while a short batch time is promoted by a low lance height at the end of the batch. The optimal control strategy for the lance height is thus a strategy in which the lance height is at its maximum value during the first part of the batch and the lance height is switched to its minimum value after the slop sensitive period has elapsed.
The batch time is shortest when the oxygen blowing rate is at its maximum value during the entire batch. However, a low oxygen blowing rate reduces the probability of slopping. The optimal control strategy for the oxygen blowing rate is, therefore, a strategy in which the oxygen blowing rate is at its maximum value during the batch and it is reduced to its minimum value during the slop sensitive period to prevent slopping.
Using the optimal strategy and a maximum oxygen blowing rate of $4.95.10^4$ $[nm^3/h]$ the batch time can on average be reduced with 61 [s] or 4.6%. Using a maximum oxygen blowing rate of $5.5.10^4$ $[nm^3/h]$ the batch time can on average even be reduced with 165 [s] or 12.4%. Due to modeling errors, this reduction in batch time may not be fully realizable when the calculated optimal strategy is applied in practice. The calculated optimal strategy, however, indicates the direction in which the currently used control strategy can be changed to reduce the batch time.

Bibliography

[1] W.F. Ramirez, Process control and identification, Academic press inc., Boston (1994)

[2] M.I. Kamien, N.L. Schwartz, Dynamic optimization the calculus of variations and optimal control in economics and management, North-Holland, Amsterdam (1991)

[3] S.K. Agrawal, B.C. Fabien, Optimization of dynamic systems, Kluwer academic publishers, Dordrecht (1999)

[4] H. Gaye, P.V. Riboud, Modele d'optimisation physio-chimique et economique de l'enfournement en acierie al'oxygene, *Revue de metallurgie*, **79**(1982), 131-140

[5] C. Ryman, M. Larsson, Reduction of CO_2 emissions from integrated steelmaking by optimised scrap strategies: Application of process intergration models on the BF-BOF system, *ISIJ International*, **46**(2006), 1752-1758

[6] H.D. Goodfellow, M. Pozzi, J. Maiolo, Dynamic process control and optimization for EAF steelmakers, *MPT international*, **6**(2006), 24-30

[7] E. Cordova, M. Kahn, D. Zuliani, B. Goldberg, J. Maiolo, Advanced dynamic control technology for EAF steelmaking and other combustion processes, *MPT international*, **2**(2007), 28-32

[8] R.D.M. MacRosty, C.L.E. Schwartz, Dynamic optimization of electric arc furnace operation, *AIChE Journal*, **53**(2007), 640-653

[9] O. Bode, R. Bruckenhaus, Optimisation of steelplant logistics at Dillinger Hutte using simulation models, In: *5th European oxygen steelmaking conference*, Aachen (2006), 411-416

[10] J. Brockhoff, P. Broersen, M. Hartwig, H. Pronk, H. ter Voort, R. Mostert, A. Snoeijer, A. Overbosch, Towards 7 million tons of liquid steel per year at BOS2 Corus strip IJmuiden, In: *5th european oxygen steelmaking conference*, Aachen (2006), 417-424

[11] G. Simms, I. Blake, Port Talbot challenges, In: *5th european oxygen steelmaking conference*, Aachen (2006), 425-432

[12] A. Berghofer, R. Kromarek, Salzgitter Flachstahl GmbH increased the efficiency of its BOF shop, In: *5th european oxygen steelmaking conference*, Aachen (2006), 477-485

[13] A.B. Snoeijer, P. Mink, M. Hartwig, H. ter Voort, J.P. Brockhoff, Improvement of process consistency at BOS no. 2 Corus IJmuiden, In: *5th european oxygen steelmaking conference*, Aachen (2006), 186-193

[14] B. Deo, P.K. Gupta, M. Malathi, P. Koopmans, A. Overbosch, R. Boom, Theoretical and practical aspects of dissolution of lime in laboratory experiments and in BOF, In: *5th European oxygen steelmaking conference*, Aachen (2006), 202-209

[15] F. Oeters, R. Scheel, Untersuchungen zur kalkauflosung in CaO-FeO-SiO2-schlacken, *Arch. eisenhuttenwes.*, **45**(1974), 575-580

10

Conclusions

The objective of this thesis is to develop a dynamic control strategy for basic oxygen steelmaking which both reduces the occurrence of slopping and increases the production capacity by reducing the batch time. This control strategy was calculated by dynamic optimization of the process. For dynamic optimization a dynamic process model, that describes the steel and slag composition, the steel temperature and slopping, was developed. Since, the development of such a model would greatly benefit from the continuous measurement of important process variables, their feasibility was investigated as well.

Chapters 1 and 2 contain an introduction and background information.

In chapter 3 the feasibility of the continuous measurement of the steel composition, the slag composition, the steel temperature and the foam height was investigated. Due to extreme process conditions most measurements were infeasible. To develop a dynamic process model, however, continuous reference measurements were needed. For validation of steel and slag composition the decarburization rate and the accumulation rate of oxygen inside the converter were used.

In chapter 4 a slop detection system was presented that can be used for the detection of slopping, since direct measurement of the foam height was not feasible. Images taken by a camera viewing the converter mouth were used to design a slop detection algorithm. The detection algorithm can detect slopping

within 5 seconds for 73% of the slopping batches. Of the non-slopping batches 94% was correctly detected as non-slopping.

The temperature and carbon concentration at the end of the batch are currently predicted by a first principles static model using the raw material additions as inputs. Chapter 5 showed that a PLS model was not a good alternative to replace this static model.

In chapter 6 a dynamic process model for the main blow was developed. This dynamic model, describing the steel and slag composition, consists of a carbon and a iron oxide balance and an additional equation describing the influence of the lance height and the oxygen blowing rate on the amount of iron droplets in the slag. Using this model the measured step responses in the decarburization rate and the accumulation rate of oxygen were described satisfactorily.

In chapter 7 the dynamic process model described in chapter 6 was extended so that it describes the entire batch. The dynamic model predicts the steel temperature, steel composition and slag composition. The model was validated using the measured decarburization rate and accumulation rate of oxygen of which the variance accounted for is 73% and 63% respectively.
The dynamic model is less accurate in the prediction of the steel temperature and steel carbon concentration at the end of the batch than the static model described in chapter 5. The dynamic model should, therefore, be used in combination with the static model.

In chapter 8 a slop probability model was described. It was shown, that the majority of slopping batches can be modeled using a statistical two layer hierarchical model. In the first layer of the model a boolean expression is used to identify the slop sensitive period. In the second layer of the model, a logistic model is used to calculate the probability of slopping. This simple model correctly detects 73% of the slopping batches and 71% of the non-slopping batches.

In chapter 9 basic oxygen steelmaking was dynamically optimized with the goal to minimize the batch time and to prevent slopping. The dynamic model described in chapters 6 and 7 was used as state equations and the slop probability model described in chapter 8 was used as a constraint. It was derived, that dynamic optimization results in a bang-bang control strategy.

Simulations showed, that by using the optimal control strategy, the batch time could be reduced with 4.6%. Because of modeling error, the reduction in batch time might deviate from this calculated reduction when the optimal control strategy is implemented. The calculated optimal control strategy is, however, an indication of how the control variables can be changed to reduce the batch time and to prevent slopping.

Acknowledgements

This thesis would not have been written without the contributions and support of colleagues, family and friends.
I first would like to thank Brian Roffel en Ben Betlem who have been my supervisors during (part of) the project. They have provided me with valuable input and support and have given me the freedom to determine the direction of the research.
Next I would like to thank Wim Prins and Rob Klinge who have been been the contact persons at Danieli Corus. Without their organizational input and financial support the project would not have been possible.
I would also like to thank the members of my promotion committee and my paranimfs for their time. I am honored that you are willing to participate in my promotion.
Furthermore, I would like to thank my co-workers at Corus, Aart Overbosch, Paul Mink, Bert Snoeijer, Elizabeth Graveland and Abha Kapilashrami the experts on the oxygen steelmaking process. The many brainstorm session and the received comment on my work were very inspiring to me. I would also like to thank them and Marcel Hartwig and Hans ter Voort from the OSF2 steelplant, for the provision of plant data.
I would like to thank several people for their contribution to parts of this thesis. Frenk van den Berg and Erwin Spelbos, who work for Corus R&D, for their contribution to the work on slop detection with the CMOS camera, Jean-Paul Fox of the University of Twente for the discussions on how to model slopping and Bastiaan Blankert, who is a former colleague, for the discussion on dynamic optimization. Furthermore, I would like to thank the many students who contributed to this thesis with their masters thesis or their internship. Bart van den Berg, Andreas Pons, Peter Schouten, Laurens van Oostveen, Sander van der Hoorn, Anton Lefeber and Ruud Schols thank you very much

for your hard work.
On a more personal note I would like to thank my direct collegues at the University of Twente Bastiaan Blankert, Edwin Zondervan and Bartie Bruggink-de Braal for the pleasant working atmosphere.
I would also like to thank my parents; Papa en mama bedankt voor jullie interesse en steun, niet alleen tijdens de afgelopen vier jaar maar ook tijdens mijn hele schoolcarriere.
Last but certainly not least I would like to thank Jeroen. Thank you very much for listening to my problems during dinner and the washing up. Especially during the times when I encountered difficulties. Not only your moral support, but also your technical advise has been invaluable to me.

List of symbols

Symbols

a	constant	$[\frac{mol}{s}]$
a_1	boundary	$[\frac{mol}{s}]$
a_2	boundary	$[\frac{mol}{s}]$
a_3	boundary	$[m]$
a_4	boundary	$[m]$
a_{scrap}	scrap dissolution rate	$[\frac{kg}{s}]$
a_T	coefficient	$[\frac{K}{mol}]$
A	frequency factor	$[\frac{1}{s}]$
A_{CaO}	addition rate of CaO	$[\frac{mol}{s}]$
A_{FeO}	addition rate of FeO	$[\frac{mol}{s}]$
A_{MgO}	addition rate of MgO	$[\frac{mol}{s}]$
A_{SiO2}	addition rate of SiO2	$[\frac{mol}{s}]$
A_{TiO2}	addition rate of TiO2	$[\frac{mol}{s}]$
b	constant	[-]
b_1	regression coefficient	[-]
b_2	regression coefficient	[-]
b_3	regression coefficient	[-]
b_4	regression coefficient	$[\frac{1}{kg}]$
b_5	regression coefficient	[-]
b_{n+1}	regression coefficient	
B	basicity	[-]
c	constant	$[\frac{mol}{ms}]$
C	carbon in steel	[mol]
$[C]$	carbon concentration	$[\frac{mol}{m^3}]$

$[C^*]$	molar carbon concentration	$[\frac{mol}{mol}]$
C_0	initial amount of carbon in steel	[mol]
C_{hm}	carbon concentration hot metal	[w%]
C_{st}	carbon concentration steel	[w%]
$C_{reaction}$	carbon that reacts	[mol]
D	set	
E	set	
Ea	activation energy	$[\frac{J}{mol}]$
Fe	iron in bath	[mol]
FeO	iron oxide in slag	[mol]
$[FeO]$	iron oxide concentration in the slag	$[\frac{mol}{m^3}]$
$[FeO^*]$	molar percentage of iron oxide in the slag	$[\frac{mol}{mol}]$
$FeO_{addition}$	iron oxide added due to additions	[mol]
FeO_{lance}	iron oxide added due to blowing of oxygen	[mol]
$FeO_{localmax}$	iron oxide content in local maximum	[mol]
f_i	state equations	
$f_{resonance}$	resonance frequency	[Hz]
F	performance functional	
g	gain	[-]
g(x)	inequality constraint	[-]
h	foam height	[m]
H	Hamiltonian	
Heavyscrap	heavy scrap weight	[kg]
H_{lance}	lance height	[m]
i	discrete time instance	[s]
J	objective function	[s]
k	constant	[-]
k_0	reaction rate constant	$[\frac{mol}{s}]$
k_{0eq}	reaction rate constant	$[\frac{mol}{s}]$
k_{Si}	reaction rate constant	$[\frac{mol}{s}]$
k_{Ti}	reaction rate constant	$[\frac{mol}{s}]$
K	step function	[-]
L	length of tube	[m]
n	stoichiometric coefficient	[-]
n_x	fraction of element X in scrap	$[\frac{mol}{kg}]$
Mn_{hm}	hot metal manganese concentration	[w%]
O	oxygen in converter	[mol]
$O_{additions}$	oxygen origination from the additions	[mol]
O_{air}	oxygen entering through the air	[mol]

O_{lance}	oxygen origination from the lance	[mol]
$O_{reactionsconverter}$	oxygen consumed by reactions in the converter	[mol]
$O_{wastegas}$	oxygen in the waste gas	[mol]
O_{Fe}	oxygen used to oxidize iron	[mol]
O_{Mn}	oxygen used to oxidize manganese	[mol]
O_P	oxygen used to oxidize phosphorous	[mol]
O_{Si}	oxygen used to oxidize silicon	[mol]
P	slop probability	[-]
P_{hm}	hot metal phosphorous concentration	[w%]
pCO_2	carbon monoxide carbon dioxide ratio	$[\frac{mol}{mol}]$
Position	position parameter	[-]
$Q_{additions}$	energy consumed by additions	[J]
$Q_{convertergas}$	energy in converter gas	[J]
$Q_{heatloss}$	energy lost to environment	[J]
$Q_{reactionsconverter}$	energy produced by reactions	[J]
$Q_{reactionswastegas}$	energy produced by reactions in the waste gas	[J]
Q_{scrap}	energy consumed by scrap	[J]
Q_{slag}	energy consumed by the slag	[J]
Q_{steam}	energy consumed by the steam	[J]
Q_{steel}	energy consumed by the steel	[J]
$Q_{wastegas}$	energy leaving in waste gas	[J]
$Q_{wastegassystem}$	energy consumed by the waste gas system	[J]
R	gas constant	$[\frac{J}{molK}]$
S_C	C dissolution rate due to scrap	$[\frac{mol}{s}]$
S_{Fe}	Fe dissolution rate due to scrap	$[\frac{mol}{s}]$
S_{Si}	Si dissolution rate due to scrap	$[\frac{mol}{s}]$
S_{Ti}	Ti dissolution rate due to scrap	$[\frac{mol}{s}]$
$[Si^*]$	silicon molar concentration	$[\frac{mol}{mol}]$
Si_{hm}	hot metal silicon concentration	[w%]
$Si_{reaction}$	silicon reacted	[mol]
t	time	[s]
t_f	final time	[s]
t_0	initial time	[s]
T	steel temperature	[K]
T_0	initial steel temperature	[K]
T_{hm}	hot metal temperature	[K]
T_{st}	steel temperature	[K]
$[Ti^*]$	titanium molar concentration	$[\frac{mol}{mol}]$
Ti_{hm}	hot metal titanium concentration	[w%]

$Ti_{reaction}$	titanium reacted	[mol]
T_{hm}	hot metal temperature	[K]
v	sound velocity	$[\frac{m}{s}]$
V_M	molar volume	$[\frac{m^3}{mol}]$
VO_2	oxygen blowing rate	$[\frac{mol}{s}]$
V_{steel}	steel volume	$[m^3]$
W_{CaO}	calcium oxide content of the slag	[kg]
W_{SiO2}	silicium oxide content of the slag	[kg]
W_{hm}	amount of hot metal charged	[ton]
W_{lime}	amount of lime charged	[ton]
W_{ore}	amount of iron ore charged	[ton]
W_{scrap}	amount of scrap charged	[ton]
W_{slag}	amount of slag charged	[ton]
WG_{CO}	volume fraction of carbon monoxide in waste gas	[-]
WG_{CO2}	volume fraction of carbon dioxide in waste gas	[-]
x_i	condition	
x_{i0}	initial condition	
x_1	model input	
x_2	model input	
x_n	model input	
X	oxidizable elements in the steel	[mol]
$X_{reaction}$	removal of element X in bath due to reactions	[mol]
X_{scrap}	bath content of element X due to scrap dissolution	[mol]
X_C	carbon concentration	[w%]
$X_{C,demanded}$	demanded carbon concentration	[w%]
XO_n	oxides in the slag	[mol]
$XO_{n,addition}$	measured amount of component XO_n added	[mol]
$\hat{y}$	modeled value	
y	measured value	
β	attenuation coefficient	$[\frac{dB}{m}]$
ΔT	model constant	[K]
ϵ	predefined error margin	[mol]
η	regression parameter for slopping	[-]
λ	costates	
ϕ_{wg}	waste gas flow	$[\frac{m^3}{s}]$
Φ	magnitude sound spectrum measured	[dB]
Φ_0	magnitude sound spectrum source	[dB]

Matrices

B	regression matrix
E	residual matrix
F	residual matrix
P	loading matrix
Q	loading matrix
T	score matrix
U	score matrix
X	data matrix
Y	data matrix

Abbreviations

EAF	electric arc furnace
BOS	basic oxygen steelmaking
FN	false negative
FP	false positive
HM	hot metal
LV	latent variable
PCA	principal component analysis
PC	principal components
PLS	partial least squares
TN	true negative
TP	true positive
VAF	variance accounted for
var	variance